

EFFECT OF WELDING PARAMETERS ON THE HOT CRACKING BEHAVIOR  
OF 7039 ALUMINUM - ZINC ALLOY

A THESIS SUBMITTED TO  
THE GRADUATE SCHOOL OF NATURAL AND APPLIED SCIENCES  
OF  
MIDDLE EAST TECHNICAL UNIVERSITY

BY

MERT AKKUŞ

IN PARTIAL FULFILLMENT OF THE REQUIREMENTS  
FOR  
THE DEGREE OF MASTER OF SCIENCE  
IN  
METALLURGICAL AND MATERIALS ENGINEERING

SEPTEMBER 2010

Approval of the thesis:

**EFFECT OF WELDING PARAMETERS ON THE HOT CRACKING  
BEHAVIOR OF 7039 ALUMINUM - ZINC ALLOY**

submitted by **MERT AKKUŞ** in partial fulfillment of the requirements for the degree of **Master of Science in Metallurgical and Materials Engineering Department, Middle East Technical University** by

Prof. Dr. Canan Özgen  
Dean, Graduate School of **Natural and Applied Sciences**

\_\_\_\_\_

Prof. Dr. Tayfur Öztürk  
Head of Department, **Metallurgical and Materials Eng.**

\_\_\_\_\_

Prof. Dr. Rıza Gürbüz  
Supervisor, **Metallurgical and Materials Eng. Dept., METU**

\_\_\_\_\_

Dr. Caner Batıgün  
Co-Supervisor, **Weld. Tech. and NDT Res./App.C., METU**

\_\_\_\_\_

**Examining Committee Members**

Prof. Dr. Bilgehan Ögel  
Metallurgical and Materials Eng. Dept., METU

\_\_\_\_\_

Prof. Dr. Rıza Gürbüz  
Metallurgical and Materials Eng. Dept., METU

\_\_\_\_\_

Prof. Dr. C. Hakan Gür  
Metallurgical and Materials Eng. Dept., METU

\_\_\_\_\_

Dr. Caner Batıgün  
Welding Tech. and NDT Res./App.C., METU

\_\_\_\_\_

Assist. Prof. Dr. Kazım Tur  
Materials Engineering Department, Atılım University

\_\_\_\_\_

**Date:** 16/09/2010

**I hereby declare that all information in this document has been obtained and presented in accordance with academic rules and ethical conduct. I also declare that, as required by these rules and conduct, I have fully cited and referenced all material and results that are not original to this work.**

Name, Last name: Mert AKKUŞ

Signature:

## ABSTRACT

### EFFECT OF WELDING PARAMETERS ON THE HOT CRACKING BEHAVIOR OF 7039 ALUMINUM - ZINC ALLOY

Akkuş, Mert

M.Sc., Department of Metallurgical and Materials Engineering

Supervisor : Prof. Dr. Rıza Gürbüz

Co-supervisor : Dr. Caner Batıgün

September 2010, 101 Pages

7039 aluminum alloys are widely being used in the aerospace, automotive and defense industries in which welding technique is used for their joining. The main problem encountered during the welding of 7039 aluminum alloy is hot cracking. The aim of this study is to understand the effect of welding parameters on the hot cracking behavior of 7039 aluminum alloy by using Modified Vareststraint Test (MVT) with Gas Tungsten Arc Welding (GTAW) technique. During tests, welding speed was selected as varying parameter, welding current was kept constant and to understand the effect of filler materials 5183 and 5356 aluminum alloy filler materials were used. It has been observed that with the change in welding speed hot cracking susceptibility of 7039 aluminum alloy changes. The effect of filler materials is found to be favorable by decreasing the hot cracking susceptibility of 7039 aluminum alloy. Filler material additions also improved the hardness of the weld metal. Based on the cracking mechanism hot cracks were investigated as solidification cracks and liquation cracks. It has been experienced that liquation cracking susceptibility of the filler material added samples has been affected from the magnesium and manganese contents of the weld seams. Effect of solidification range on liquation cracking was also justified with differential thermal analyses. With the micro examinations the intergranular structure of hot cracking is revealed.

In addition, the characterization and growth properties of the hot cracks under cyclic load were tried to be understood and the fractography of these cracks were taken.

Keywords: Hot cracking, Modified Varestraint Test, 7039 aluminum alloy

## ÖZ

### 7039 ALÜMİNYUM - ÇİNKO ALAŞIMINDA, KAYNAKLAMA İŞLEMİNİN SICAK ÇATLAMA DAVRANIŞI ÜZERİNDEKİ ETKİLERİNİN İNCELENMESİ

Akkuş, Mert

Yüksek Lisans, Metalurji ve Malzeme Mühendisliği Bölümü

Tez Yöneticisi : Prof. Dr. Rıza Gürbüz

Ortak Tez Yöneticisi : Dr. Caner Batıgün

Eylül 2010, 101 Sayfa

7039 alüminyum alaşımı havacılık, otomotiv ve savunma sanayilerinde yaygın bir şekilde kullanılmakta ve bu alaşımlar sanayide genellikle kaynak teknolojisi yoluyla birleştirilmektedir. 7039 alüminyum alaşımlarının kaynatılması sırasında karşılaşılan en yaygın problem sıcak çatlama olmaktadır. Bu çalışmada, Modified Vrestraint Test (MVT) yöntemi ve Gaz Tungsten Ark Kaynağı (GTAK) kullanarak 7039 alüminyum alaşımının çeşitli kaynak parametreleri altında sıcak çatlama eğilimi ve çatlaklara bağlı kırılma davranışı incelenmiştir. Testlerde sabit kaynak akımı ve değişken kaynak hızlarının kullanılmasının yanında 7039 alüminyum alaşımı üzerinde 5183 ve 5356 alüminyum alaşımı dolgu malzemeleri kullanarak ve kullanmadan kaynak işlemleri gerçekleştirilmiştir. İncelemelerde kaynak hızındaki değişimin 7039 alüminyum alaşımının sıcak çatlama davranışını değiştirdiği ve dolgu malzemesi kullanımının 7039 alüminyum alaşımının sıcak çatlama davranışını azalttığı görülmüştür. Ayrıca, dolgu malzemesi kullanımı kaynak bölgesinin sertliğinde artış sağlamıştır. Sıcak çatlaklar, çatlama mekanizmasına bağlı olarak ya katılma ya da erime çatlakları olarak ortaya çıkmaktadırlar. Dolgu malzemesi kullanılan testlerde erime çatlama davranışı kaynak metalindeki magnezyum ve mangan miktarları ile ilişkilendirilebilmektedir. Katılma aralığının erime çatlama davranışına etkisi diferansiyel termal analiz yoluyla da doğrulanmıştır. Mikro incelemeler sonucunda sıcak çatlakların taneler arası yapısı gözlemlenmiştir. Son

olarak sıcak çatlakların tekrarlı yükleme altında karakterizasyonu ve büyüme özellikleri incelenmiş, fraktografik incelemelerde bulunulmuştur.

Anahtar Kelimeler: Sıcak çatlama, Modified Vareststraint Test, 7039 alüminyum alaşımı

To my family



## ACKNOWLEDGEMENTS

I would like to express my deepest and sincere gratitude to my thesis supervisor Prof. Dr. Rıza Gürbüz for his valuable guidance and supervision.

I would also like to thank to my thesis co-supervisor Dr. Caner Batıgün for his encouraging guidance and continuous support throughout the thesis.

I am grateful to all members of Welding Technology & Nondestructive Testing Research/Application Center for their assistance during the experiments and FNSS Savunma Sistemleri A.Ş. for providing the samples. My special thanks to my friend Murat Tolga Ertürk for making the processes easy at Welding Technology & Nondestructive Testing Research/Application Center.

Support of Göksu Gürer during fatigue tests; technical assistance of researchers at Thermal Analysis Laboratory of METU Central Laboratory during Differential Thermal Analysis; helps of technicians at Foundry Laboratory of Metallurgical and Materials Engineering Department during chemical analysis and support of researchers at SEM Laboratory of Metallurgical and Materials Engineering Department during SEM examinations are gratefully acknowledged.

I am grateful to my employer TÜBİTAK, to my superiors and my colleagues for providing convenience during my M.S. studies.

I want to extend my appreciation to all my friends for their moral support and friendship.

Finally, I would like to dedicate this study to my parents for supporting and encouraging me throughout all my life.

## TABLE OF CONTENTS

<b>ABSTRACT</b> .....	iv
<b>ÖZ</b> .....	vi
<b>ACKNOWLEDGEMENTS</b> .....	ix
<b>TABLE OF CONTENTS</b> .....	x
<b>LIST OF TABLES</b> .....	xiv
<b>LIST OF FIGURES</b> .....	xv
<b>CHAPTERS</b>	
<b>1. INTRODUCTION</b> .....	1
1.1 Aim of the Study .....	1
<b>2. THEORY</b> .....	3
2.1 Properties of Aluminum and Aluminum Alloys .....	3
2.2 Arc Welding .....	5
2.2.1 Gas Tungsten Arc Welding (GTAW) .....	5
2.3 Weld Structure .....	8
2.3.1 Weld Metal .....	8
2.3.2 Partially Melted Zone (PMZ) .....	10
2.3.3 Heat Affected Zone (HAZ) .....	10
2.4 Weld defects .....	11
2.4.1 Porosities .....	11

2.4.2	Tungsten and Oxide Inclusions .....	13
2.5	Cracking.....	13
2.5.1	Hot cracking.....	13
2.6	Methods to Evaluate Hot Cracking.....	23
2.6.1	Modified Varestraint Test.....	24
<b>3.</b>	<b>LITERATURE REVIEW .....</b>	<b>25</b>
3.1	Hot Cracking Formation .....	25
3.2	Effect of Filler Material and Chemical Composition .....	25
3.3	Effect of Strain.....	26
3.4	Effect of Welding Speed.....	27
<b>4.</b>	<b>EXPERIMENTAL PROCEDURE.....</b>	<b>29</b>
4.1	Material.....	29
4.2	Experimental Setup.....	32
4.2.1	MVT Equipment.....	32
4.2.2	Specimen Preparations for MVT and Test Procedure .....	36
4.2.3	Chemical Analysis .....	39
4.2.4	Crack Length Measurements .....	40
4.2.5	Metallographic Examinations.....	41
4.2.6	Differential Thermal Analysis (DTA) .....	43
4.2.7	Hardness Test.....	44
4.2.8	Fatigue Test .....	44

4.2.9	SEM Examinations .....	45
<b>5.</b>	<b>RESULTS .....</b>	<b>47</b>
5.1	Results Related with the Test Methodology .....	47
5.2	Results of the Chemical Analysis .....	47
5.3	Hot cracking Susceptibility of 7039 Aluminum Alloy .....	48
5.4	Results of the Crack Length Measurements .....	50
5.5	Results of Metallographic Examinations .....	57
5.5.1	Results of Macrostructure Examinations .....	57
5.5.2	Results of Microstructure Examinations .....	59
5.6	Results of the Differential Thermal Analysis (DTA) .....	70
5.7	Results of the Hardness Test .....	73
5.8	Results of the Fatigue Test .....	75
5.9	Results of SEM Examinations .....	78
5.9.1	SEM Examinations of the Welded Samples .....	78
5.9.2	SEM Examinations of Fatigue Tested Samples .....	82
<b>6.</b>	<b>DISCUSSION .....</b>	<b>86</b>
6.1	Hot cracking behavior of 7039 aluminum alloy .....	86
6.2	Effect of welding parameters on the hot cracking susceptibility .....	86
6.2.1	Effect of welding parameters on the liquation cracking susceptibility .....	87
6.3	Effect of filler materials on the hot cracking susceptibility .....	88
6.4	Effect of filler materials on hardness .....	88

6.5 Behavior of hot cracks under fatigue test .....	88
<b>7. CONCLUSION</b> .....	90
<b>REFERENCES</b> .....	92
<b>APPENDICES</b> .....	96
A. PHASE DIAGRAM OF Al-Mg-Zn .....	96
B. CRACK LENGTH AND NUMBER MEASUREMENT RESULTS.....	97

## LIST OF TABLES

### TABLES

Table 1 Chemical composition of the 7039 aluminum alloy .....	31
Table 2 Tensile test results of the obtained 7039 aluminum alloy.....	31
Table 3 The composition of the filler materials [46] .....	32
Table 4 Welding parameters and conditions .....	35
Table 5 The grouping of the samples .....	37
Table 6 Composition of the reagents .....	40
Table 7 Reagents used for macro and microexaminations.....	42
Table 8 The composition of the weld seams produced by MVT method .....	47
Table 9 Fatigue life of the samples .....	76
Table 10 Length of the final cracks of the fatigue tested samples .....	77
Table B1 Crack length measurement results for 7039 aluminum alloy set .....	97
Table B2 Crack length measurement results for 7039-5183 aluminum alloy set .....	98
Table B3 Crack length measurement results for 7039-5356 aluminum alloy set .....	99
Table B4 The length and location of liquation cracks of 7039-5183 aluminum alloy .....	100
Table B5 The length and location of liquation cracks of 7039-5356 aluminum alloy .....	101

## LIST OF FIGURES

### FIGURES

Figure 1 Polarities for GTAW [6].....	7
Figure 2 Cleaning of the Ar+ ions for positive tungsten electrode [6] .....	7
Figure 3 Effect of temperature gradient and growth rate on solidification of weld metal [6] .....	9
Figure 4 Effect of welding speed and welding current on temperature gradient [6] .	10
Figure 5 Solubility of hydrogen in aluminum [2] .....	12
Figure 6 Tensile and compressive stress zone during welding [15] .....	15
Figure 7 Effect of liquid film to the strain distribution [16] .....	16
Figure 8 Stages of hot cracking [16].....	17
Figure 9 Hot cracking tendency and solidification stages (Borland's theory) [19]..	19
Figure 10 Relation between total crack length and mean grain size of Al-2%Zn-2%Mg [20] .....	20
Figure 11 Liquation cracking mechanism in PMZ [22].....	21
Figure 12 Effect of heat input on liquation cracking [6].....	22
Figure 13 Effect of grain size on liquation cracking [6] .....	23
Figure 14 Modified Varestraint Test [31] .....	24
Figure 15 The microstructure of the obtained 7039 aluminum alloy plate (a) parallel to the rolling direction (b) perpendicular to the rolling direction. Keller Etching.....	30

Figure 16 The microstructure of the obtained 7039 aluminum alloy plate before etching.....	30
Figure 17 Power Source of the MVT Equipment .....	33
Figure 18 Electronic Control Unit of the MVT Equipment.....	33
Figure 19 Welding and Bending Unit of the MVT Equipment .....	34
Figure 20 Calculation of the strain developed during MVT method [38] .....	34
Figure 21 Scheme for the samples .....	36
Figure 22 Excessive heat caused melting of the specimen .....	38
Figure 23 Specimen preparation method used in the study of Savage and Lundin [27] .....	38
Figure 24 Unmelted part observed on the cross section of the sample.....	39
Figure 25 Method to measure crack lengths .....	41
Figure 26 Location where the macro and microexaminations were done .....	42
Figure 27 Fractured surfaces taken to SEM examinations.....	45
Figure 28 a) Liquation cracks formed in the HAZ region of 7039-5183 set (welding speed: 65 mm/min) b) Solidification cracks formed in the weld part of 7039-5183 set (welding speed: 55 mm/min) .....	49
Figure 29 Centerline crack observed during welding of 7039 aluminum alloy (welding speed: 60 mm/min) .....	49
Figure 30 Total crack length measured for the three different aluminum alloy sets .	50
Figure 31 Maximum crack length measured for the three different aluminum alloy sets.....	51
Figure 32 Number of total cracks counted for the three different aluminum alloy sets .....	51



Figure 33 Average crack length calculated for the three different aluminum alloy sets .....	52
Figure 34 Effect of welding speed on the total crack length for the whole sets .....	53
Figure 35 Effect of welding speed on the maximum crack length for the whole sets .....	53
Figure 36 Effect of welding speed on the total crack number for the whole sets .....	54
Figure 37 Effect of welding speed on the total liquation crack length for the weld seams produced by filler materials.....	55
Figure 38 Effect of welding speed on the maximum liquation crack length for the weld seams produced by filler materials.....	55
Figure 39 Macro-photos of the weld region of the samples.....	58
Figure 40 Weld and parent metal regions of 7039-5183 aluminum alloy welded with 50 mm/min welding speed and 120 A drop current. Keller etching.....	59
Figure 41 Weld structure of 7039-5183 aluminum alloy welded with 65 mm/min welding speed and 120 A drop current. Keller etching.....	60
Figure 42 Weld metal of 7039-5356 aluminum alloy welded with 55 mm/min welding speed and 120 A drop current. Keller etching.....	61
Figure 43 Weld metal of 7039-5183 aluminum alloy welded with 55 mm/min welding speed and 120 A drop current. Keller etching.....	61
Figure 44 Solidification crack at the weld metal of 7039-5183 aluminum alloy welded with 50 mm/min welding speed and 120 A drop current. Keller etching. ....	62
Figure 45 Solidification crack at the weld metal of 7039-5356 aluminum alloy welded with 60 mm/min welding speed and 120 A drop current. Keller etching. ....	63
Figure 46 Porosities around the weld metal of 7039-5183 aluminum alloy welded with 60 mm/min welding speed and 120 A drop current. Keller etching.....	64

Figure 47 Liquation crack at the PMZ and HAZ of 7039-5356 aluminum alloy. Weck reagent.....	65
Figure 48 Precipitates formed at the weld metal of 7039 aluminum alloy welded with 60 mm/min welding speed and 120 A drop current. Weck etching.....	66
Figure 49 Precipitates formed at the weld metal of 7039 aluminum alloy welded with 60 mm/min welding speed and 120 A drop current. Weck etching.....	66
Figure 50 Intergranular liquation cracks observed for (a) 7039-5183 aluminum alloy (b) 7039-5356 aluminum alloy welded with 60 mm/min welding speed and 120 A drop current. Weck reagent.....	67
Figure 51 SEM-EDX analysis taken from the cracking region of 7039 aluminum alloy.....	68
Figure 52 SEM-EDX analysis taken from the cracking region of 7039-5183 aluminum alloy .....	69
Figure 53 Crack tip radius range for the whole sets .....	70
Figure 54 Heat flow versus temperature graph showing the heating stage of the 7039 aluminum alloy .....	71
Figure 55 Heat flow versus temperature graph showing the heating stage of the 7039-5183 aluminum alloy.....	72
Figure 56 Heat flow versus temperature graph showing the heating stage of the 7039-5356 aluminum alloy.....	73
Figure 57 Hardness profile along the cross section of the 7039 aluminum alloy.....	74
Figure 58 Hardness profile along the cross section of the 7039-5183 aluminum alloy .....	74
Figure 59 Hardness profile along the cross section of the 7039-5356 aluminum alloy .....	75

Figure 60 Macro-photos of the fatigue fractured surface of 7039 aluminum alloy...	76
Figure 61 Macro-photos of the fatigue fractured surfaces of 7039-5183 and 7039-5356 aluminum alloys.....	77
Figure 62 Fractography of a liquation crack of 7039-5183 aluminum alloy.....	79
Figure 63 Fractography of a liquation crack of 7039-5183 aluminum alloy. The crack formation is intergranular.....	79
Figure 64 Fractography of the solidification cracks located at the weld metal of 7039-5183 aluminum alloy.....	80
Figure 65 Fractography of a solidification crack located at the weld metal of 7039-5356 aluminum alloy.....	81
Figure 66 Fractography of a solidification crack located along the fusion line of 7039 aluminum alloy.....	81
Figure 67 Dendritic morphology observed at the weld metal of 7039-5356 aluminum alloy.....	82
Figure 68 SEM photographs of the parent metal and weld metal of the fatigue tested samples.....	83
Figure 69 SEM photograph showing the ductile fracture of the 7039 aluminum alloy taken after fatigue test.....	84
Figure 70 Cracks that were formed just under the surface of the 7039 aluminum alloy.....	85
Figure A1 Liquidus projection of Al-Mg-Zn.....	96

# CHAPTER 1

## INTRODUCTION

### 1.1 Aim of the Study

Aluminum alloys are becoming more and more favorable in different industrial fields. Their easy fabrication, good physical and mechanical properties and also lightweightness makes them preferable over conventional materials. Especially aerospace, automotive and defense industries benefit from the high toughness and low density of the aluminum alloys.

Aluminum alloys used in these industries are joined mostly by welding applications. Gas tungsten arc welding (GTAW) and gas metal arc welding (GMAW) techniques are widely used for the welding of these alloys. However during welding, related with some properties of the aluminum alloys certain problems may show up. Hot cracking is one of the critical problems that occur during welding of the aluminum alloys, particularly for heat treatable aluminum alloys. Considering the crack formation mechanism, hot cracking is observed either as solidification cracking or liquation cracking. High thermal conductivity of aluminum alloys, stress acting on the system, chemical composition or alloy precipitates may be the cause of the hot cracking during welding. Depending on various parameters, hot cracking can be prevented by doing some modifications in some properties of the alloys or by controlling the welding parameters.

Discussions on hot cracking phenomena were started long time ago, several theories and discussions were put forward in the mid of 20<sup>th</sup> century. Later on, methods to evaluate the hot cracking susceptibility were introduced. Modified Varestraint Test (MVT) is one of these test methods that evaluate the hot cracking susceptibility. In this test method the sample is welded and at the same time bended under a

predefined stress, thereby the formation of hot cracks is triggered. The hot cracking susceptibility is evaluated by measuring the total crack length and total number of the cracks that form across weld metal, partially melted zone and heat affected zone. Besides, maximum crack length measurements are also determinant in evaluating hot cracking susceptibility.

In this study, a member of 7xxx aluminum alloy series; 7039 aluminum alloy is used. The main alloying element of 7039 aluminum alloy is zinc but it also contains significant amount of magnesium. This alloy is widely used in the applications that require high strength and good weldability. Therefore understanding the welding characteristics in connection with hot cracking susceptibility is necessary for these alloys. Until this time some studies were conducted in order to understand the welding of 7039 aluminum alloys, to find optimum welding techniques for this alloy and also to find optimum filler materials. However not a detailed study were conducted to understand the hot cracking phenomena of this alloy. Considering the trend in the use of 7039 aluminum alloy in the industry, a study to understand the hot cracking behavior of this alloy is necessary. Therefore the aim of this study came up as to understand the cracking behavior and observe the effect of welding parameters on the hot cracking susceptibility of the 7039 aluminum alloy.

Through this study several MVT tests combined with GTAW were conducted to understand the hot cracking susceptibility of the 7039 aluminum alloy. During welding, welding speed was selected as varying parameter and welding current was kept constant. To understand the effect of chemical composition 5183 and 5356 aluminum alloy filler materials were used. Crack observations, metallographic examinations, thermal analyses, hardness and fatigue tests were carried out in order to understand the effect of welding parameters on the hot cracking behavior of 7039 aluminum alloy.

## CHAPTER 2

### THEORY

#### 2.1 Properties of Aluminum and Aluminum Alloys

Having low specific gravity makes aluminum and its alloys preferable for particular applications; such as marine, automobile, aircraft industries. Joining of aluminum parts are mostly carried out by welding process in the industry. Although welding of aluminum is widely used in these sectors, some properties that aluminum have in nature (i.e. high thermal conductivity, high thermal expansion) may cause problems during welding process [1].

Aluminum melts around 650°C and melting point of its alloys varies from (350°C - 650°C). Relative to steel, aluminum removes heat from the welding region five-six times faster than the steel does. It's relatively high thermal conductivity makes it necessary to use higher heat inputs for the welding of aluminum [2].

The relatively high thermal expansion and contraction of aluminum and its alloys may cause cracking problems during the heating and cooling steps of the welding process. Aluminum alloys have a relatively low ductility and strength at the temperatures near their melting point. If they are welded under stress and strain they are more likely to crack. The composition, welding speed or welding current can be regarded as the main factors that affect hot cracking [1].

Aluminum and its alloys are very likely to react with oxygen, which may cause serious problems in welding. When it is open to air an aluminum-oxide thin film occurs across the surface which should be removed before the welding in order to start the welding process. Oxide formed on the surface may cause corrosion or may lower the quality of the welding. In this study, oxide layer is removed by mechanical

brushing prior to welding. Porosity problems are also encountered in welding of aluminum and its alloys. The main reason of the gas porosity in aluminum welds is that aluminum in the molten state can easily absorb hydrogen element whereas in the solid state the solubility of hydrogen in aluminum becomes lower. Hydrogen that was solved in the liquid state precipitates during solidification and forms porosities. The source of absorbed hydrogen can be the moisture on the metal surface, atmosphere or flame [1].

In order to prevent some weaknesses that pure aluminum possesses during welding (i.e. low strength) aluminum is welded in its alloy form. When aluminum is alloyed with other metals, the combination is an attractive element with wide range of attractive properties [3].

As a major classification, aluminum alloys can be divided into two groups: wrought alloys and cast alloys. Basically wrought aluminum alloys are defined as the alloys that are mechanically worked. The two groups of aluminum alloys can be further classified with respect to their temper conditions; non heat treatable aluminum alloys and heat treatable aluminum alloys. Non-heat treatable alloys can be defined as the aluminum alloys which gain its strength through cold working or solid solution strengthening. As a difference from heat treatable aluminum alloys they cannot form second-phase precipitates that improve their strength. Whereas heat treatable aluminum alloys can be strengthened by heat treatment. They are mostly preferred in aerospace, marine and transportation applications since they present good strength while having low density [4]. Heat treatable aluminum alloys are prone to weld cracking. Weld cracking can be prevented by selecting the suitable filler material or by modifying the welding parameters. 2xxx (Al-Cu), 6xxx (Al-Mg-Si) and 7xxx (Al-Zn) series are the typical heat treatable aluminum alloys.

This thesis focuses on 7039 aluminum alloy which is a member of Al-Zn-Mg series, or in other words 7xxx series. The heat treatable 7xxx series involve zinc (Zn) as a major alloying element and also a significant amount of magnesium. Other than these several elements may exist in the chemical composition. The characteristic property

of these alloys is that; they provide the highest strength of all aluminum alloys because of the zinc, magnesium and copper elements that they contain [4].

## **2.2 Arc Welding**

Welding of aluminum alloys are carried out most effectively by Gas Tungsten Arc Welding (GTAW) or Gas Metal Arc Welding (GMAW). In this study GTAW is used for the welding of the 7039 aluminum alloy.

### **2.2.1 Gas Tungsten Arc Welding (GTAW)**

Arc is created between a non-consumable tungsten electrode and metal and passes through an inert atmosphere. One of the main advantages of GTAW is that the heat is concentrated on a narrow region that results a narrow heat affected zone. Another advantage is that since the tungsten electrode is non-consumable, metal spattering does not occur across the arc [5].

Tungsten electrode is used during GTAW because tungsten can withstand to higher temperatures by its high melting point. The cleanness of the tungsten electrode is an important factor. They are produced with a cleaned surface and with a certain diameter. Tungsten electrodes are supplied with several compositions and pure tungsten is used mostly with AC (alternating current) welding [5]. During the experiments tungsten electrode with a green color code is used. The green color symbolizes the pure tungsten electrode which is usually used for AC welding. One another factor for the electrode is its tip diameter. For a better arc, the tip of the electrode is shaped into a balled end which helps to achieve a more stabilized current.

During GTAW, shielding gas is used in order to protect the weld pool from the atmospheric gases and it provides a uniform metal transfer and stabilizes the arc. The shielding gas used in welding of 7039 aluminum alloy consist of argon which is an inert gas and does not react with the materials that presents in welding. Having lower ionization potential, argon gas ensures easier arc initiation with respect to helium gas [4]. Besides, as a consequence of argon being heavier than helium, effective



shielding of the system and cleaning of oxides are achieved with argon gas [1]. In order to improve the control of gas flow onto the weldment or heat resistant ceramic or alumina nozzles are used. Their resistance to high temperature makes them use in these specific applications. The tungsten electrode passes through the ceramic nozzle at the tip and the amount of the electrode extends beyond the tip of the nozzle is an important factor. Before each experiment the difference between the tip of electrode and nozzle is calibrated [5].

As stated above, melting during welding process is achieved by the arc initiated between tungsten electrode and the metal surface and this arc can be achieved either by direct or alternating current. Polarity of the current plays also an important role in welding. In this study, alternating current is used which provides oxide cleaning effect and successive penetration. Alternating current combines the two advantages of “direct current with electrode positive” and “direct current with electrode negative”. When the electrode is positive, the electrons jump from negative workpiece to positive electrode and so the heat is carried by electrons to the tip of the electrode. Whereas when the electrode is negative, electrons are carried from tungsten to the workpiece and accordingly heat carried by electrons to the workpiece results in deeper penetration (Figure 1). For the positive electrode, positive  $\text{Ar}^+$  ions hit to the workpiece and breaks the aluminum oxide bonds that are formed on the aluminum alloy surface (Figure 2).

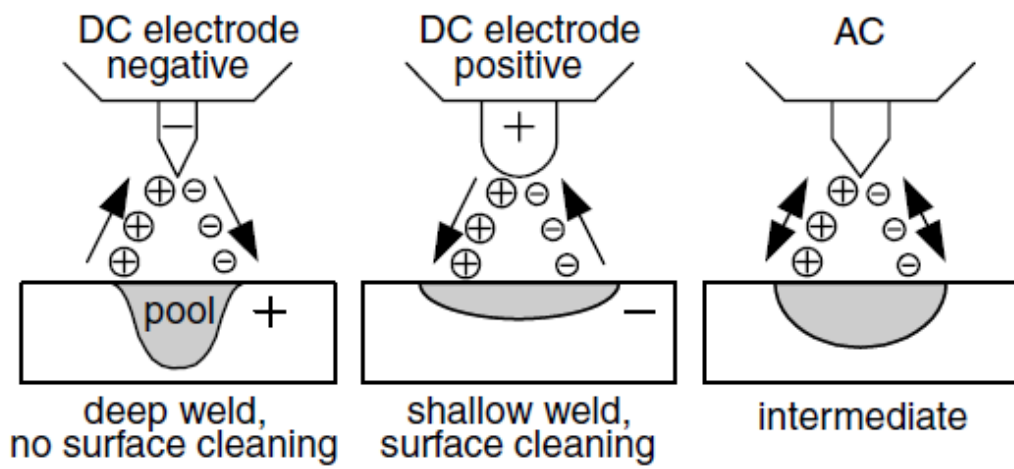


**Figure 1** Polarities for GTAW [6]

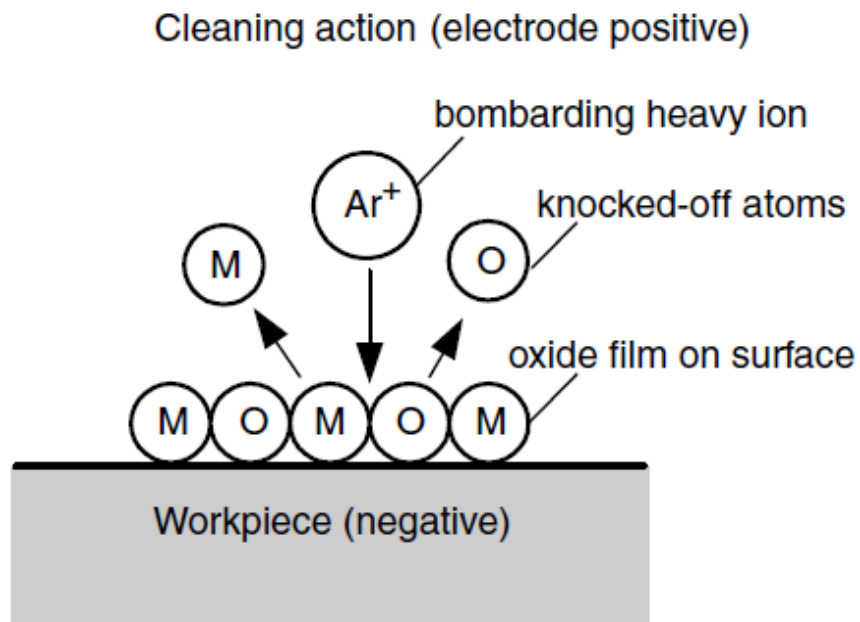


**Figure 2** Cleaning of the  $Ar^+$  ions for positive tungsten electrode [6]

## **2.3 Weld Structure**

During welding, as the heat resulting from the arc concentrates on the weld pool the other regions are affected relatively less from the heat. Considering the transverse cross section, this results in the formation of zones across weldment. These zones can be either seen by naked eye or by chemical etching and named as weld metal, partially melted zone (PMZ), heat affected zone (HAZ). Besides these, the remaining part of the metal can be named as parent metal which is less affected by the heat evolved during welding. Weld metal is the region that is melted during welding. At the final state, this zone consists of parent metal and filler material if added. Partially melted zone lies just outside the weld pool where liquation occurs during welding. Heat-affected zone is the area located between PMZ and parent metal at which the temperatures are too low to melt the metal and also high enough to alter microstructure of the metal [6, 7].

### **2.3.1 Weld Metal**

Weld metal is the area that is melted during welding, as a result of arc initiated between metal and electrode. This area is strongly affected by the welding parameters and the filler materials used.

In order to understand the effects of the welding parameters it is better to focus on solidification concepts. Welding parameters considered in this study, i.e. welding speed and welding current, affect directly solidification microstructure and solidification mode. Solidification microstructure is represented by multiplying temperature gradient ( $G$ ) and growth rate ( $R$ ) whereas solidification mode is represented by dividing temperature gradient ( $G$ ) into growth rate ( $R$ ). Altering welding speed and welding current affects the morphology of the solidification structure  $GR$  and also the size of the solidification mode  $G/R$  (Figure 3). For example, increase in welding current results in a decrease in temperature gradient and similarly increase in welding speed may decrease the temperature gradient at the end of weld pool and increase growth rate as shown in the Figure 4 for the 1100 aluminum. Therefore; change in the welding parameters can modify the solidification

mode and solidification structure which may directly affect the hot cracking mechanism. Savage et al. [8] studied the effect of growth rate and temperature gradient on the solidification mechanics and concluded that welding parameters have an impact on the solidification structures.

Welding parameters have also effect on the weld pool shape. Relatively low welding speeds and heat input produce more elliptical weld pool whereas higher welding speeds and higher heat inputs (high currents) cause tear dropped shape. High heat input and welding speed may cause heterogeneous nucleation at the center of the weld.

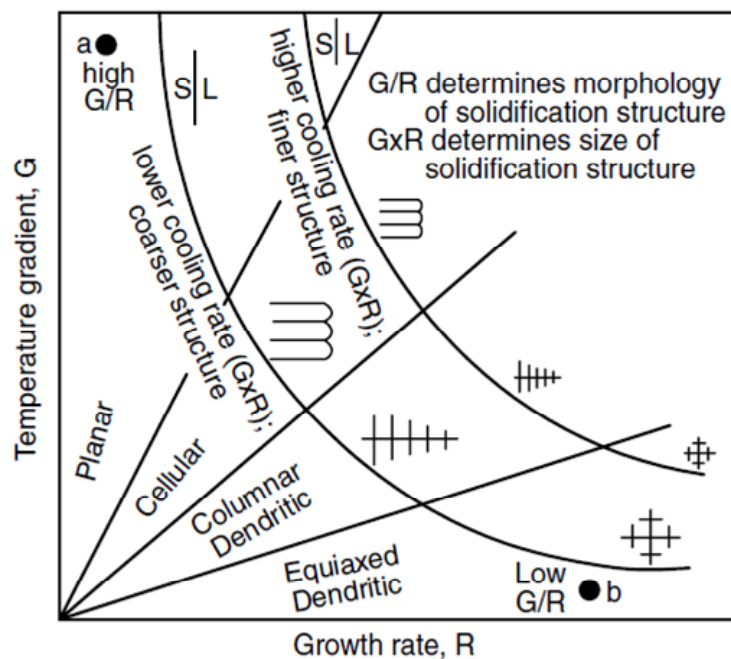


**Figure 3** Effect of temperature gradient and growth rate on solidification of weld metal [6]

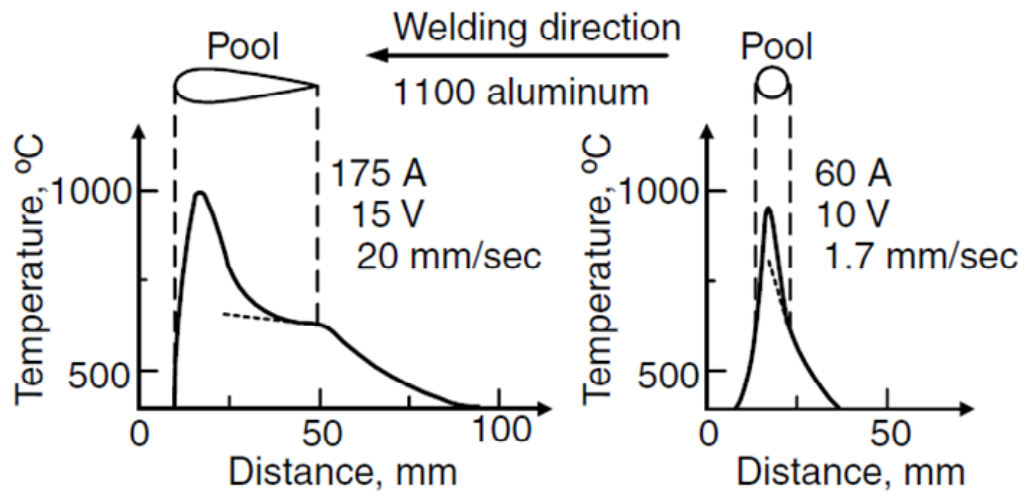


**Figure 4** Effect of welding speed and welding current on temperature gradient [6]

### 2.3.2 Partially Melted Zone (PMZ)

This zone lies just beside the fusion line at which the temperatures fall between liquidus and solidus temperatures. Across this zone melting is incomplete and this zone can be easily seen for the aluminum alloys that have wider solidification range.

This zone is very prone to hot cracking which will be discussed in the upcoming chapters. Grain boundary liquation may be seen in this zone and the regions where liquid films exist are known as weak regions. Therefore, presence of grain boundary liquation causes loss in strength across this zone which may cause hot cracking under strain and stress.

### 2.3.3 Heat Affected Zone (HAZ)

Heat affected zone lies between partially melted zone and parent metal. This zone is affected by the high temperatures that come up during welding but no melting occurs across this zone. The heat affects the microstructure of the parent metal in this zone and alters the mechanical properties. Previously strengthened alloys may lose their strength when subjected to heat during welding. In case of loss in strength in this

zone, post weld heat treatment is necessary in order to recover the mechanical properties.

## **2.4 Weld defects**

Practically, during welding observing a discontinuity or defect is expectable. Producing a perfect weld is nearly impossible and actually it is not always necessary if the discontinuities remain between the tolerance limits. If a defect presents in/on the weldment that exceeds the tolerance limits then it may cause the final weld product rejectable.

The main types of the weld discontinuities observed during arc welding can be given as follows: Process-related discontinuities (undercut, tungsten inclusions, porosities, lack of penetration, arc strike, incomplete fusion, overlaps, melt-through shrinkage voids, oxide inclusions etc); metallurgical discontinuities (cracks, fisheyes, segregations) [4]. It will be useful to get idea about the possible weld defects in order to distinguish hot cracks.

### **2.4.1 Porosities**

Porosities occur due to the entrapped gas during solidification of the weld metal. In aluminum alloys the main reason of the porosity is hydrogen that has high solubility in liquid aluminum and in contrast low solubility in the solid state of aluminum. This sudden fall in solubility of hydrogen cause the hydrogen to be trapped in the aluminum (alloy) (Figure 5).

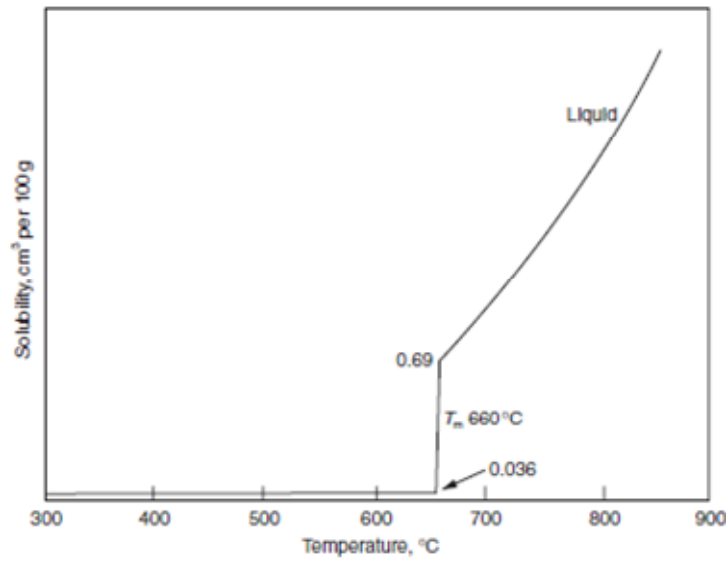


**Figure 5** Solubility of hydrogen in aluminum [2]

Rate of absorption of hydrogen depends on the arc current and weld speed. Increasing the arc current results increase in the temperature of the weld pool. As the temperature of the system increases the hydrogen absorption rate of the system increases. Reducing the welding speed will increase the solidification time which will allow the hydrogen to get evolved from the system. In addition to the factors given above, the composition of the aluminum alloy is another factor that is determinant in the porosity formation. Using magnesium in the filler material can reduce the porosity problem. It is found that magnesium increases the solubility of hydrogen [2]. At this point the choice of filler material becomes important. The reason of the hydrogen can be due to contamination in the presence of moisture or due to shielding gas used. The purity of the shielding gas may affect the hydrogen contamination. In order to avoid contamination, the parent metal should be mechanically cleaned (i.e. wire brushing) prior to welding and welded in a short period of time after cleaning. Brushing removes the oxide layer that may be a source of hydrogen.

### **2.4.2 Tungsten and Oxide Inclusions**

These inclusions are observed during GTAW. They are defined as the foreign particles found in the parent metal resulted from the non-consumable tungsten electrode. The reason of the tungsten inclusion may be dipping of the electrode into the parent metal. Although the melting point of the tungsten is very high, using high currents may cause tungsten to melt and dissolve into the weld pool [5]. Besides tungsten inclusions, aluminum and its alloys can easily form oxides (i.e.  $Al_2O_3$ ) and the oxides that are not melted can be mixed into the weld pool.

This study will mainly focus on the cracking behavior of the 7039 aluminum alloy:

## **2.5 Cracking**

Cracks form when the stress localized in a region exceeds the strength of the material. A crack forms when there exist a discontinuity that raises stress, a particle that has low fracture toughness or tensile stress [9].

The orientation of the crack with respect to the weld axis in the weldment is either longitudinal or transverse. Longitudinal cracks are parallel to the weld axis whereas transverse cracks are perpendicular to the weld axis. Longitudinal cracks can be either at weld metal or on side regions [5].

Cracks that form across the weldment can be classified into two according to the mechanism responsible for cracking: hot cracking and cold cracking. This study focuses on hot cracking behavior of 7039 aluminum alloy.

### **2.5.1 Hot cracking**

Hot cracking is a main problem in welding since it reduces the strength of the weldment dramatically. The relatively high thermal coefficient of aluminum and its alloys makes it more susceptible to hot cracking when compared with steel [10].

Hot cracking depends both on metallurgical, i.e. phase relations and mechanical factors, i.e. stress-strain distributions [11, 12].



Metallurgical factors are mostly related with the segregation of the constituents and presence of liquid phases along the grain boundaries during solidification. In addition, the grain structure during solidification, the solidification temperature range, the weld metal composition etc. are also regarded as the metallurgical factors [4].

Mechanical factors are mostly related with the stress and strain concepts. Amount of restraint applied on the system, design of the joint, size and thickness of the weld, thermal distribution among the sample etc. can be regarded as the critical factors that affect directly the hot cracking behavior of the material. In addition, localized stresses trigger the cracking formation during welding. Combined with the metallurgical factors, mechanical factors can be very critical for hot cracking during welding.

Based on the cracking mechanism hot cracking can be divided into two forms: solidification cracking and liquation cracking.

#### **2.5.1.1 Solidification cracking**

Solidification cracking generally appears in the weld zone and along the centre of the weld [13]. During solidification, liquid film existing between the dendrites separates the grains from one another. Also during solidification, due to shrinkage and thermal contraction, if the metal cannot contract freely stress is induced [6]. Therefore, if a stress (tensile) presents between these grains, they separate from each other easily. In other words solidification cracking occurs intergranularly (i.e. between the grains or along the grain boundary) and reveals a dendritic morphology.

The factors affecting solidification cracking can also be explained in two concepts; metallurgical and mechanical. According to Kou et. al. [14], solidification cracking depends on some metallurgical and mechanical aspects. Metallurgical factors can be given as; presence of low soluble alloying elements, range of solidification temperature, the amount and distribution of liquid, brittleness and ductility of the solidifying structure and surface tension whereas mechanical factors can be exemplified as strain and stress acting on the system.

## Mechanical Factors

During welding and solidification, aluminum is exposed to thermal alterations. During solidification aluminum tends to shrink and upon this shrinkage if the induced stress exceeds the stress of metal that is solidifying, occurrence of cracking is inevitable. Chihoski et. al. [15] has studied the stress zones across the weldment and concluded that if tensile stresses appear on the mushy zone the probability of the cracking increases. From Figure 6 the tensile and compressive stress zones can be seen. The stress abbreviation  $T_1$  shown on the Figure 6 occurs in response to  $C_1$  that is induced as a result of the heating effect of the torch. Zero stress occurs on the weld pool and tension ( $T_s$ ) occurs near the weld pool or over the mushy zone due to shrinkage. Compressive stress represented by  $C_2$  occurs in response to expansion and finally tensile stress  $T_2$  occurs due to shrinkage against fixed weld metal.

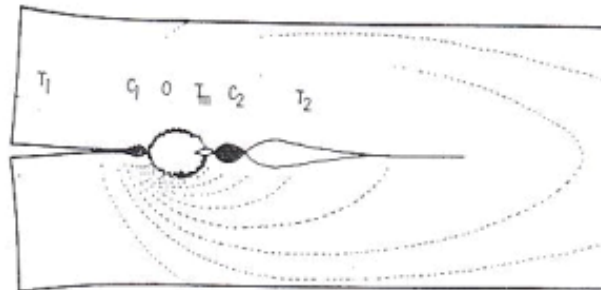


**Figure 6** Tensile and compressive stress zone during welding [15]

Another important mechanical factor that affects solidification cracking is the amount of strain acting on the intergranular liquid film [11]. According to Pellini [16], the intergranular liquid film is a relatively weak region and tears apart under a strain. Figure 7 shows the strain distribution at three different stages during solidification. At the stage where liquid film exists between grains, or along grain

boundaries, the strain acting on the system has more detrimental effect with respect to the stage 1 at which mushy zone exists and stage 3 at which solid phases dominate.

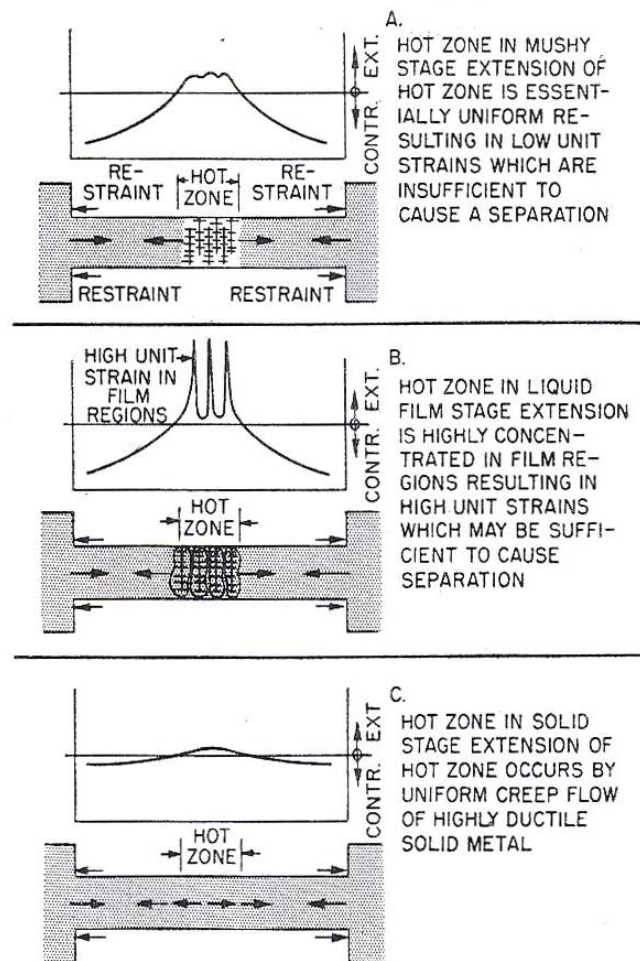


**Figure 7** Effect of liquid film to the strain distribution [16]

Figure 8 shows the dependence of hot cracking on segregates and tensile forces. As the torch passes across the segregate region, liquid film forms between the grains. Melting occurs as a consequence of thermal gradient formed perpendicular to the

weld. At the first stage as shown in the stated figure, compressive forces induce at the HAZ region in response to expansion of the weld metal. However at the following stage, tensile forces induce as a result of contraction and at the final stage as a result of concentrated strain on the crack position, cracking occurs.

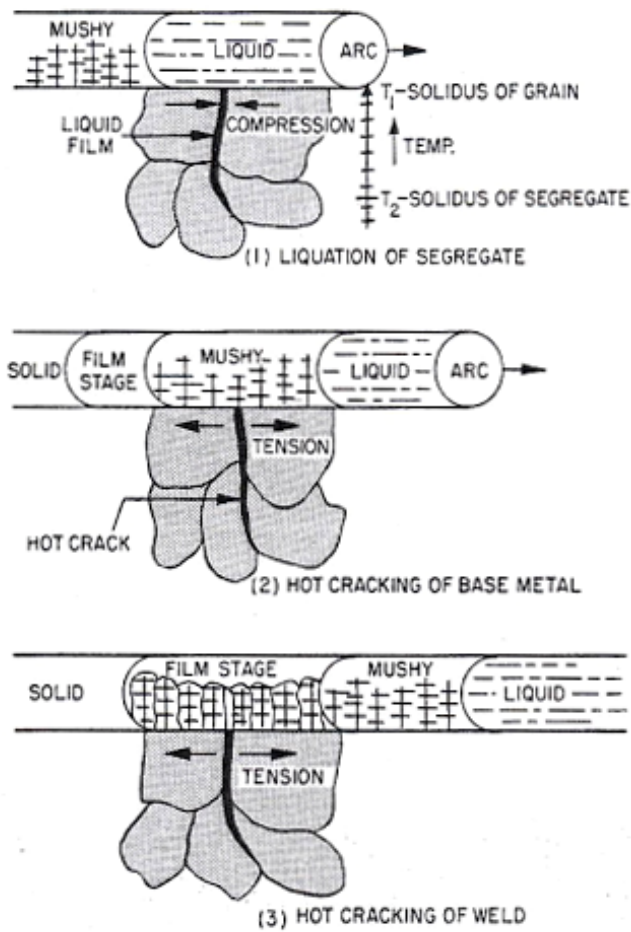


**Figure 8** Stages of hot cracking [16]

## **Metallurgical Factors**

Aluminum alloys having wider solidification range are more prone to solidification cracking. Alloys having wider solidification range possess mushy zone more during solidification which means that they are more open to solidification cracking resulting from solidification shrinkage [17]. This can be further explained by brittleness temperature range (BTR) concept. According to this, during solidification or below liquidus at a certain temperature, crystals nucleate, grow and form a relatively brittle structure. The temperature which crystals show brittle structure is called coherent temperature. However upon further cooling the structure becomes more ductile up to a certain temperature which is called nil-ductility temperature. The temperature range between this coherent and nil ductility temperature is called brittle temperature range. Solidification cracking susceptibility increases by the increase in brittle temperature range [18]. Brittle temperature range depends on the solidification range in so that when solidification range increases brittle temperature range also increases.

Presence of low soluble alloying elements has also an effect in solidification cracking. During solidification due to this low solubility the growing grains push them towards to the centre of the weld. As a final state, these alloying elements form as low melting phases and remain as liquid films exhibiting low strength along the grain boundaries.

The effect of liquid films existing along grain boundaries can be further discussed by the Borland's theory. Borland [19] looks into solidification concept in terms of four stages. Borland states that, in the first stage of solidification, both the phases exist as free with respect to each other. In the following stage the movement of the solid phases is getting restricted whereas the liquid phase is still able to move. This movement enables the cracks to be healed. In the third stage the movement of liquid phase is being restricted by the increased number of solid fraction. This stage defines the critical solidification range at which healing of cracks is relatively hard with respect to the prior stage. At the final stage complete solid phases are observed and cracking due to liquid phase is not seen (Figure 9).

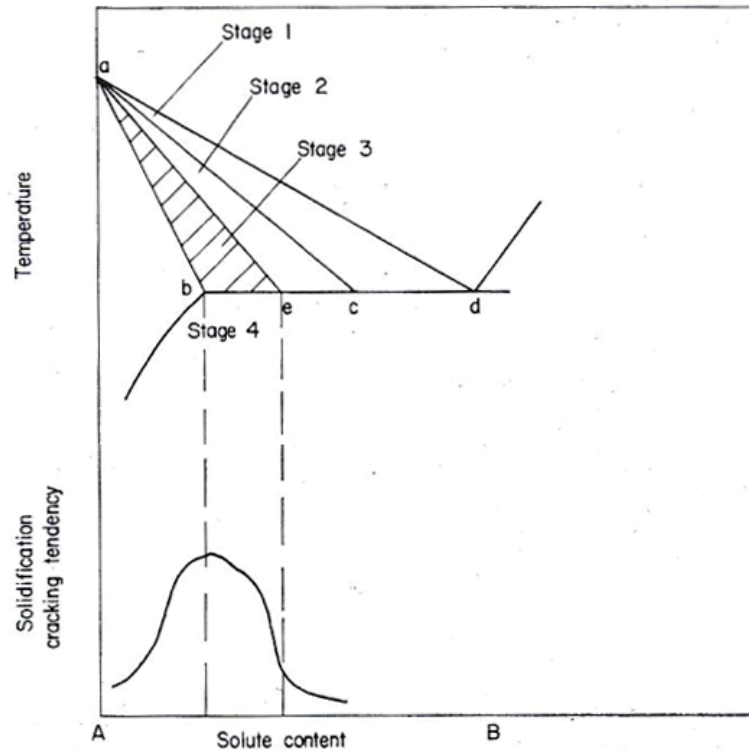


**Figure 9** Hot cracking tendency and solidification stages (Borland's theory) [19]

Another important factor affecting the solidification cracking is the grain size. Aluminum alloys having finer grain size are less susceptible to solidification cracking. Fine grained aluminum has more success in healing and feeding of liquid which reduces the cracking probability. Another useful fact of fine grained morphology is that the grain boundary area is relatively more with respect to coarse grained morphology. Therefore low melting point constituents are less concentrated on the grain boundaries in the case of low grained structure [6, 12]. Matsuda et. al. [20] showed that increasing grain size increases the crack susceptibility (Figure 10). Addition of alloying elements has significant effect in decreasing grain size and accordingly the crack susceptibility

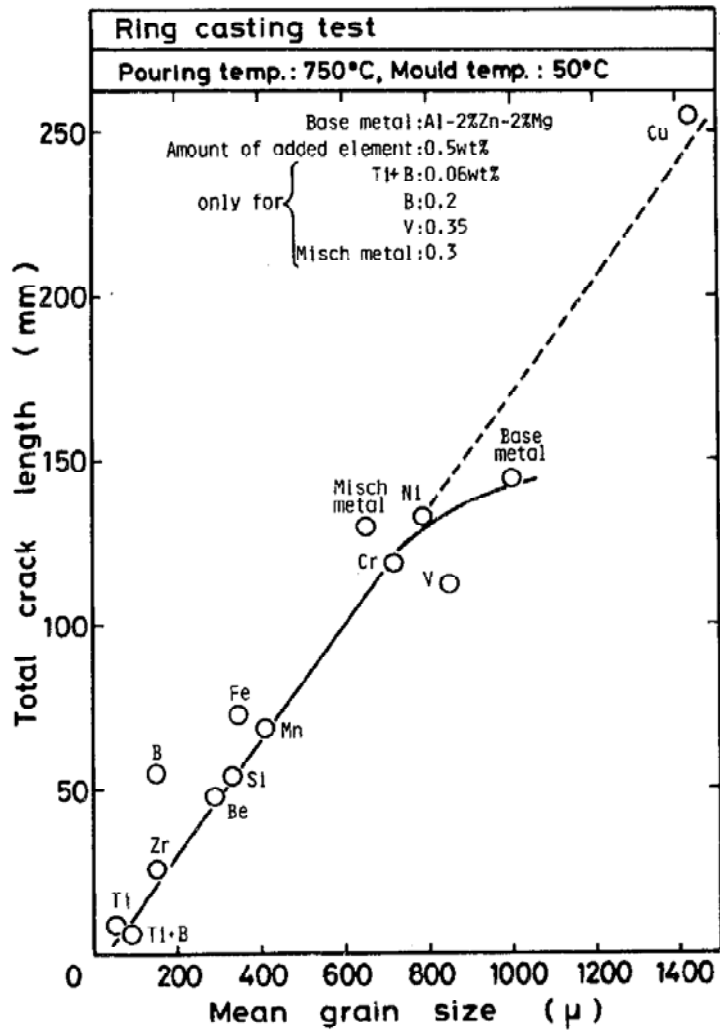


**Figure 10** Relation between total crack length and mean grain size of Al-2%Zn-2%Mg [20]

### 2.5.1.2 Liquefaction cracking

Liquation cracking mainly occurs in the heat affected zone and partially melted zone [13]. It resembles to solidification cracking by being intergranular; however dendritic morphology is not seen for liquation cracking.

As discussed previously, Partially Melted Zone (PMZ) is the zone outside of the fusion line and the temperature of this zone lies between solidus and liquidus temperatures. During welding, the alloy is subjected to heat which raises the temperature of the fusion zone and causes the low melting point constituents to melt along the grain boundaries. Under a sufficient stress or strain these weak regions have high tendency to apart from each other and cracking occurs. Therefore; liquation cracks form along the grain boundaries in the PMZ (Figure 11) [21, 22].

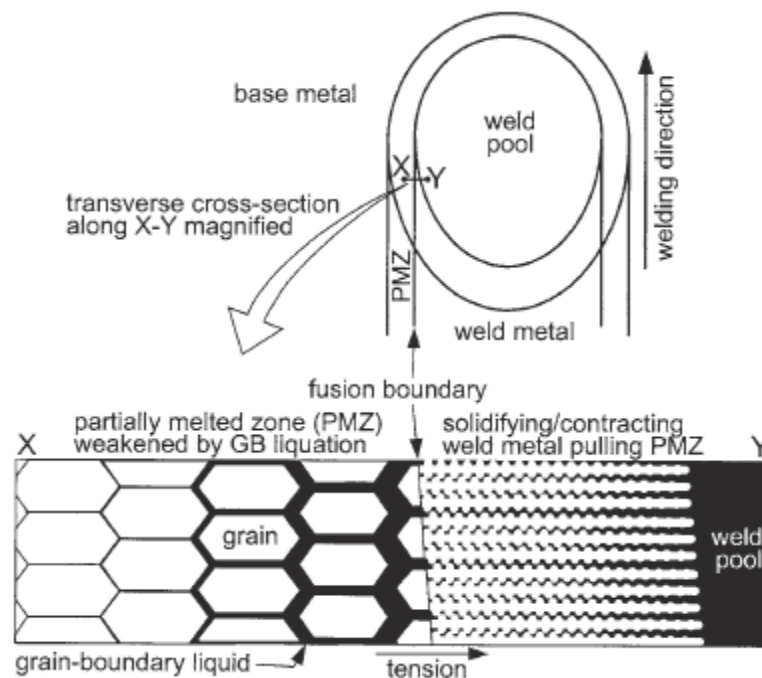


**Figure 11** Liquation cracking mechanism in PMZ [22]

There are several factors that affect liquation cracking in aluminum alloys. Similar to solidification cracking; grain size, strain and stress acting on the system, the range of solidification, welding parameters can affect the occurrence of liquation cracking. As the solidification range increases the PMZ becomes wider and more prone to



cracking under sufficient stress. Also the more the fraction of liquid presenting during solidification is, the wider the PMZ becomes. Decreasing welding speed or in other words increasing heat input [23] directly increases the fraction of liquid presenting during solidification and the size of PMZ (Figure 12).

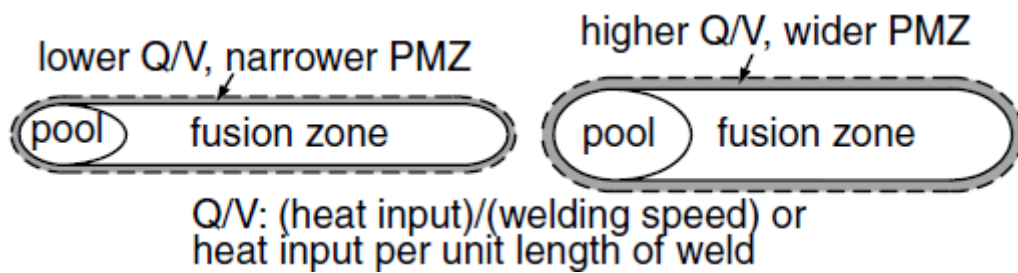


**Figure 12** Effect of heat input on liquation cracking [6]

Similar to solidification cracking, liquation cracking also occurs under a sufficient stress or strain. Therefore if the alloy is welded under restraint, the probability of the liquation cracking increases.

Grain size is another factor for the liquation cracking. As the grain size decreases the grain boundary area accordingly increases. When the alloy has more grain boundary area the ratio of the solute segregates along the grain boundary decreases. Remembering that liquation cracking is the result of the solute segregates along the grain boundary; decreasing grain size improves the liquation crack resistivity (Figure 13).

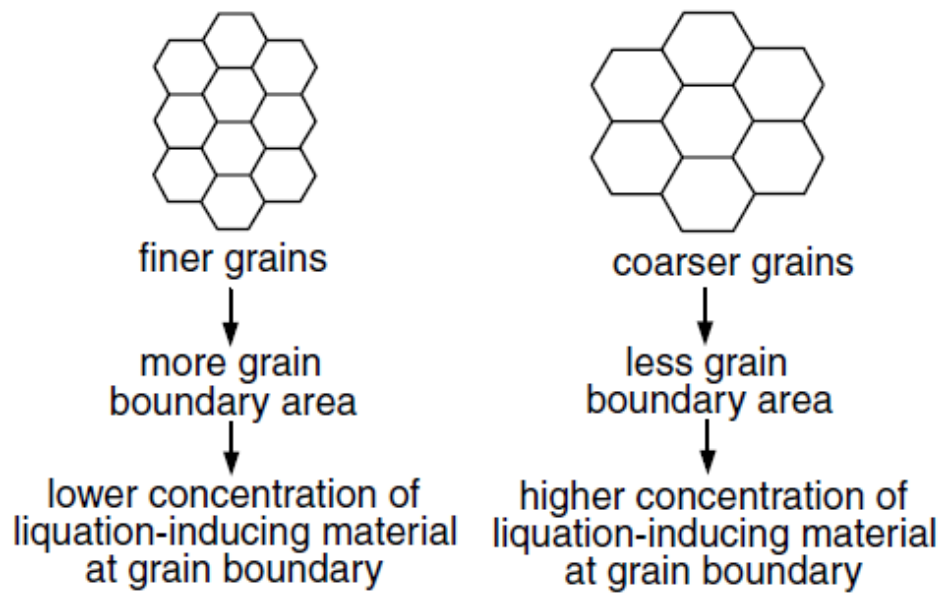


**Figure 13** Effect of grain size on liquation cracking [6]

## 2.6 Methods to Evaluate Hot Cracking

There are several test methods to evaluate the hot cracking susceptibility. For the evaluation methods based upon crack length measurements, the load can be externally or internally applied. Transverse Varestraint Test, Modified Varestraint Test (MVT) can be given as examples of externally loaded weldability tests. For the self restraint tests, most known examples are circular patch test, Houldcroft test, t-fillet test etc. The self restraint tests are not suitable to evaluate the effect of strain on hot cracking susceptibility. Externally loaded tests help us to evaluate both mechanical parameters and welding parameters [24, 25]. In this study, Modified Varestraint Test was used to evaluate the hot cracking behavior of the 7039 aluminum alloy. It enables us to evaluate the crack formation quantitatively in a reproducible way.

### 2.6.1 Modified Varestraint Test

This method is highly practical to evaluate the weldability and also hot cracking susceptibility [26]. In this method, material is bended under a defined stress during welding. As a consequence of bending a local strain occurs on and around the weld pool where liquid, semi-solid, solid phases coexist. When the critical value for cracking is exceeded, solidification and liquation cracking occur which can be easily seen on the surface of the weldment. With this test, effect of welding parameters, effect of filler materials and effect of bending rate in terms of hot cracking can easily be evaluated [27-29]. The test results of the MVT Method can be evaluated in terms of total crack length, maximum crack length and total crack number. The cracks occurred during this test are evaluated and measured by using stereomicroscope and the number and length of these cracks are recorded.

The main advantage of this test is that both the solidification crack at the weld metal and liquation crack at the HAZ and PMZ regions can be evaluated at the same time [30]. A schematic representation for the MVT method is given at Figure 14.

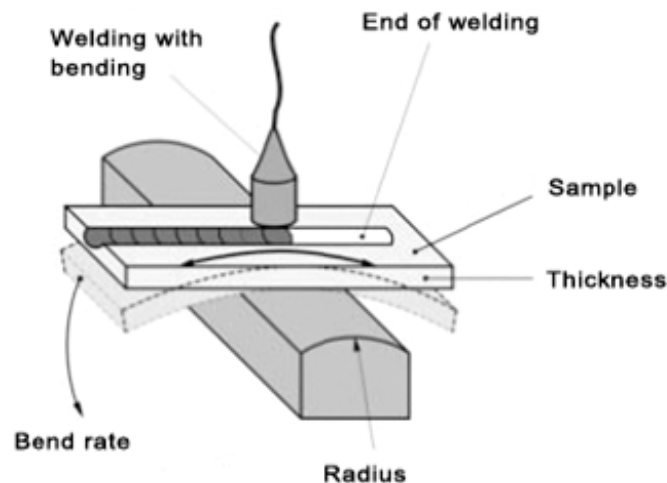


**Figure 14** Modified Varestraint Test [31]

## CHAPTER 3

### LITERATURE REVIEW

#### 3.1 Hot Cracking Formation

According to Hemsworth et. al. [32] hot cracking in non-ferrous alloys occurs as in two major types; cracking due to segregation and ductility-dip cracking. Cracks occurring due to segregation appear either as solidification cracks at weld metal or liquation cracks in HAZ or in PMZ. The main reason of these cracks is the segregates or phases with low melting point along the grain boundaries or in other words the intergranular films.

Cheng, C.M.; Chou, C.P. [10] studied the effects of thermal cycles and strain level on the hot cracking formation of the heat treatable aluminum alloys by using Spot Vareststraint Test. They concluded that number of thermal cycles does not affect the hot cracking in the weld zone but it has an effect on the HAZ region. The appearance of the cracks at the weld metal is different from the cracks in the HAZ region such that smooth pores exist between the grains and partially melting occurs in the HAZ region. SEM analysis of the crack regions shows that liquation cracking in the HAZ occurs as in two forms. Liquation cracking occurs as a result of melting of segregates along the grain boundaries or melting of the grain boundaries itself. Batıgün et. al. has also concluded in his study that hot cracks form along the grain boundaries. Besides, he also showed in his study that the length and number of cracks increase in the HAZ region when relatively large grains form across this region [28].

#### 3.2 Effect of Filler Material and Chemical Composition

Robinson I.B. and Baysinger F.R. [33] studied the effects of filler materials on the welding of 7039 aluminum alloy. They stated that 5183 and 5356 aluminum alloys

are the suitable filler materials for the welding of the 7039 aluminum alloy in the automotive industry. Changing the filler material type affects the cracking tendency of the 7039 aluminum alloy. Gibbs F.E. [34] discussed in his study the effective filler materials that could be used for the welding of 7039 aluminum alloy. Through his study, effect of elements on the mechanical properties of the 7039 aluminum alloy were discussed and he tried to present an optimum filler material composition that would improve the mechanical properties of the 7039 aluminum alloy.

Tirkes S. [24] studied the hot cracking susceptibility of the twin roll cast Al-Mg alloys and found that hot cracking susceptibility is dependent on the Mg amount. With the addition of Mg content, solidification range of the alloys changes and therefore hot cracking susceptibility changes. Similarly, Kim et. al. [35] concluded in his study that alloying elements and especially Mn has an effect on the hot cracking behavior. He stated that adding Mn element decreases the mushy zone size and therefore enhances the hot cracking susceptibility. He also investigated the effects of Cr on the hot cracking susceptibility.

Cicala E. [36] concluded in his study that since the presence of filler material changes the chemical composition, it is expected that addition of filler material also affects the mechanical properties of as-welded product and hot cracking in particular. Matsuda F. [37] approached to the issue from a different aspect. He stated that hot cracking depends on the grain size and if the additional element has an effect on the size of the grain it is natural to expect the effect of additional elements on the hot cracking behavior.

### **3.3 Effect of Strain**

Strain presenting on the welding area is an important factor that affects the hot cracking susceptibility of the alloys. Caymaz F. [38] has studied effects of strain on the hot cracking behavior of the aluminum alloys during welding by using MVT method. Hot cracking occurs as a consequence of strain acting on the system that exceeds the strength of the solidified weld metal. Hot cracking susceptibility of the alloys is evaluated by measuring the total crack length, maximum crack length and

total crack number. As the strain rate increases the total crack length, maximum crack length and total crack number increase that means amount of strain has a pronounced effect on hot cracking tendency.

Cheng, C.M.; Chou, C.P. [10] found the similar effect of strain on the hot cracking that hot cracking susceptibility increases with the increasing strain in the weld zone and HAZ region.

### **3.4 Effect of Welding Speed**

Brungraber R.J. and Nelson F.G. [39] studied the effect of weld parameters on the strength of HAZ and penetration depth and showed that they are directly related with the following formula " $EI/Vt$ " where E: potential difference (v) I: current (amp), V: traveling speed (ipm), t: plate thickness (inch). The amount of the penetration is directly related with the given function which gives a measure for the heat input.

Liptak J.A. [40] investigated the effect of welding parameters on the depth of penetration. Penetration amount is directly related with the welding parameters such as, current, voltage, welding speed, tungsten electrode shape etc. Accordingly, he stated that penetration amount increases when the welding current increases and the travelling speed decreases. In another study of Liptak J.A. [41], effect of welding parameters (i.e. welding speed, welding current) on the lack of fusion during the welding of 7039 aluminum alloy was covered. Faster welding speeds have decreasing effect on the amount of the liquid metal around the weld pool and decreases the possibility of lack of fusion defect.

Regarding the effects of welding speed on the hot cracking behavior of the alloys, several different ideas were put forward by different authors. Studies in the literature focusing at the effects of welding speed on hot cracking were compiled in the study of Coniglio et. al. [42]. He figured out that different studies have different approaches in explaining the effects of welding speed on hot cracking behavior. Some studies in the literature stated that increase in welding speed has a positive effect in weldability; in other words when the welding speed increases hot cracking decreases. On the other hand several studies assert the contrary. For example; Cicala

E. [36] focused on the hot cracking behavior in Al-Mg-Si alloy laser welding and stated that welding speed is the one of the most effective factor on avoiding hot cracking. In his study, he found that welding speed has a direct effect on mechanical properties of the laser welded Al-Mg-Si alloy and concluded that lower welding speeds engendered less crack formation. Similarly, Shibahara M. [43] correlated welding speed with hot cracking in his study carried out with Houldcroft Test and concluded that with lower welding speeds, shorter hot cracks are obtained. On the contrary, Chihoski R.A. [15] emphasizes that increasing welding speed results in the improvement of weldability and thereby hot cracking susceptibility. He explains this with the occurrence of stress fields during welding. With increasing welding speed compressive stresses form in the mushy zone that has repressive effect in the hot cracking formation.

Johnson L. [44] showed the effect of strain patterns during welding and stated that during welding high strains occur parallel and perpendicular to the direction of welding. In addition, effect of welding parameters on the strain patterns was also discussed in the mentioned study. Changing welding parameters resulted in different strain patterns such that in higher welding speeds, higher strains may occur as a result of higher thermal gradients.

In another study of Chihoski R.A. [45], the situation is clearly explained. He indicated that a fixed ideal welding speed cannot be assigned for different aluminum alloys. Every aluminum alloy has its optimum welding speed that possesses minimum hot cracking for certain conditions.

To summarize, so many studies tried to explain the effects of welding speed on the hot cracking behavior of different materials and these studies revealed that different mechanisms are determinant in the formation of hot cracks.

## CHAPTER 4

### EXPERIMENTAL PROCEDURE

In this study, effects of welding on the hot cracking behavior of 7039 aluminum alloy were evaluated by using Modified Vareststraint Test (MVT) method. Different welding speeds and filler materials were applied in order to understand the effects of welding on the hot cracking.

The experiments were carried out at the METU Welding Technology and Non-Destructive Testing Research / Application Center of the Middle East Technical University (METU).

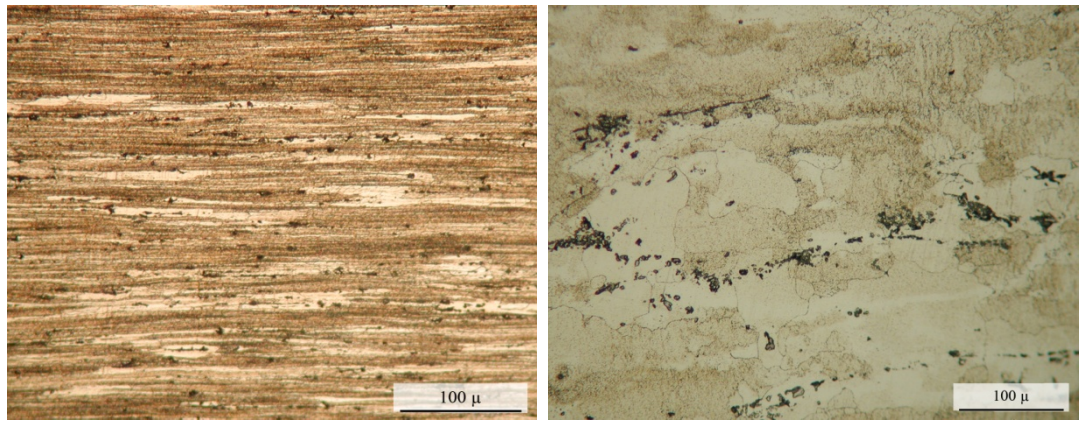
#### 4.1 Material

The material, 7039 aluminum alloy, is produced by Alcoa Inc. and obtained from FNSS Savunma Sistemleri A.Ş in the form of hot rolled plates. 7039 aluminum alloy is widely used in the construction of armor plates, missile parts, pressure vessels, storage tanks etc.

The plates were previously hot rolled and then heat treated in the T61 condition. During heat treatment they were first solution treated and afterwards aged artificially.

The micrographs of the obtained plates that were taken in longitudinal and transverse rolling direction can be seen in Figure 15. Figure 16 shows the micrograph of the alloy as unetched. The precipitates can easily be seen.





(a)

(b)

**Figure 15** The microstructure of the obtained 7039 aluminum alloy plate (a) parallel to the rolling direction (b) perpendicular to the rolling direction. Keller Etching.

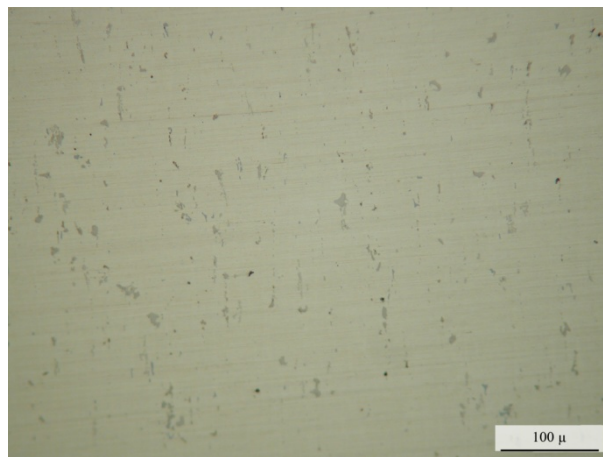


**Figure 16** The microstructure of the obtained 7039 aluminum alloy plate before etching

The chemical composition of the obtained 7039 aluminum alloy plate is given in the Table 1. Chemical composition is found by applying chemical analysis by Spectrometer located at the Metallurgical and Materials Engineering Department at Middle East Technical University.

**Table 1** Chemical composition of the 7039 aluminum alloy

Material	Elements								
	Cu	Si	Mn	Mg	Zn	Fe	Cr	Ti	Al
7039	0,0763	0,122	0,303	2,41	4,55	0,374	0,161	0,06	bal.

The tensile test results of the obtained 7039 aluminum alloy in accordance with EN 895 are given in the Table 2.

**Table 2** Tensile test results of the obtained 7039 aluminum alloy

	Transverse rolling direction	Longitudinal rolling direction
Tensile strength (MPa)	436	441
0.2% tensile yield strength (MPa)	392	399
Elongation %	10,21% (L <sub>0</sub> : 137 mm)	11,03% (L <sub>0</sub> : 136 mm)

In order to evaluate the effect of filler materials, 5183 and 5356 aluminum alloys were used as filler materials. The filler materials are obtained in the form of wires. The nominal composition of these filler materials that is received from the producer are given in Table 3.

**Table 3** The composition of the filler materials [46]

Material	Elements								
	Cu	Si	Mn	Mg	Zn	Fe	Cr	Ti	Al
5183	<0,05	<0,25	0,6- 1,0	4,3- 5,2	<0,0068	<0,4	0,1- 0,3	0,07- 0,15	bal.
5356	<0,05	<0,25	0,1- 0,2	4,5- 5,6	<0,0050	<0,4	0,1- 0,3	0,07- 0,15	bal.

## 4.2 Experimental Setup

### 4.2.1 MVT Equipment

The hot cracking behavior of the materials was tested by using Modified V restraint Test (MVT) method. MVT system is manufactured by “Rehm Schweisstechnik” and consists of three main bodies. The power is supplied to Welding and Bending Unit by Power Source (Figure 17); the system is controlled by Electronic Control Unit (Figure 18) and the tests are carried out by the Welding and Bending Unit (Figure 19).

MVT Equipment consists of an automatic torch controlled by the Electronic Control Unit. Adjustment of the torch and welding parameters with the help of control units ensured the reproducibility of the tests.

The bending unit of the MVT system consists of two upper and one lower dies. The applied strain during MVT method can be altered by changing the radius of the dies. During the tests, lower die with 250 mm radius was selected which corresponds to 2% strain value for the 10 mm thick samples. The amount of strain is calculated as shown in the Figure 20.



**Figure 17** Power Source of the MVT Equipment



**Figure 18** Electronic Control Unit of the MVT Equipment



**Figure 19** Welding and Bending Unit of the MVT Equipment

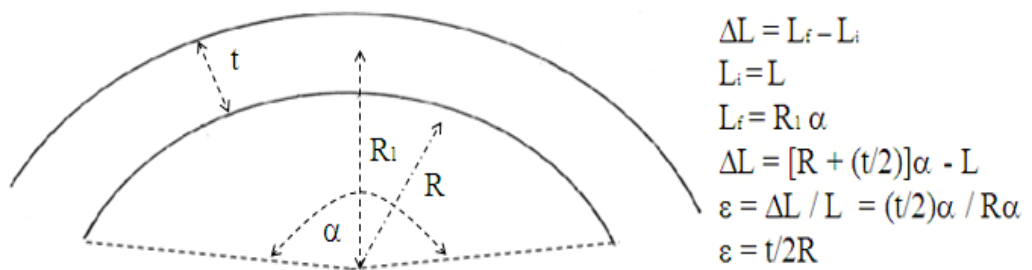


**Figure 20** Calculation of the strain developed during MVT method [38]

The parameters and conditions for welding can be found in Table 4.

**Table 4** Welding parameters and conditions

<b>Test Type</b>	<b>Varestraint Test Method</b>
Welding Type	Gas Tungsten Arc Welding
Power Source	Rehm Invertig 250 GV
Polarity	Alternating Current (AC)
Applied Strain	2%
Shielding Gas	Argon
Gas Flow Rate	10 lt/min
Welding Speed	50-55-60-65-70 mm/min
Welding Current	120 A
Electrode Type	Pure Tungsten Electrode
Electrode Diameter	2.4 mm
Electrode Tip Angle	90°
Distance from Electrode Tip to Weldment	2 mm
Distance from Nozzle Tip to Weldment	4 mm

When the power is off, the position of the electrode inside the torch should be adjusted. In order to adjust the position of the electrode inside the torch, the torch is first pushed from the above against a rubber calibration surface and the electrode gets its position.

Before starting welding, it should be checked that the gas and the cooling water are turned on.

#### 4.2.2 Specimen Preparations for MVT and Test Procedure

The samples are provided as in hot rolled form and shaped into the form with dimensions as follows; 100x40x10 mm (Figure 21).

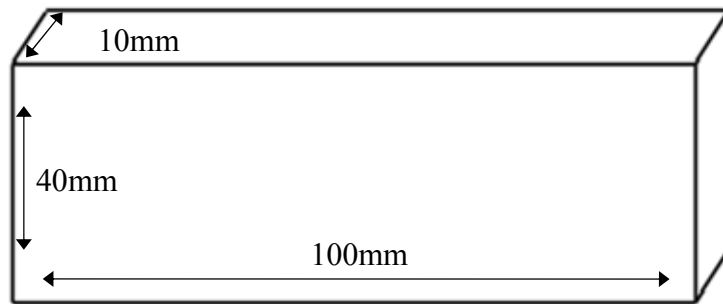


**Figure 21** Scheme for the samples

Prior to each test the two surfaces of the material and the tip of the electrode were ground by brush and emery papers in order to remove the oxide layer and ease the flow of the arc. The samples were ground in longitudinal direction in order to differentiate them from the cracks. Following, alcohol was applied to the surfaces in order to remove the unwanted particles from the surface.

The samples were grouped as shown in Table 5.

**Table 5** The grouping of the samples

Set #	Sample Number	Sample Material	Filler Material Used	Welding Speed	Drop Current
Set 1 7039	1	Al-Zn 7039	No filler material is used.	50 mm /min	120 A
	2	Al-Zn 7039	No filler material is used.	55 mm /min	120 A
	3	Al-Zn 7039	No filler material is used.	60 mm /min	120 A
	4	Al-Zn 7039	No filler material is used.	65 mm /min	120 A
	5	Al-Zn 7039	No filler material is used.	70 mm /min	120 A
Set 2 7039- 5183	6	Al-Zn 7039	Al-Mg 5183	50 mm /min	120 A
	7	Al-Zn 7039	Al-Mg 5183	55 mm /min	120 A
	8	Al-Zn 7039	Al-Mg 5183	60 mm /min	120 A
	9	Al-Zn 7039	Al-Mg 5183	65 mm /min	120 A
	10	Al-Zn 7039	Al-Mg 5183	70 mm /min	120 A
Set 3 7039- 5356	11	Al-Zn 7039	Al-Mg 5356	50 mm /min	120 A
	12	Al-Zn 7039	Al-Mg 5356	55 mm /min	120 A
	13	Al-Zn 7039	Al-Mg 5356	60 mm /min	120 A
	14	Al-Zn 7039	Al-Mg 5356	65 mm /min	120 A
	15	Al-Zn 7039	Al-Mg 5356	70 mm /min	120 A

As shown in the Table 5, welding current value was selected as 120 A and tests were carried out with welding speed ranging from 50 to 70 mm/min. In order find an optimum current and welding speed several parameter optimization studies were carried out prior to welding tests. With 120 A current, welding speed values below 50 mm/min caused excessive heat concentrated on the region which resulted in melting of the sample (Figure 22). On the other side, when welding speeds above 70 mm/min are used, insufficient penetration is obtained.





**Figure 22** Excessive heat caused melting of the specimen

In order to ensure sufficient mixing of the filler materials with weld metal, filler materials first placed into a nut shaped on the surface of the samples and they were melted manually and then ground prior to MVT test. The specimen preparation can be schematized as shown in the Figure 23.

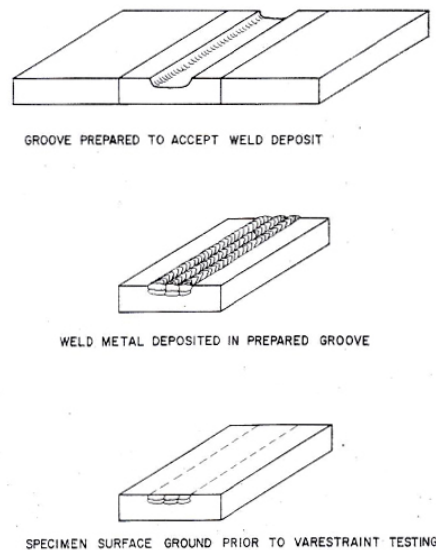


**Figure 23** Specimen preparation method used in the study of Savage and Lundin [27]

However this method, can be named as “one step welding”, resulted in insufficient mixing of the filler materials and parent metal; such that unmelted regions were observed on the cross section of the samples (Figure 24). Therefore the method was altered such that; instead of placing the filler material into a cavity, they were fed manually during manual welding prior to MVT test. This method, “two steps welding” ensured enough fusion and mixing of filler materials and parent metal.



**Figure 24** Unmelted part observed on the cross section of the sample

#### **4.2.3 Chemical Analysis**

The aim of performing chemical analysis was to obtain the chemical composition of the weld seams produced by MVT method and correlate them with hot cracking if possible. The chemical analyses were applied on the weld seam of the three sets of samples produced by MVT method with 50, 60, 70 mm/min welding speeds and 120 A drop current. Special attention was given that the area at which the analyses were taken lie in between the boundaries of the weld seam. Although there is a diffusion reality between the weld metal and parent metal, the chemical composition of the weld seam (or weld metal) was expected to be different from the chemical composition of the parent metal. In a study of Batıgün et. al. [46] this was exemplified with the loss in magnesium content in the weld metal. As a result of the heat generated during welding, some magnesium amount can evaporate from the

weld metal. For this reason chemical analyses were directly taken from the weld seam of the alloy sets.

The chemical analyses were performed by Spectrometer located at the Metallurgical and Materials Engineering Department at Middle East Technical University.

#### 4.2.4 Crack Length Measurements

After accomplishing the welding tests, the weldments were taken to the laboratory in order to carry out the crack length measurements. Two steps etching were used in order to observe surface morphology and to determine the number and the length of the cracks. The welding surfaces of the samples were first etched with modified Adler solution. Etching was carried out until the oxide layer is removed. After applying modified Adler solution, the samples were rinsed and then dipped into Lukewarm solution to have a clean surface prior to crack length observations. The composition of the reagents can be found in the Table 6.

**Table 6** Composition of the reagents

Reagent	Amount	
Adler	25 ml	Distilled water
	50 ml	HCl (Hydrochloric acid)
	15 gr	[FeCl <sub>3</sub> .6H <sub>2</sub> O] (Ferric chloride)
	3 gr	[(NH <sub>4</sub> ) <sub>2</sub> (CuCl <sub>4</sub> ).2H <sub>2</sub> O] (Ammonium chlorocuprate)
Modified Adler	100 ml	Adler solution
	1 gr	[K <sub>2</sub> S <sub>2</sub> O <sub>5</sub> ] (Potassium metabisulphite)
	70 ml	Distilled water
Lukewarm	50 ml	Distilled water
	50 ml	HNO <sub>3</sub> (Nitric acid)

After rinsing, crack length measurements were carried out by using Nikon SMZ-2T stereomicroscope at 25X magnification. Prior to measurements the microscope was calibrated. The hot cracking behavior of the samples was evaluated by measuring the length of each crack using the stereomicroscope ruler and then summing up the total number and length of the cracks. Special attention should be given to the location of the cracks, such that the cracks that were located in the welding zone, PMZ and HAZ region were taken into consideration. A scheme for measuring the cracks and method for representation of the measurements were given in Figure 25.

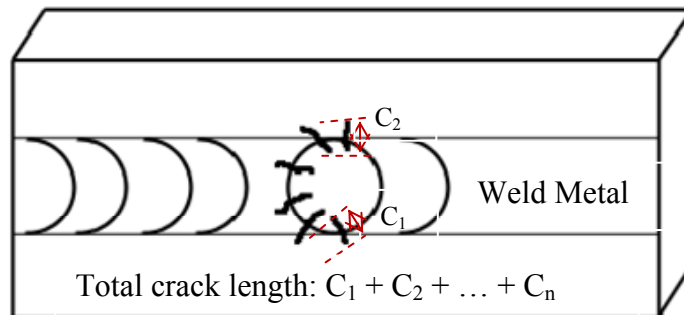


**Figure 25** Method to measure crack lengths

#### 4.2.5 Metallographic Examinations

Macrostructure and microstructure examinations were carried out after crack length measurements. The samples were cut and shaped into desired form to perform these examinations. The location where the macro and micro examinations were done is shown at the Figure 26.

The side surface where the microstructure (Keller etching) and macrostructure (Flick etching) photos were taken

The top surface where the microstructure photos were taken (Weck etching)

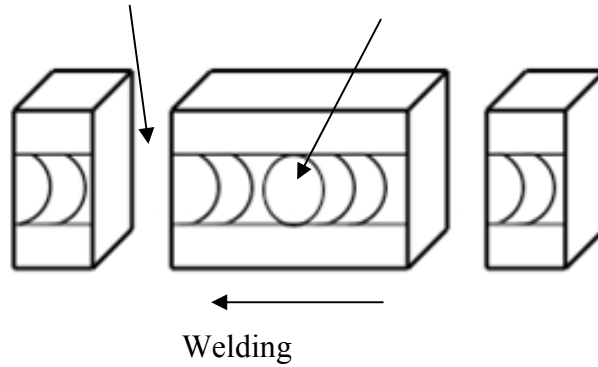


**Figure 26** Location where the macro and microexaminations were done

The reagents used to reveal the micro and macrostructure of the samples were shown in the Table 7.

**Table 7** Reagents used for macro and microexaminations

	Reagent	Amount	
Macrostructure	Flick	90 ml	H <sub>2</sub> O
		15 ml	HCl (Hydrochloric acid)
		10 ml	HF (Hydrogen fluoride)
Microstructure	Keller	190 ml	H <sub>2</sub> O
		3 gr	HCl (Hydrochloric acid)
		5 gr	NH <sub>3</sub> (Ammonia)
		1 gr	HF (Hydrogen fluoride)
	Weck	4 gr	KMnO <sub>4</sub> (Potassium Permanganate)
		1 gr	NaOH (Sodium Hydroxide)
		100 ml	Slightly warmed distilled water

#### **4.2.5.1 Macrostructure Examinations**

Macrostructure photos of the samples were taken to observe the penetration during the welding. The surface of the samples were ground with 800 grit emery paper and then polished with 6 and 1  $\mu\text{m}$  grain sized diamond powder. Then, they were etched by Flick reagent in order to reveal the microstructure of the weld area. The photos of the etched surfaces are taken by scanners.

#### **4.2.5.2 Microstructure Examinations**

Microstructure examinations were carried out to observe the general cracking behavior of the samples. Microstructure examinations were done both on the top surface of the material and on the side surface of the material. The tests were carried out by Nikon OPTIPHOT Microscope and 50x, 100x, 200x, 400x, 600X magnifications were applied. Since the side surfaces of the materials were previously ground to observe the macrostructure, only polishing with 6  $\mu\text{m}$  grain sized diamond powder was done. However, to reveal the microstructure Keller reagent was applied to the side surfaces. The top surfaces of the samples were ground and polished similarly and etched this time by Weck reagent. Between all the tests, the samples were rinsed by alcohol in order to remove the surface contaminants.

In between the microstructure examinations crack tip radius measurements were carried out for the whole sets and a crack tip radius range for the whole sets were established.

#### **4.2.6 Differential Thermal Analysis (DTA)**

Differential Thermal Analyses were performed with Setaram Setsys TG/DTA test machine at Thermal Analysis Laboratory of METU Central Laboratory. Considering the effect of solidification range on the hot cracking susceptibility of the alloys, DTA was made in order to observe and compare the solidification range of the 7039, 7039-5183 and 7039-5356 alloys. In order to produce samples for DTA, two steps welding were performed and 60 mm/min welding speed and 120 A drop current were applied during the MVT test. Then one sample from the welding region of each set (7039,

7039-5183 and 7039-5356) were taken. Samples were heated with a 10°C/min heating rate above their liquidus temperature (700°C). The graphs were recorded as a function of heat flow and temperature and endothermic and exothermic peaks were plotted.

#### **4.2.7 Hardness Test**

Hardness measurements were performed by Vickers Hardness Test at 5 kg of load (HV5) at METU Welding Technology and Non-Destructive Testing Research / Application Center.

The measurements were taken from the 7039, 7039-5183 and 7039-5356 aluminum alloys that were welded with 50 mm/min welding speed and 120 A drop current. Special attention was given to perform the measurements at the same time interval in order to avoid the effect of natural aging.

#### **4.2.8 Fatigue Test**

In addition to hardness test, fatigue tests were carried out on three point bending specimens by using MTS machine at Department of Metallurgical and Materials Engineering at METU. Considering the dimensions and form of the MVT samples three point bending test was selected as the fatigue test method.

The aim of the fatigue tests was to observe the growth properties of the hot cracks that were formed during MVT method, under cyclic load. In particular, the growth properties of the hot cracks in the weld metal and heat affected zone were intended to be studied. Especially, crack growth in the weld metal which is directly affected from the addition of filler materials was also investigated.

Fatigue samples were produced by MVT method with 60 mm/min welding speed and 120 A drop current. The tests were performed under a sinusoidal 900 kg load (min and max load range: 0-950 kg) and 7 Hz frequency.

#### 4.2.9 SEM Examinations

SEM examinations were accomplished at SEM Laboratory of Department of Metallurgical and Materials Engineering at METU.

Prior to SEM examinations, 7039, 7039-5183 and 7039-5356 samples were prepared by MVT method with 60 mm/min welding speed and 120 A drop current. Then they were fractured from the bending region into two pieces; so that the fracture region shall reveal the inside of hot cracks (Figure 27). The fracture surfaces were taken to SEM and hot cracks were elaborately investigated.

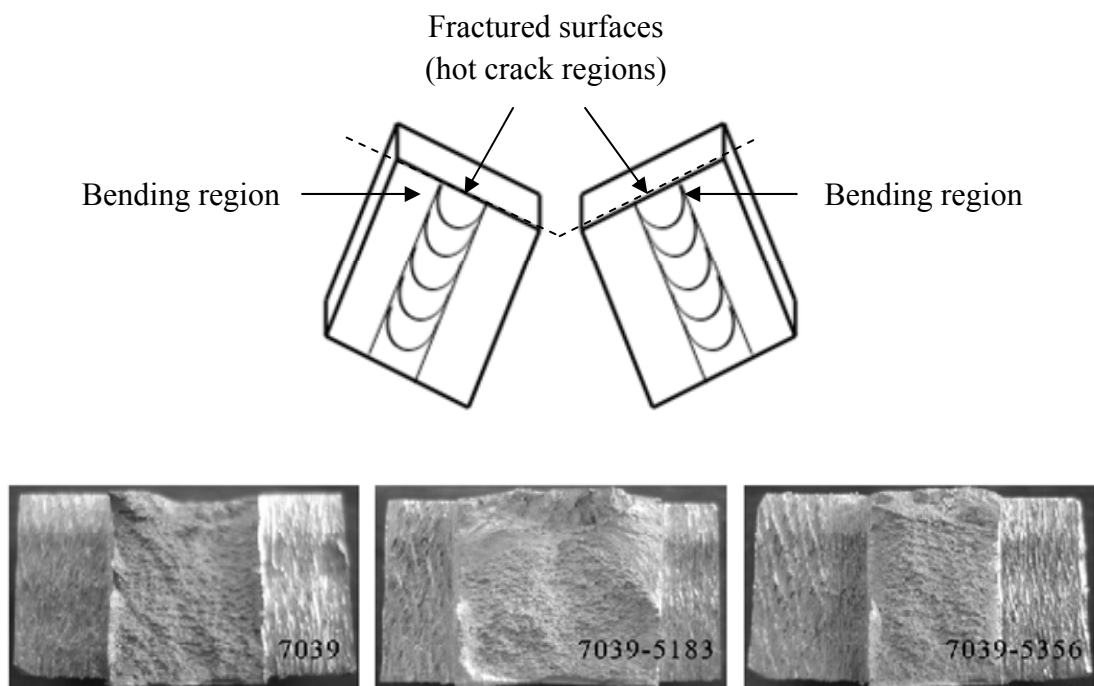


**Figure 27** Fractured surfaces taken to SEM examinations



As the samples were fractured from the bending region in which hot cracks presented, the fractured surface directly exposed the deep inside of the hot cracking regions. In between the SEM examinations EDX analyses were mainly performed on the grain junctions. The aim to perform EDX analyses was to come upon any possible precipitate located at these regions.

In addition to that, the fatigued samples were taken into SEM Laboratory. The fracture surfaces formed as a result of fatigue test were investigated under SEM.

## CHAPTER 5

### RESULTS

The aim of the study is to understand the effects of welding process on the hot cracking behavior of the 7039 aluminum alloy. The hot cracking tests were run with Modified Vareststraint Test (MVT) method and the following results were obtained:

#### 5.1 Results Related with the Test Methodology

7039-5183 and 7039-5356 sets were welded by two step welding and 7039 sets were welded only by MVT method. This resulted in better penetration in the weld metal and ensured enough mixing of filler materials and parent metal. Since two steps welding provided two passes during welding, deeper penetration is obtained for the filler material sets. The difference between the sets can be seen in the Figure 39.

#### 5.2 Results of the Chemical Analysis

Chemical composition of the weld seams of the samples produced by MVT method is shown in Table 8.

**Table 8** The composition of the weld seams produced by MVT method

Sample	Elements								
	Cu	Si	Mn	Mg	Zn	Fe	Cr	Ti	Al
7039	0,09	0,099	0,284	2,45	4,42	0,211	0,172	0,07	bal.
7039-5183	0,0587	0,0929	0,4067	3,1367	3,1067	0,2543	0,1417	0,0733	bal.
7039-5356	0,0563	0,0886	0,2257	3,3333	2,9533	0,2753	0,1527	0,0749	bal.

In related with the chemical composition of the weld seams several different phases may appear for the 7039 aluminum alloy. For the 7039 aluminum alloy it is probable to see  $Mg_3Zn_3Al_2$  and  $MgZn_2$  with the compositions given above. In the presence of silicon (Si) it is highly probable to see  $Mg_2Si$ . According to the literature it is also probable to observe  $(FeCr)Al_7$  phase. For the 7039-5183 aluminum alloy,  $Mg_3Zn_3Al_2$ ,  $Mg_2Si$  and for the 7039-5356 alloy  $Mg_5Al_8$ , are expected to be seen. [47]

### **5.3 Hot cracking Susceptibility of 7039 Aluminum Alloy**

Hot cracking susceptibilities of the specimens were assessed by using MVT method. Three sets of specimens were prepared and these sets were welded by applying five different welding speeds. In order to understand the effect of filler materials on hot cracking two sets were welded with the addition filler materials (5183 and 5356 aluminum alloys) and one set was welded without using any filler material. All the tests showed that 7039 aluminum alloy is susceptible to hot cracking under applied strain. Analyses with stereomicroscope have shown the presence of two types of hot cracking depending on the location. In the weld metal there were solidification cracks, whereas in the HAZ and PMZ regions liquation cracks were observed. In addition to these, some cracks lay both in the HAZ and weld metal (Figure 28).

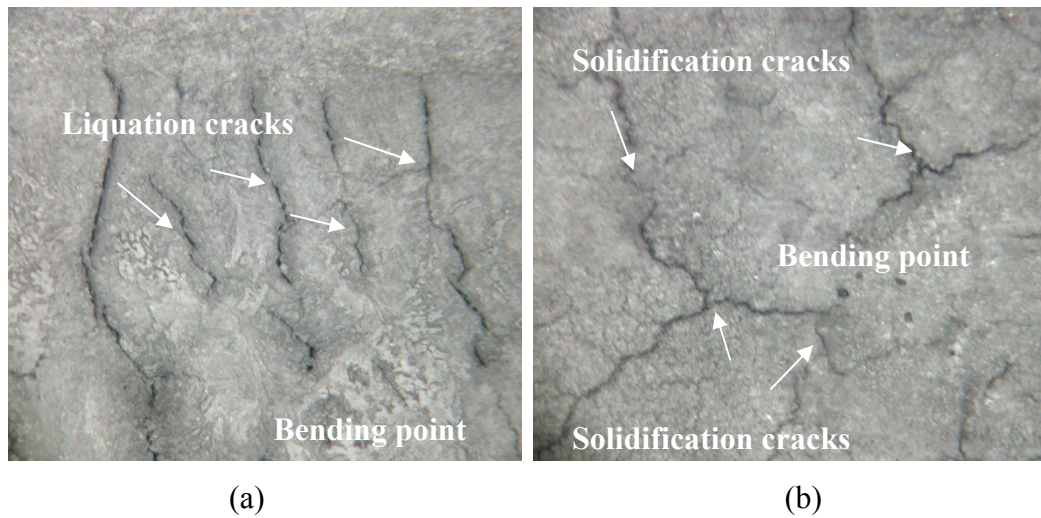


**Figure 28** a) Liquation cracks formed in the HAZ region of 7039-5183 set (welding speed: 65 mm/min) b) Solidification cracks formed in the weld part of 7039-5183 set (welding speed: 55 mm/min)

In addition to the solidification and liquation cracks, centerline cracks were observed far away from the bending point on the surface of the weldments (Figure 29). The main reason of the formation of these types of cracks is the low melting point segregates concentrated on the centerline of the samples.

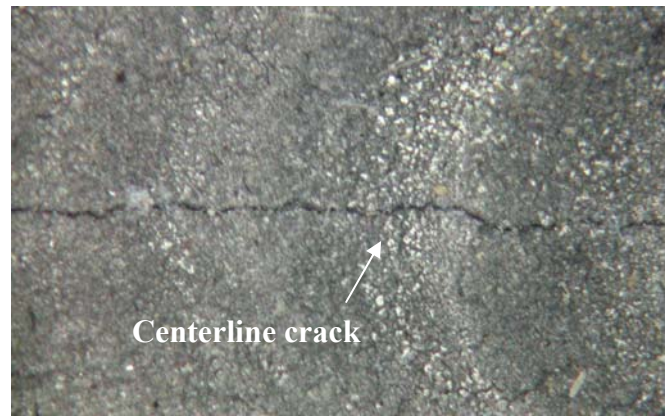


**Figure 29** Centerline crack observed during welding of 7039 aluminum alloy (welding speed: 60 mm/min)

#### 5.4 Results of the Crack Length Measurements

The hot cracks of the sets were compared in terms of total crack length, total crack number, maximum crack length and average crack length. Also, the total crack length of solidification and liquation cracks were also compared by varying the welding speed. Figure 30 shows the effect of using filler materials during welding on the hot cracking susceptibility. 7039 aluminum alloy is found to be less susceptible to hot cracking when filler materials are used during welding. When we compared the hot cracking susceptibilities of the aluminum alloys that were welded with the 5183 and 5356 filler materials, it was found that aluminum alloys welded with 5183 are more prone to hot cracking as compared to the aluminum alloys welded by using 5356 aluminum alloy filler material. As can be seen from the Figures 30-32 total number of cracks occurred after MVT method are less for the 7039-5356 aluminum alloy when compared to the other sets. Similarly, total length of the cracks and maximum crack length observed for the 7039-5356 aluminum alloy are less with respect to other sets. The length and number of the cracks for the whole sets can be seen at the Appendix Tables B1 to B3.

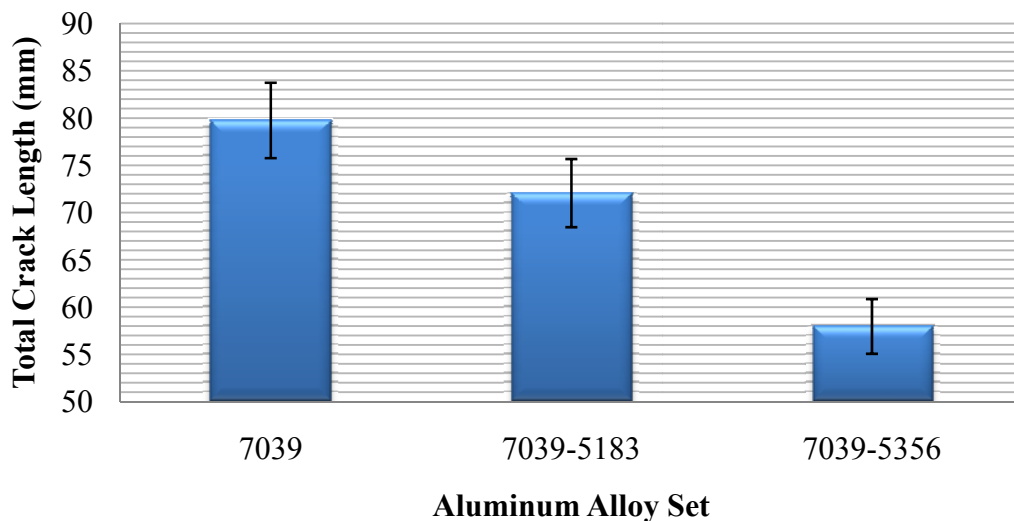


**Figure 30** Total crack length measured for the three different aluminum alloy sets

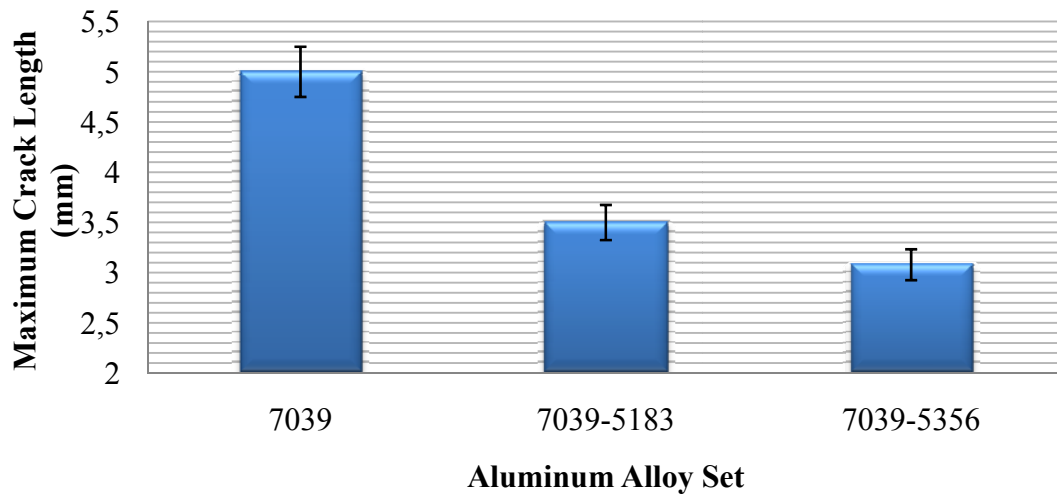


**Figure 31** Maximum crack length measured for the three different aluminum alloy sets

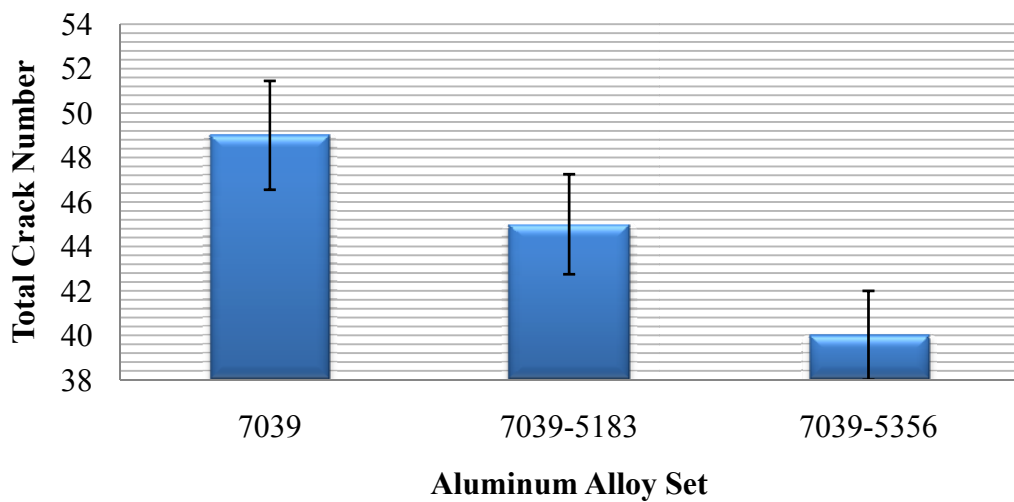


**Figure 32** Number of total cracks counted for the three different aluminum alloy sets

In addition, the average crack length calculated for the three aluminum alloy sets is compared at the Figure 33.

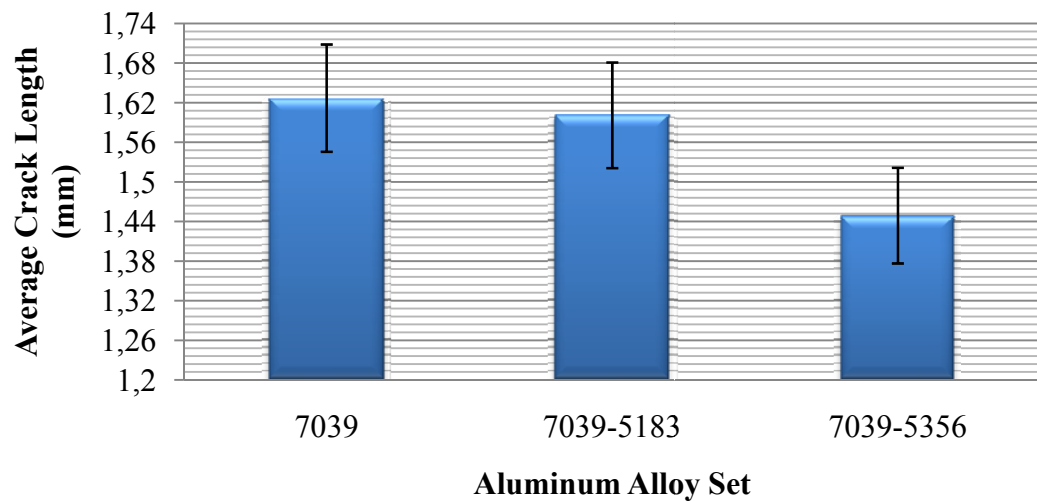


**Figure 33** Average crack length calculated for the three different aluminum alloy sets

Figures 34-36 show the effect of welding speed on the total crack length, maximum crack length and total crack number for the whole sets. For the whole sets when the welding speed increases, a decreasing trend in the total crack length, maximum crack length and total crack number is observed. However for the whole sets, the graphs reach a down peak for definite a welding speed.

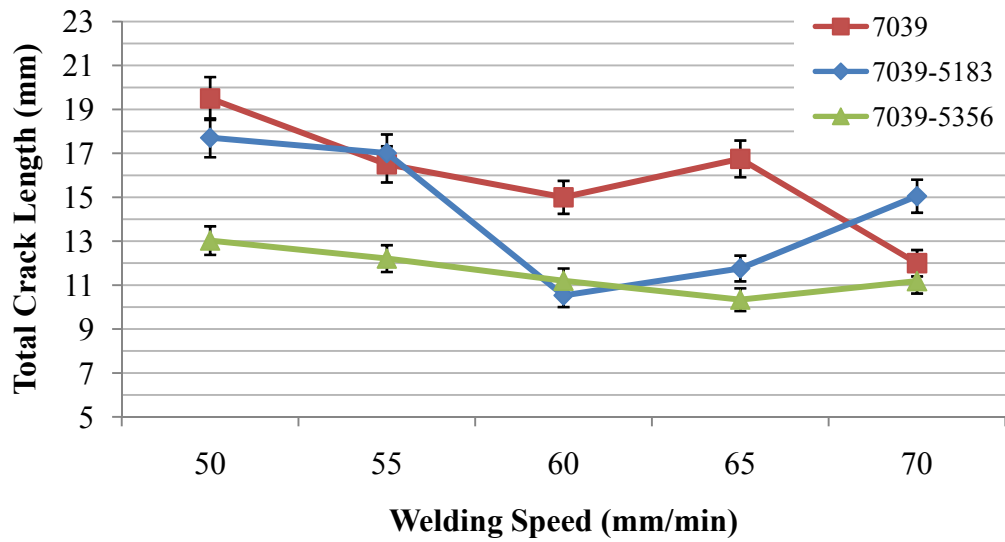


**Figure 34** Effect of welding speed on the total crack length for the whole sets

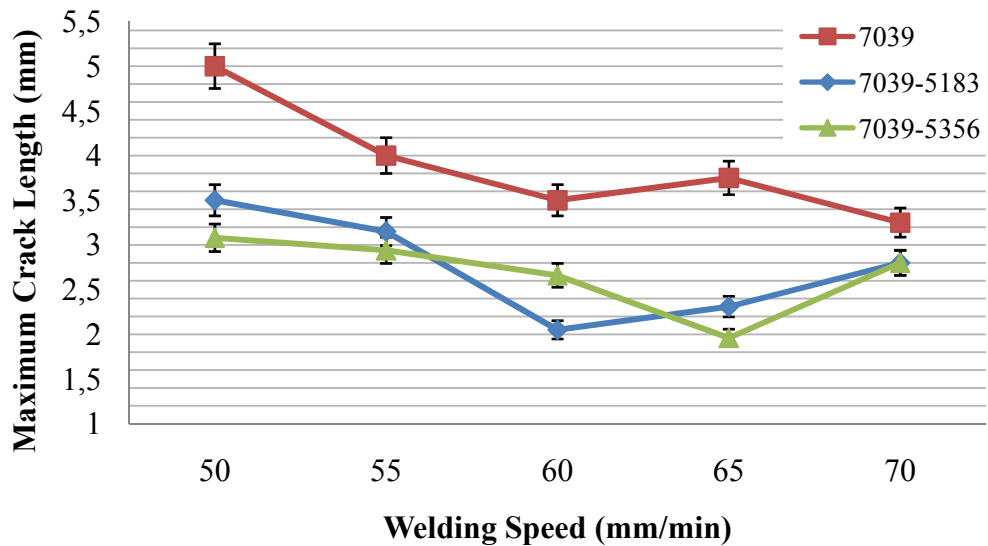


**Figure 35** Effect of welding speed on the maximum crack length for the whole sets



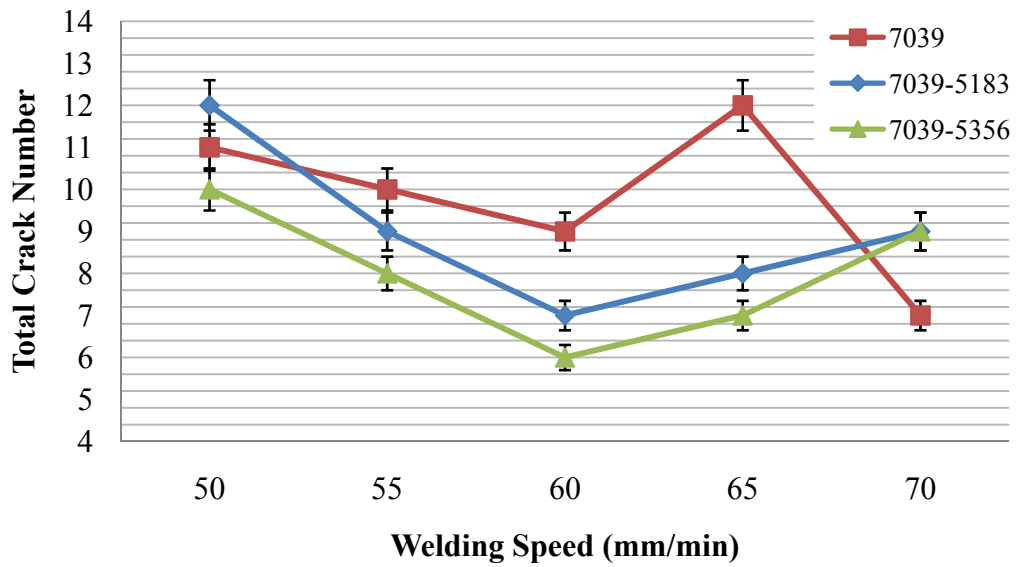


**Figure 36** Effect of welding speed on the total crack number for the whole sets

As stated before, hot cracks are seen either as solidification and liquation cracks. Weld seam of 7039 produced without the addition of filler materials showed negligible amount of liquation cracks. Even more, the cracks observed as liquation cracks started from the weld metal and extended to the PMZ region for the weld seams of 7039 aluminum alloy set. Therefore, number of liquation cracks will be compared between the weld seams of 7039-5183 and 7039-5356.

The results of the liquation crack length measurements of 7039-5183 and 7039-5356 set showed that 7039-5356 aluminum alloy set is more prone to liquation cracking with respect to 7039-5183 aluminum alloy set. For both of the sets total liquation crack length and maximum crack length observed on the weld seam decrease as the welding speed increase (Figures 37-38).

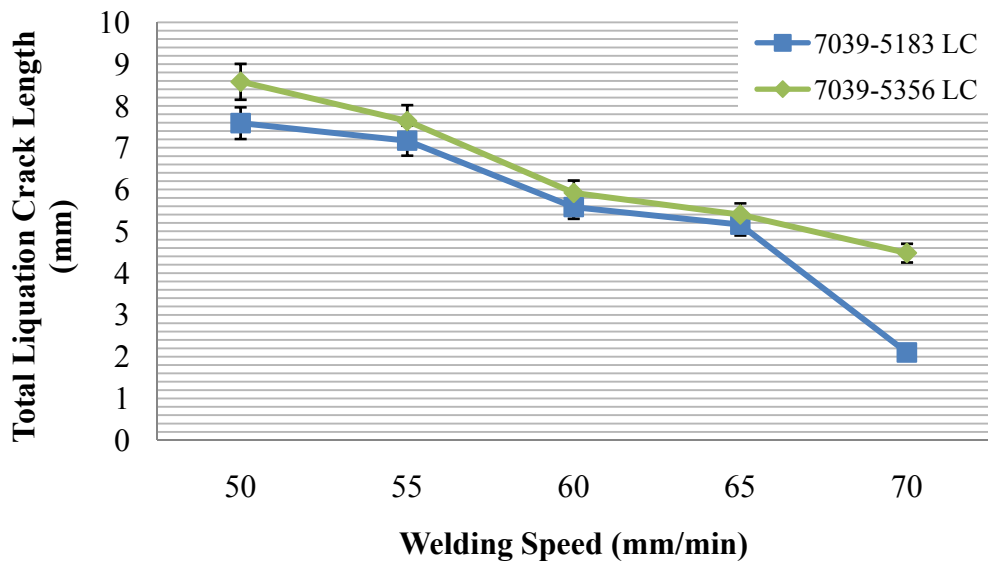


**Figure 37** Effect of welding speed on the total liquation crack length for the weld seams produced by filler materials

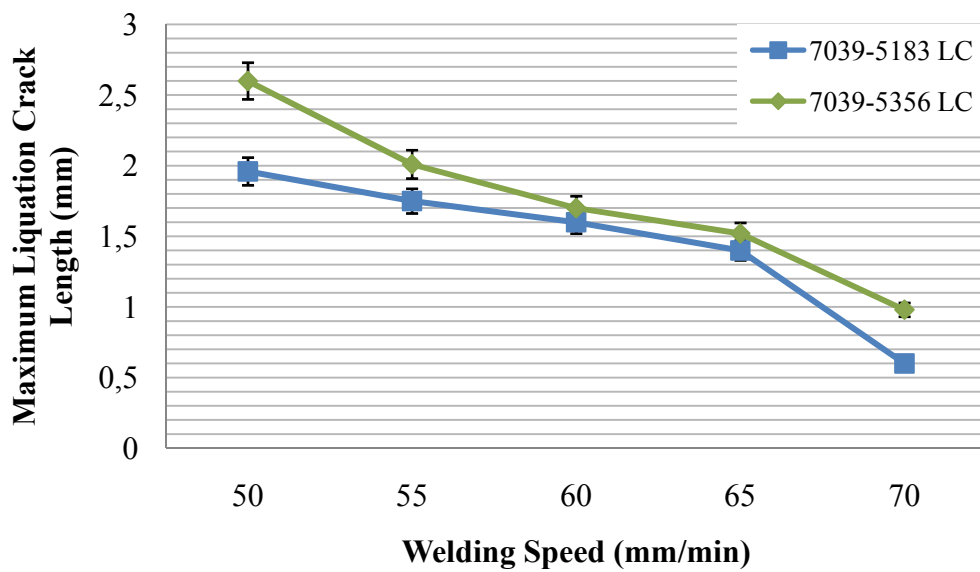


**Figure 38** Effect of welding speed on the maximum liquation crack length for the weld seams produced by filler materials

When the solidification crack susceptibility is compared between the weld seams produced by the addition of the filler alloys, it is found that there is no significant difference between these sets in terms of total solidification crack length and maximum solidification crack length.

In the Appendix Tables B4-B5, the length and the location of the liquation cracks for the 7039-5183 and 7039-5356 aluminum alloy sets were shown. Most of the liquation cracks formed almost perpendicular to the welding direction.

## **5.5 Results of Metallographic Examinations**

### **5.5.1 Results of Macrostructure Examinations**

In order to ensure sufficient mixing of filler material and parent material in the weld region, two steps welding were applied to the 7039-5183 and 7039-5356 sets. As a result of the two steps welding, deeper penetration was observed for the declared sets. In addition to this, as can be seen from the Figure 39, as the welding speed increase from 50 to 70 mm/min penetration amount decreases for the whole sets. The reason can be explained by the heat amount acting on the surface of the samples. As the welding speed decrease more amount of heat is expected to act on the samples.

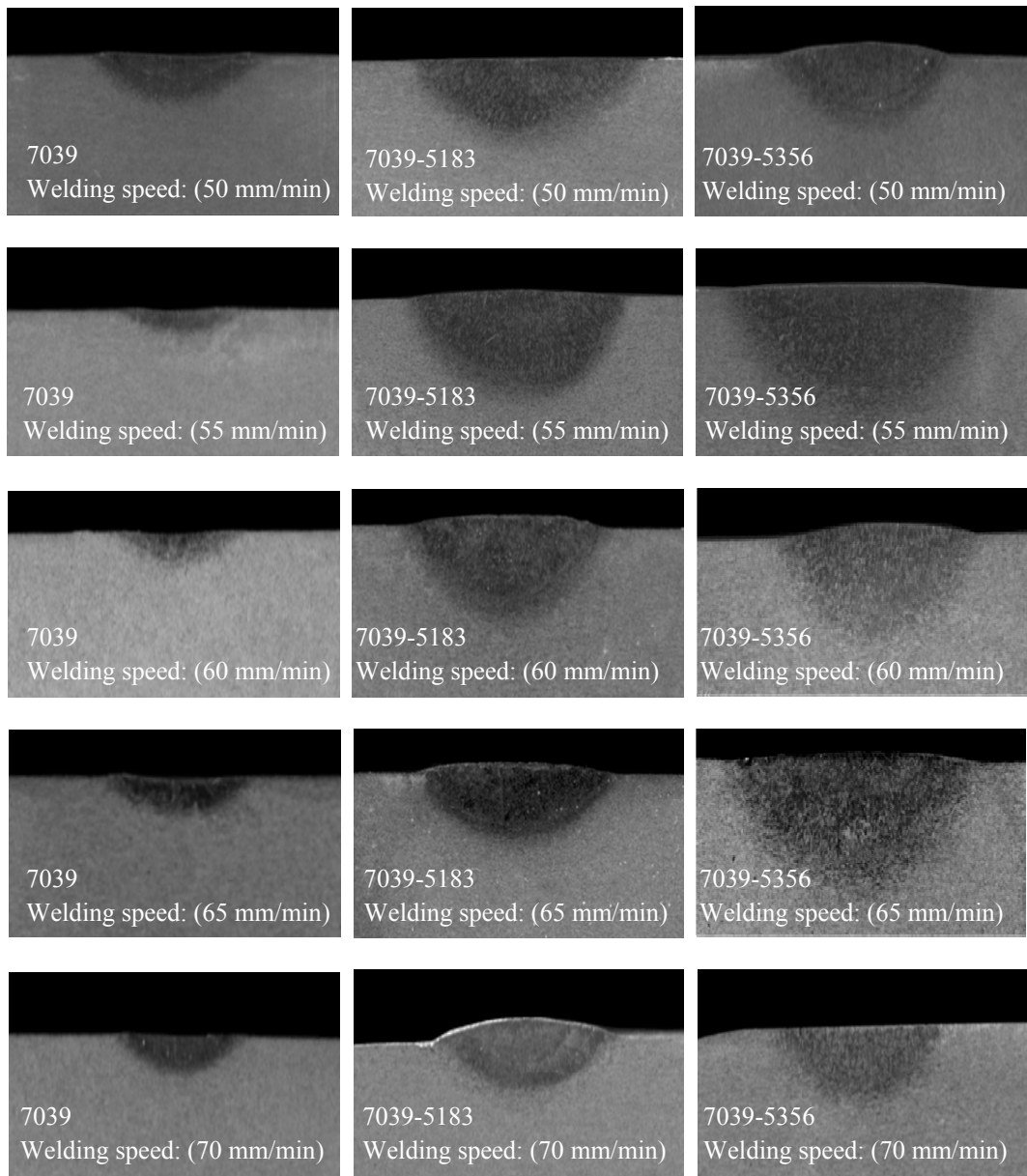
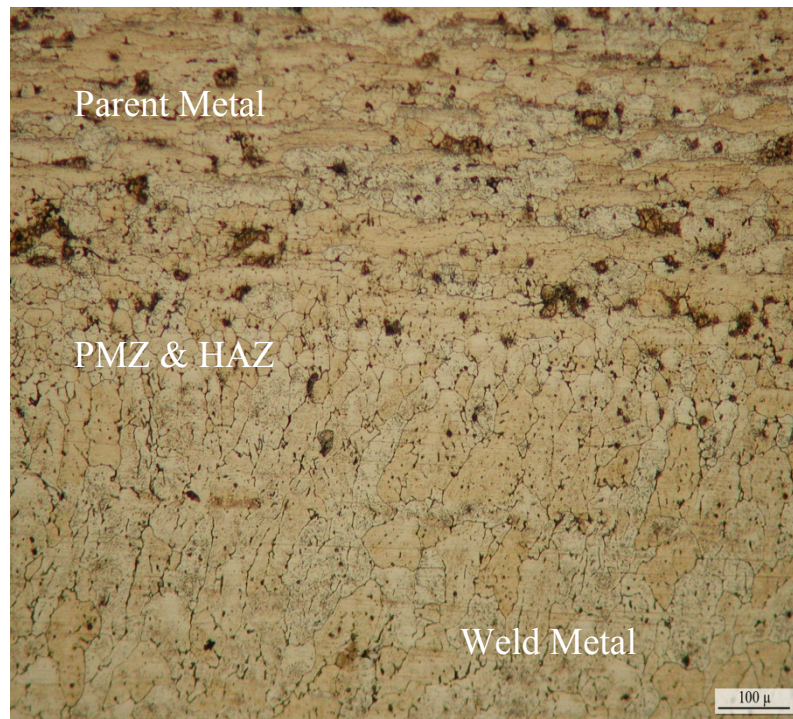


**Figure 39** Macro-photos of the weld region of the samples

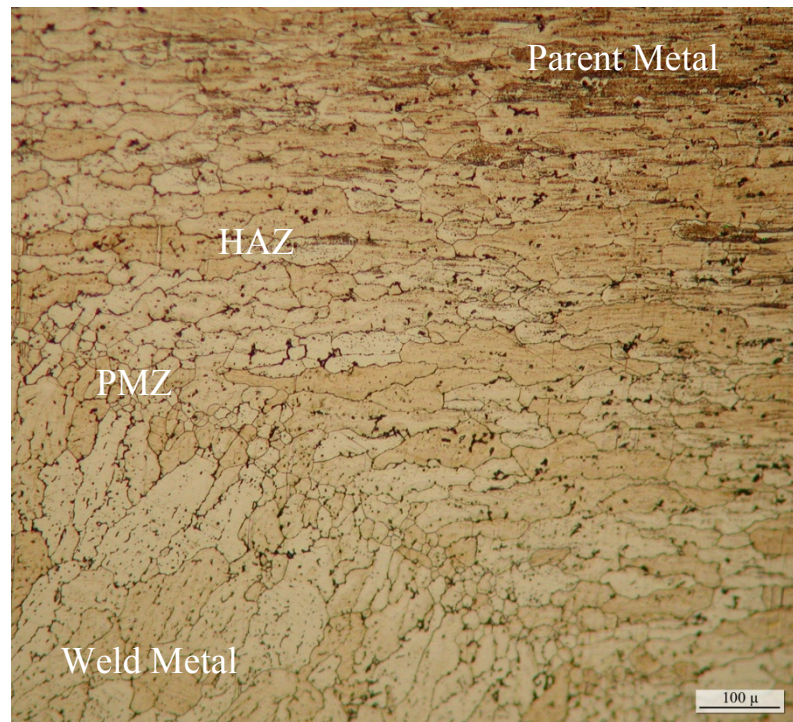
### 5.5.2 Results of Microstructure Examinations

Microstructure examinations were done at the cross section of the samples and also some were carried out at the top surface where bending was applied.

Figures 40-41 show the weld structure of the 7039-5183 aluminum alloy. The effect of welding speed on the grain size can be seen from the figures. The 7039-5183 alloy welded with 50 mm/min welding speed has coarse grains with respect to 7039-5183 alloy welded with 65 mm/min welding speed. With decreasing welding speed, weld metal average grain size increases from approximately 49,1  $\mu\text{m}$  to 67,6  $\mu\text{m}$ . The reason is that higher heat amount generated with the slower speeds causes the grains to grow.



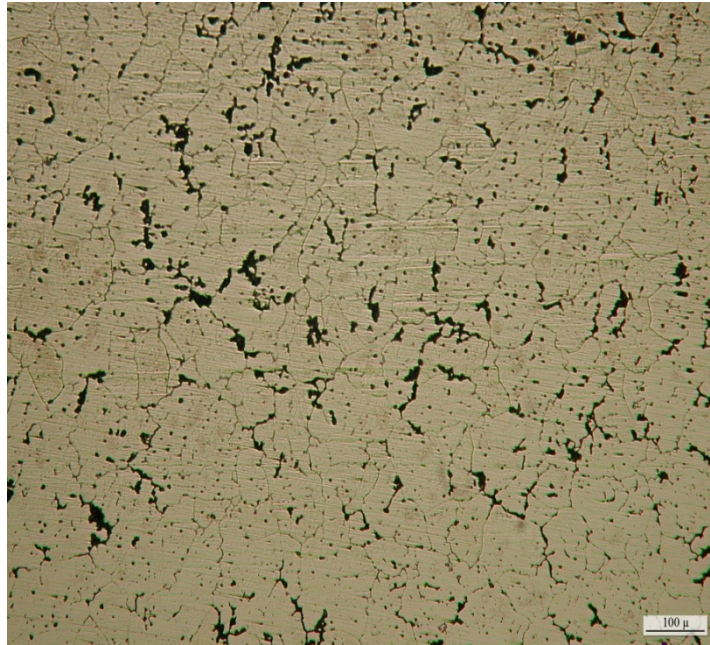
**Figure 40** Weld and parent metal regions of 7039-5183 aluminum alloy welded with 50 mm/min welding speed and 120 A drop current. Keller etching.



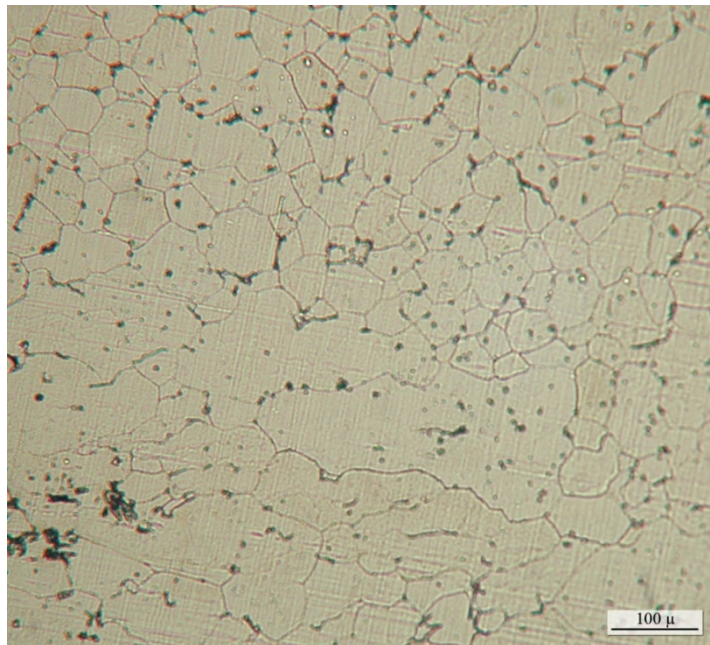
**Figure 41** Weld structure of 7039-5183 aluminum alloy welded with 65 mm/min welding speed and 120 A drop current. Keller etching.

From the Figure 42 the precipitates along the grain boundaries (dark areas) can be easily seen. These precipitates or second phase particles may initiate the crack formation under sufficient strain.

Figure 43 shows the weld metal of 7039-5183 aluminum alloy.



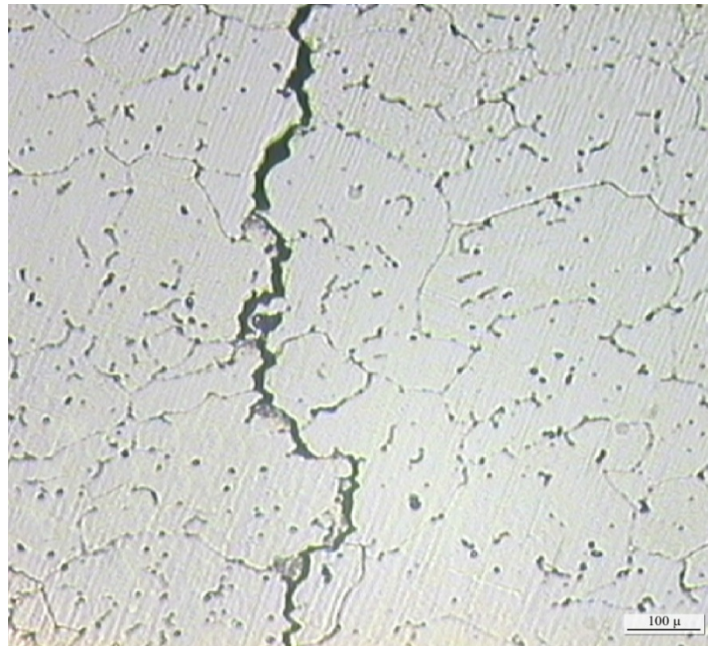
**Figure 42** Weld metal of 7039-5356 aluminum alloy welded with 55 mm/min welding speed and 120 A drop current. Keller etching.



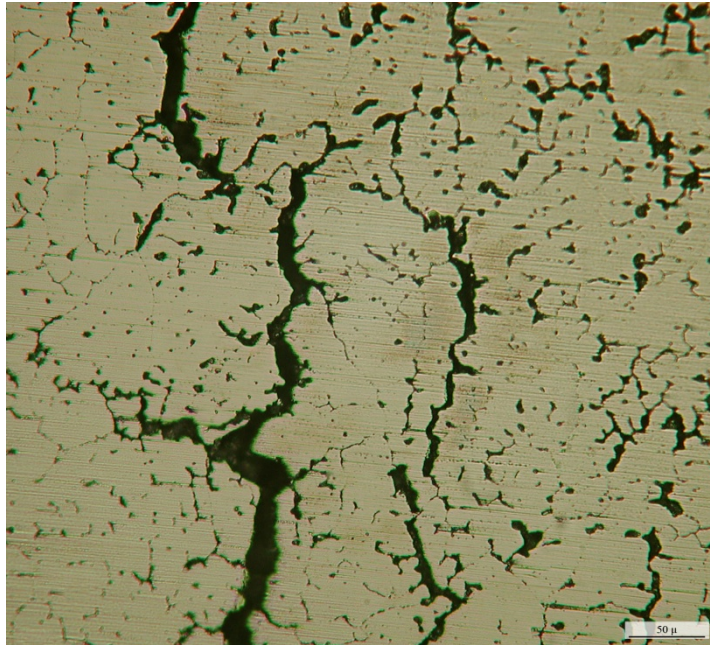
**Figure 43** Weld metal of 7039-5183 aluminum alloy welded with 55 mm/min welding speed and 120 A drop current. Keller etching.



Figures 44-45 show the solidification cracks formed along the grain boundaries at the weld metal. Their intergranular structure can be understood from these figures.

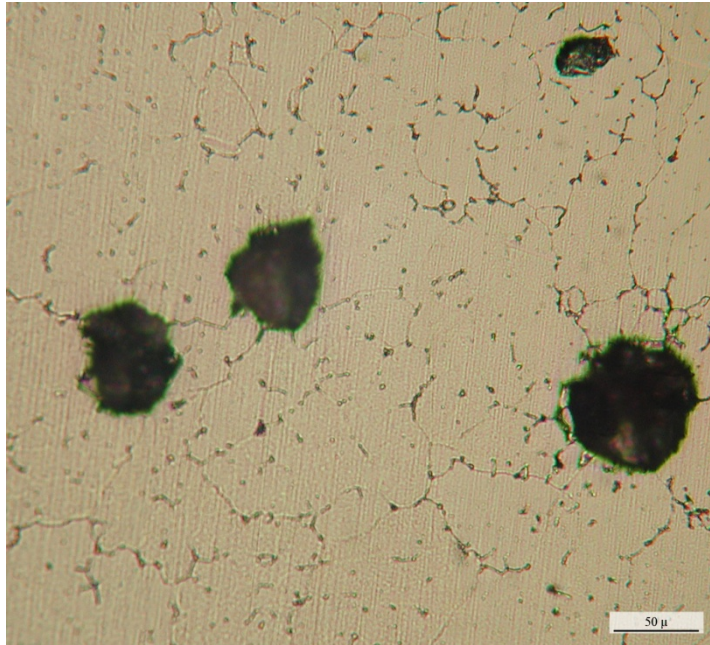


**Figure 44** Solidification crack at the weld metal of 7039-5183 aluminum alloy welded with 50 mm/min welding speed and 120 A drop current. Keller etching.



**Figure 45** Solidification crack at the weld metal of 7039-5356 aluminum alloy welded with 60 mm/min welding speed and 120 A drop current. Keller etching.

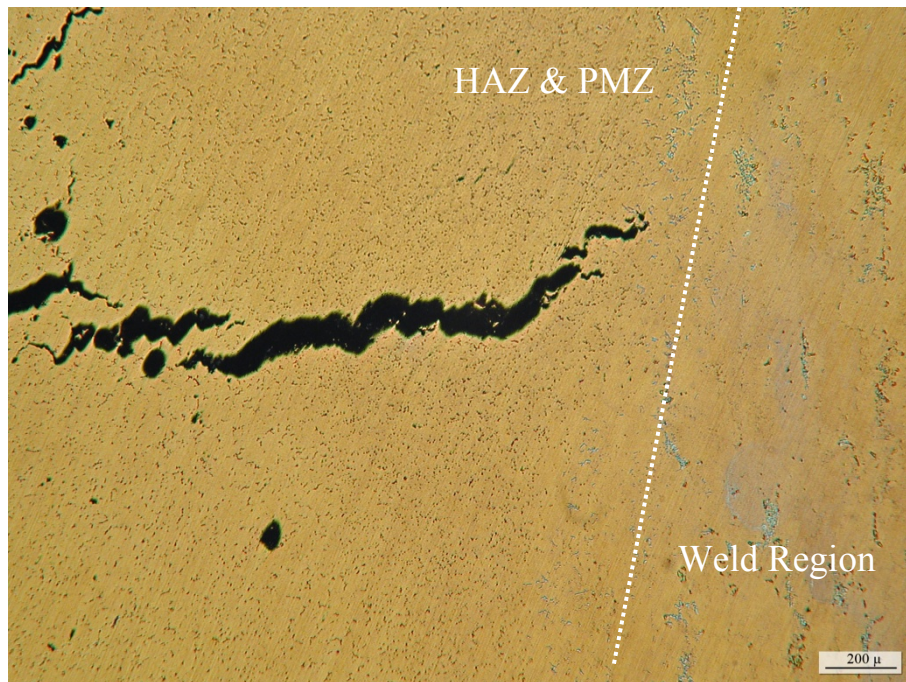
It is known that porosities are common problem for aluminum alloys. In the Figure 46 the porosities formed during the welding of 7039-5183 aluminum alloy can be easily seen.



**Figure 46** Porosities around the weld metal of 7039-5183 aluminum alloy welded with 60 mm/min welding speed and 120 A drop current. Keller etching.

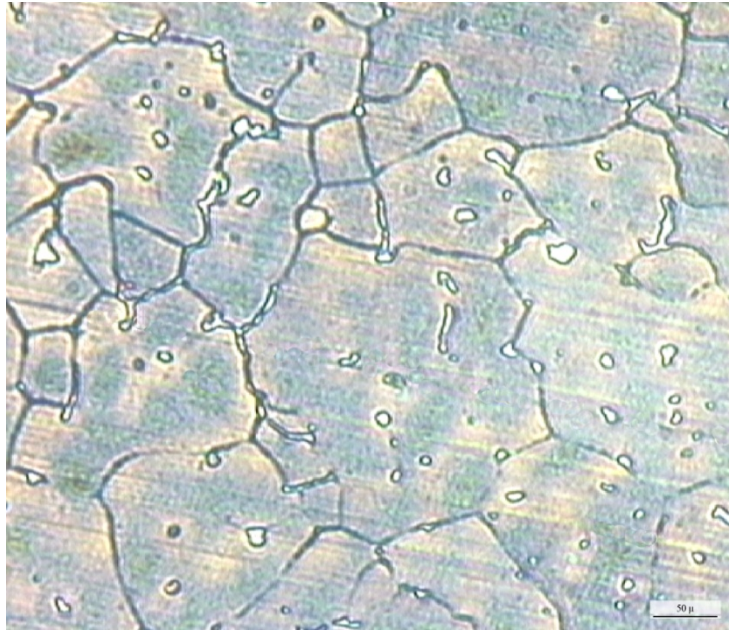
In addition to the micrographs taken from the cross section, microstructure of the top surface was also examined. The top surface is etched by using Weck reagent.

Figure 47 shows liquation cracks at the top surface of 7039-5356 aluminum alloy. The crack lies along PMZ and HAZ. The grains are not apparent due to insufficient etching.



**Figure 47** Liquation crack at the PMZ and HAZ of 7039-5356 aluminum alloy. Weck reagent.

Figures 48-49 show the precipitates formed at the weld metal of the 7039 aluminum alloy welded with 60 mm/min welding speed. Especially the precipitates along the grain boundaries and at the grain boundary junctions are noticeable.



**Figure 48** Precipitates formed at the weld metal of 7039 aluminum alloy welded with 60 mm/min welding speed and 120 A drop current. Weck etching.

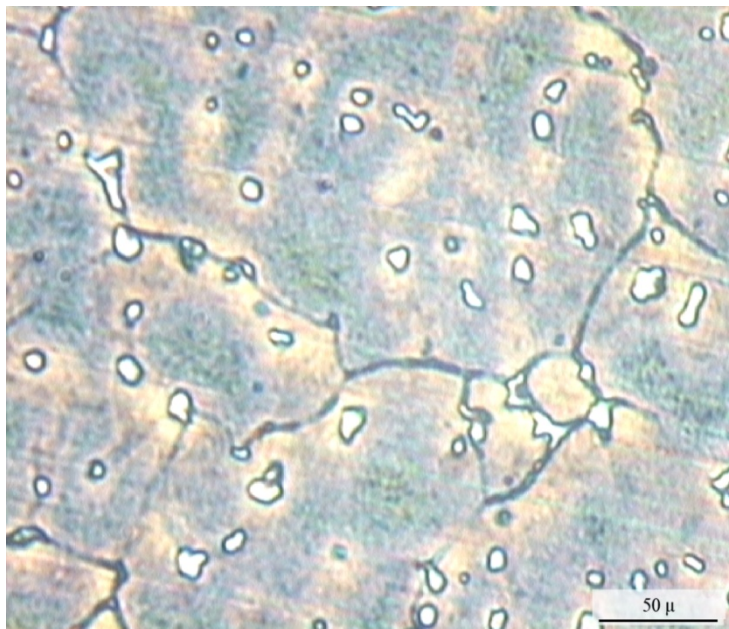


**Figure 49** Precipitates formed at the weld metal of 7039 aluminum alloy welded with 60 mm/min welding speed and 120 A drop current. Weck etching.

For the 7039-5183 and 7039-5356 aluminum alloys, precipitate films along the grain boundaries were observed. These precipitates may be the reason of the intergranular liquation crack formation (Figure 50).

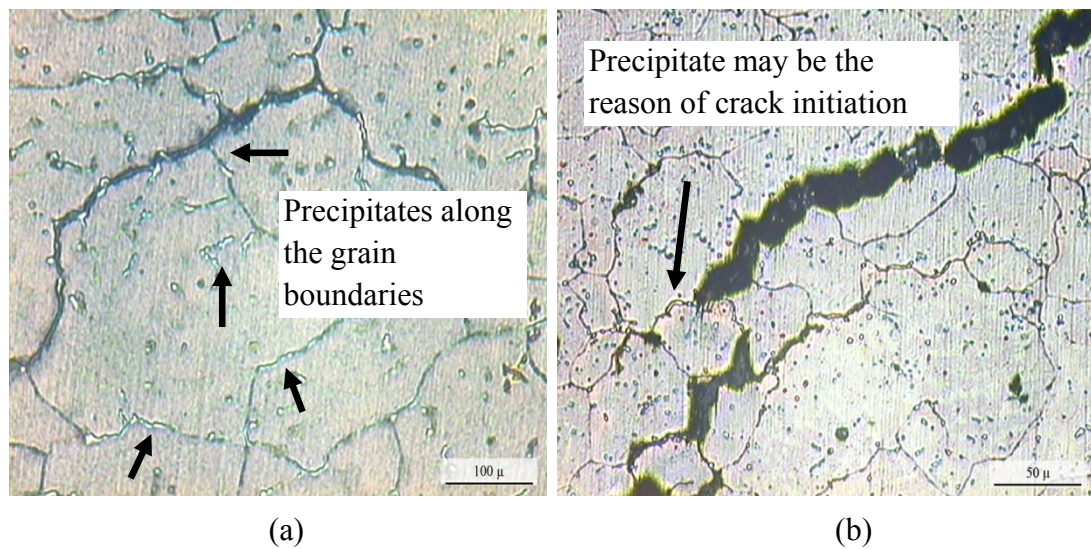


**Figure 50** Intergranular liquation cracks observed for (a) 7039-5183 aluminum alloy (b) 7039-5356 aluminum alloy welded with 60 mm/min welding speed and 120 A drop current. Weck reagent.

As stated in the “Experimental Procedure” part, it is probable to see different phases for the 7039 aluminum alloy. In this sense in order to identify precipitates correctly literature was surveyed and SEM-EDX analysis was taken from the hot cracking regions. As can be seen from the SEM-EDX analysis shown at Figure 51, iron (Fe) and chromium (Cr) elements present near the crack region. When this result is compared with the literature it can be claimed that the observed precipitates for the 7039 aluminum alloy exhibit  $(\text{FeCr})\text{Al}_7$  phase. The region, where the SEM-EDX analysis was taken, contains Zn as the twice amount of Mg. According to the

literature [47], when the Zn:Mg ratio is more than 2 it is probable to see  $MgZn_2$  phases. Therefore for the 7039 aluminum alloy,  $(FeCr)Al_7$  phases are accompanied with  $MgZn_2$  phases having elongated and discontinuous form [48].

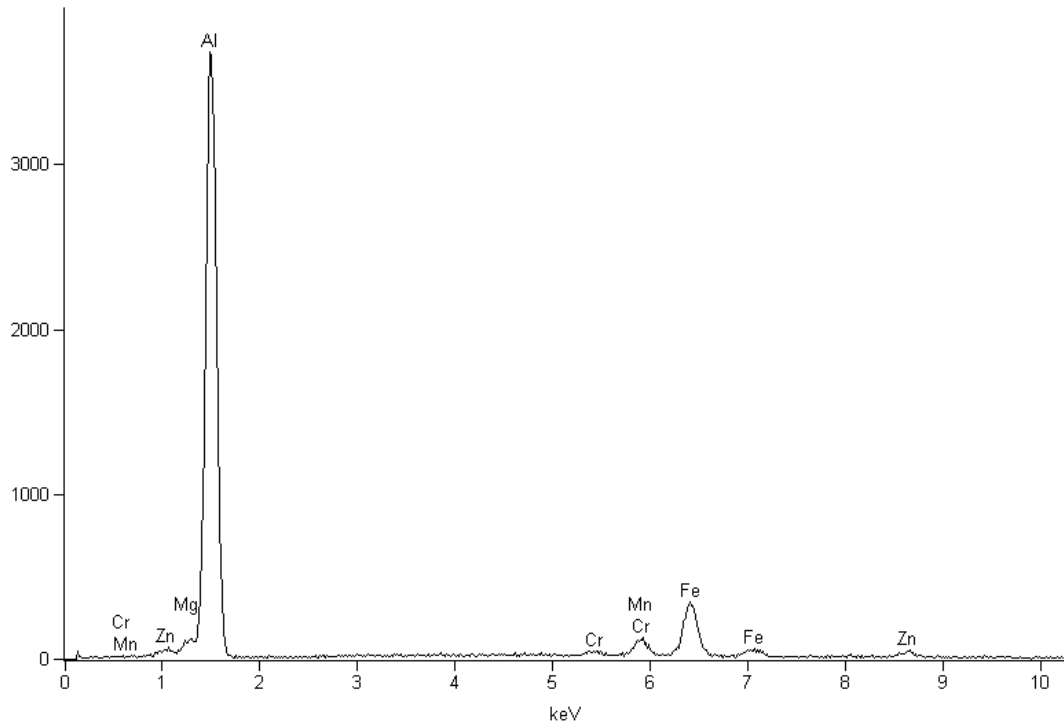


**Figure 51** SEM-EDX analysis taken from the cracking region of 7039 aluminum alloy

SEM-EDX analysis taken from the 7039-5183 and 7039-5356 aluminum alloys resembled each other (Figure 52). The cracking regions contain mostly Mg and Zn elements. Referring to their chemical composition and literature [47], it may be stated that the presenting phases are  $Mg_3Zn_3Al_2$ .

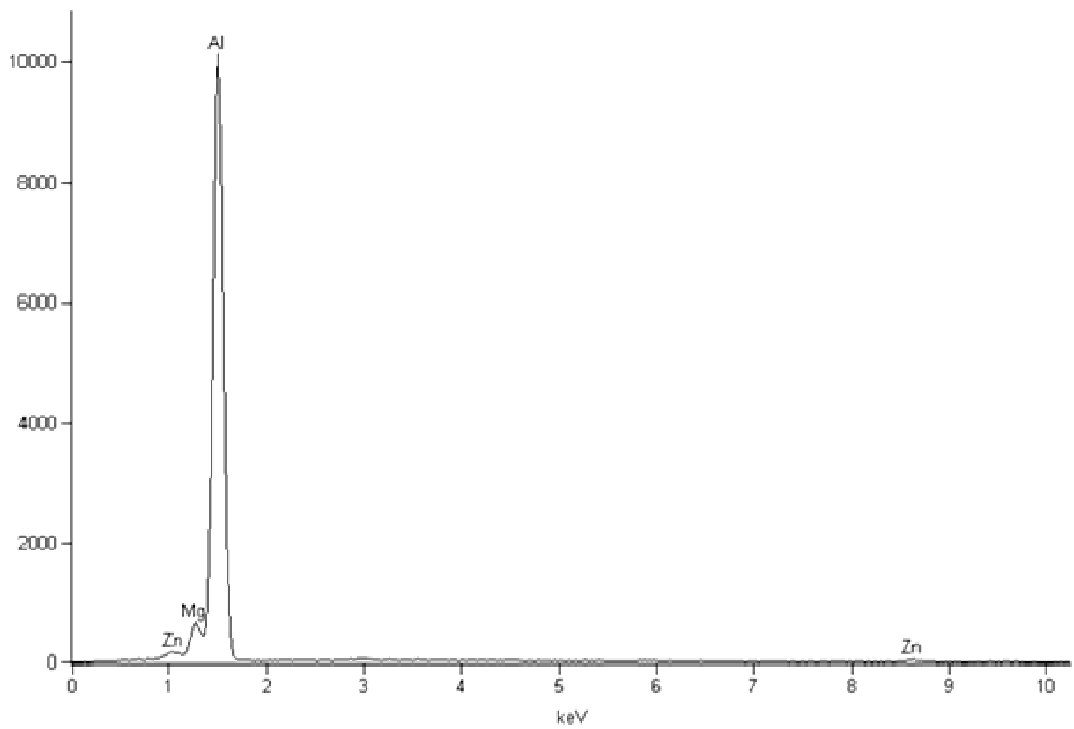


**Figure 52** SEM-EDX analysis taken from the cracking region of 7039-5183 aluminum alloy

In addition to the microstructure examinations, crack tip radius measurements were also carried out. Figure 53 shows some examples of cracks and a range for the crack tip radius for the whole sets.



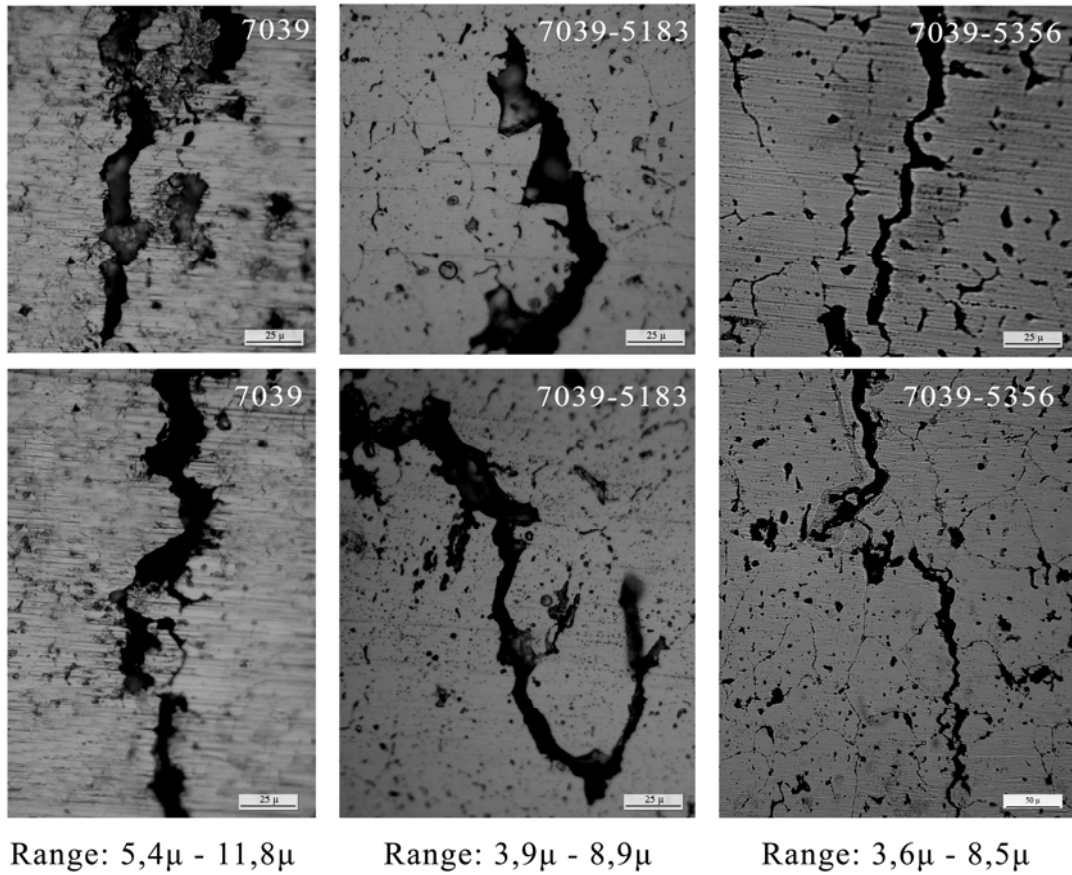


**Figure 53** Crack tip radius range for the whole sets

### 5.6 Results of the Differential Thermal Analysis (DTA)

Hot cracking susceptibility is also related with the solidification range of the alloys. Thermal analyses allowed measuring the solidus and liquidus temperatures of the alloys and surely the solidification range. Figure 54 shows the heating stage of the 7039 aluminum alloy above its liquidus temperature. The liquidus temperature of this alloy is found by the peak point which shows 644°C and the onset point represents the temperature for the beginning of the endothermic reaction which is 619 °C. The liquidus temperatures were found by considering the heating stage of the alloys since cooling stage can mislead to different results due to undercooling effect [49].

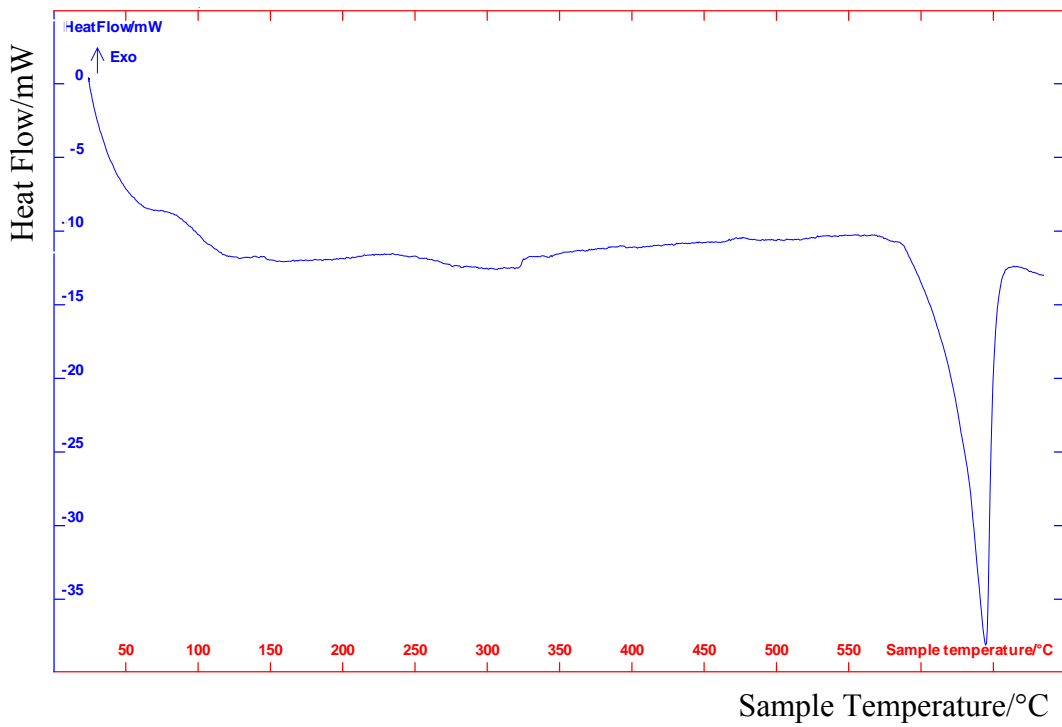


**Figure 54** Heat flow versus temperature graph showing the heating stage of the 7039 aluminum alloy

Thermal analysis result of the 7039-5183 and 7039-5356 sets were compared below. Figure 55 shows the heating stage of the 7039-5183 alloy. At 619°C first liquid formation started and total completion of the melting was at 644°C.

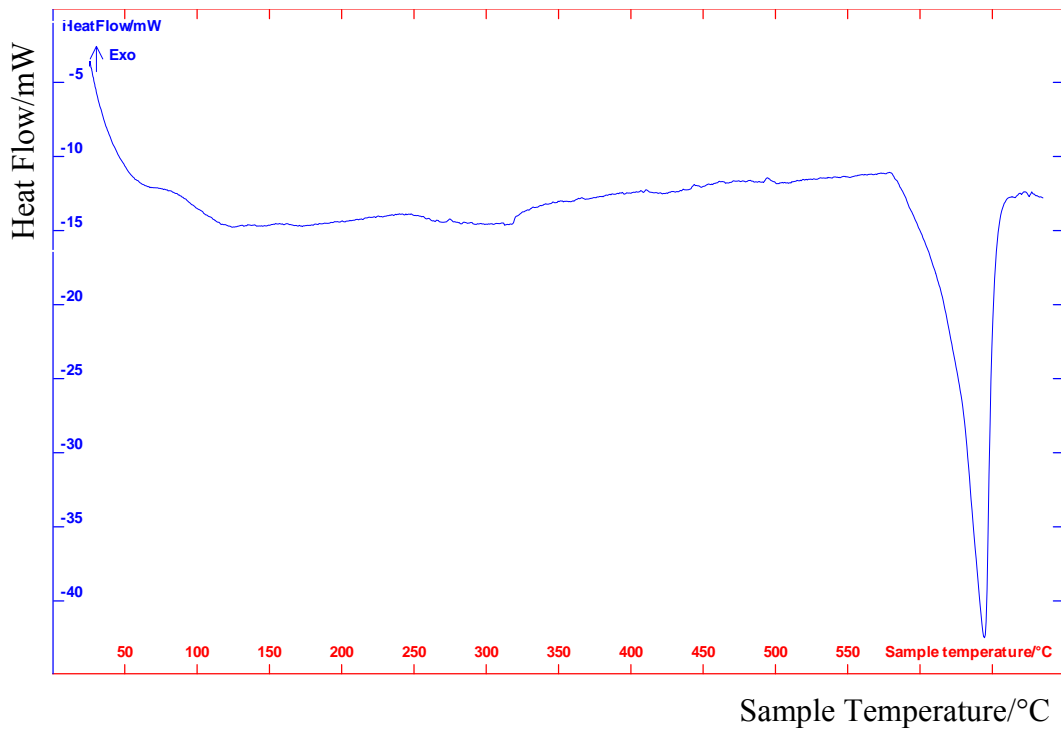


**Figure 55** Heat flow versus temperature graph showing the heating stage of the 7039-5183 aluminum alloy

Figure 56 shows the heating stage of the 7039-5356 aluminum alloy. First liquid formation started at 617°C and melting was completed at 644°C.

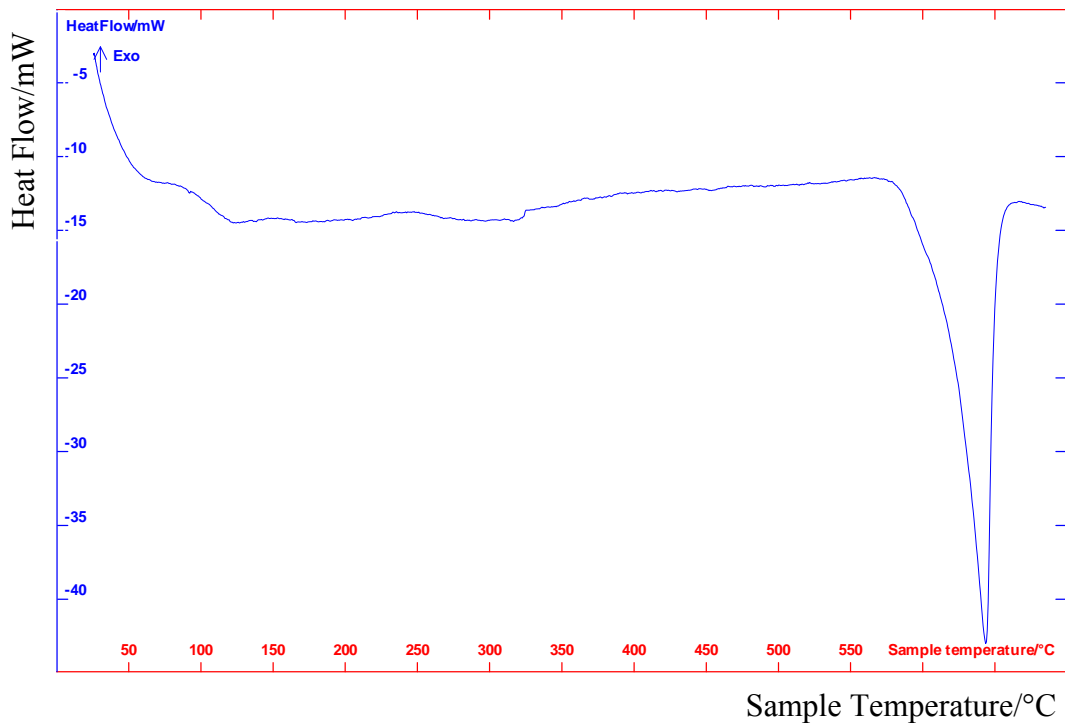


**Figure 56** Heat flow versus temperature graph showing the heating stage of the 7039-5356 aluminum alloy

The solidification range for the 7039-5183 aluminum alloy is calculated as 25 °C whereas the solidification range of the 7039-5356 aluminum alloy is calculated as 27 °C. The small difference between their solidification ranges is due to the effect of magnesium on the solidification range of the alloys.

### 5.7 Results of the Hardness Test

Vickers Hardness Measurements revealed the following graphs for the 7039, 7039-5183 and 7039-5356 aluminum alloys (Figures 57-59).

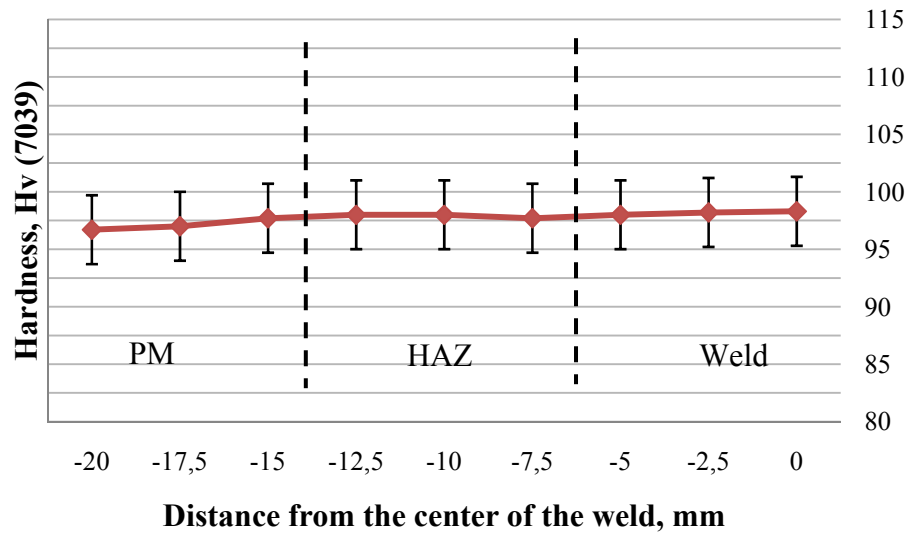


Figure 57 Hardness profile along the cross section of the 7039 aluminum alloy

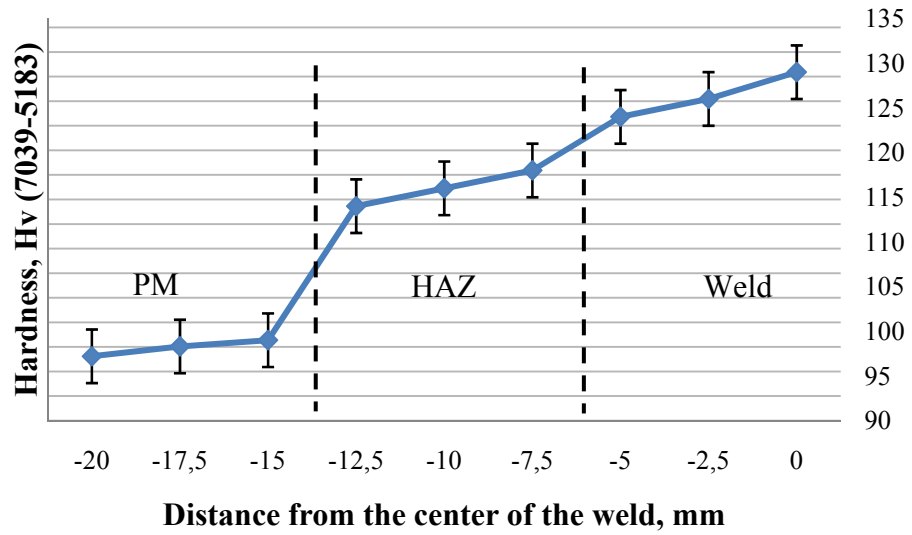
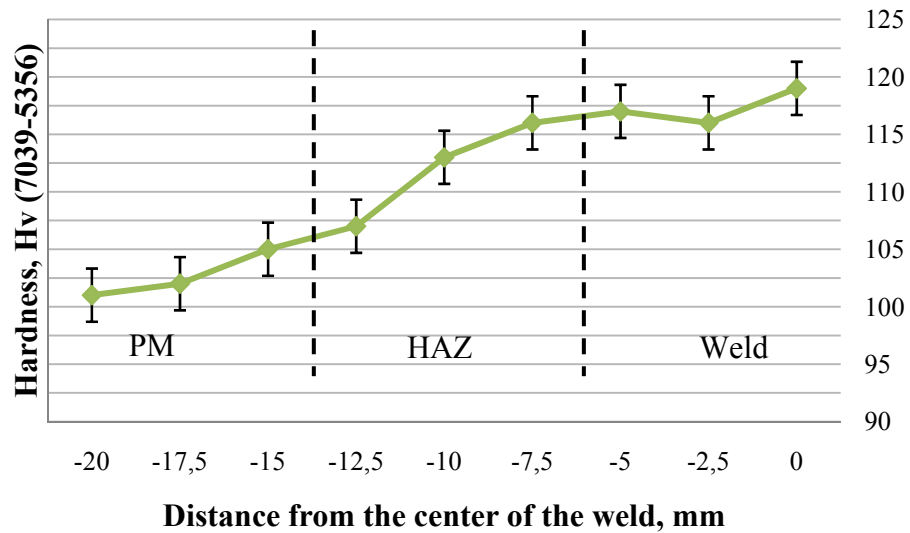


Figure 58 Hardness profile along the cross section of the 7039-5183 aluminum alloy



**Figure 59** Hardness profile along the cross section of the 7039-5356 aluminum alloy

No significant difference was observed between the samples that were welded with different welding speeds.

### 5.8 Results of the Fatigue Test

7039, 7039-5183 and 7039-5356 aluminum alloy sets produced with MVT method were fatigue tested to observe the characterization and growth properties of the hot cracks under cyclic load.

Fatigue life of the samples under a sinusoidal 900 kg load is shown in Table 9. Table 9 also shows the maximum crack length of the samples measured after MVT method prior to fatigue tests (60 mm/min welding speed, 120 A welding current). Accordingly, the 7039 aluminum alloy which possessed longest crack after MVT method, had the least fatigue life among the other sets.

**Table 9** Fatigue life of the samples

<b>Aluminum Alloy</b>	<b>Number of cycles</b>	<b>Maximum Crack Length (MVT)</b>
7039	$2,1 \times 10^5$ cycles	3,5 mm
7039-5183	$3,6 \times 10^5$ cycles	2,05 mm
7039-5356	$3,8 \times 10^5$ cycles	2,66 mm

Macro-photos of the fractured surfaces that are subjected to fatigue test gave clues related with the growth properties of the cracks. The fractured surface of the 7039 aluminum alloy revealed the initiation point of the cracks along the fusion line and weld metal. These cracks extended towards the parent metal under cyclic load (Figure 60).



**Figure 60** Macro-photos of the fatigue fractured surface of 7039 aluminum alloy.

The fractured surfaces of the 7039-5183 and 7039-5356 aluminum alloys revealed the initiation point of the cracks in the PMZ and HAZ regions (Figure 61). Unlike 7039 aluminum alloy, the cracks started to grow from the PMZ and HAZ region (and little from weld metal) towards the parent metal under cyclic load.

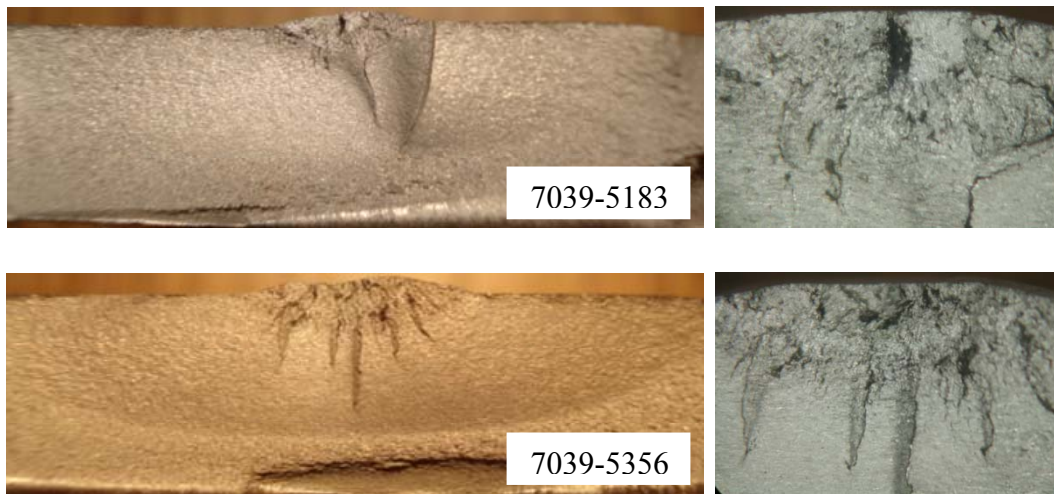


**Figure 61** Macro-photos of the fatigue fractured surfaces of 7039-5183 and 7039-5356 aluminum alloys.

Table 10 shows a comparison between the sets in terms of longest fatigue crack length, their initiation point and aspect ratio and aspect ratio of the initial cracks. Longest crack length represents the length measured just before the fracture. The longest crack was observed for the 7039 aluminum alloy and on the other part the shortest one was observed for the 7039-5183 aluminum alloy. Aspect ratio of the cracks was found by dividing the depth into the half surface length.

**Table 10** Length of the final cracks of the fatigue tested samples

<b>Aluminum Alloy</b>	<b>Longest fatigue crack</b>	<b>Initiation point</b>	<b>Aspect ratio of the longest fatigue cracks</b>	<b>Aspect ratio of the initial cracks</b>
7039	4,3 mm	Fusion line	0,23	0,22
7039-5183	3,5 mm	HAZ / PMZ	0,29	0,53
7039-5356	3,9 mm	HAZ / PMZ	0,26	0,47



In addition to the findings given above, striations were searched during SEM examinations. However no striation was observed; therefore crack growth rate could not be studied.

## **5.9 Results of SEM Examinations**

### **5.9.1 SEM Examinations of the Welded Samples**

SEM Examinations were carried out at the laboratories of the Metallurgical and Materials Engineering Department of Middle East Technical University. The fracture surfaces of the cracks were taken to the SEM examination to get information about the hot cracking properties of the alloys. SEM photographs were taken from the specimen welded with 60 mm/min welding speed and 120 A drop current.

As stated before hot cracks are in intergranular type. As a form of hot cracks, liquation cracks also occur intergranularly. The main reason of the liquation cracking is the low melting point constituents forming along the grain boundaries. Figure 62 shows an example of a liquation crack of 7039-5183 alloy and Figure 63 shows the intergranular form of the liquation crack of 7039-5183 alloy. The photos are taken from the PMZ of the alloy.

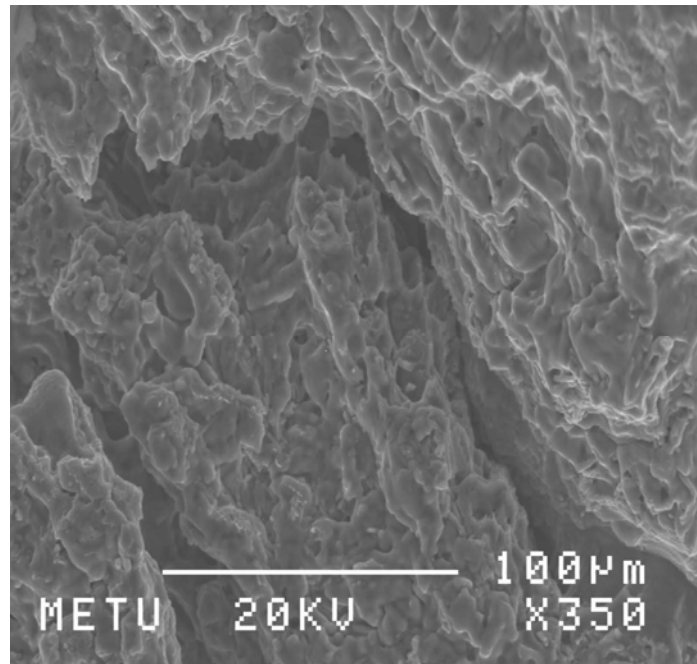


**Figure 62** Fractography of a liquation crack of 7039-5183 aluminum alloy.

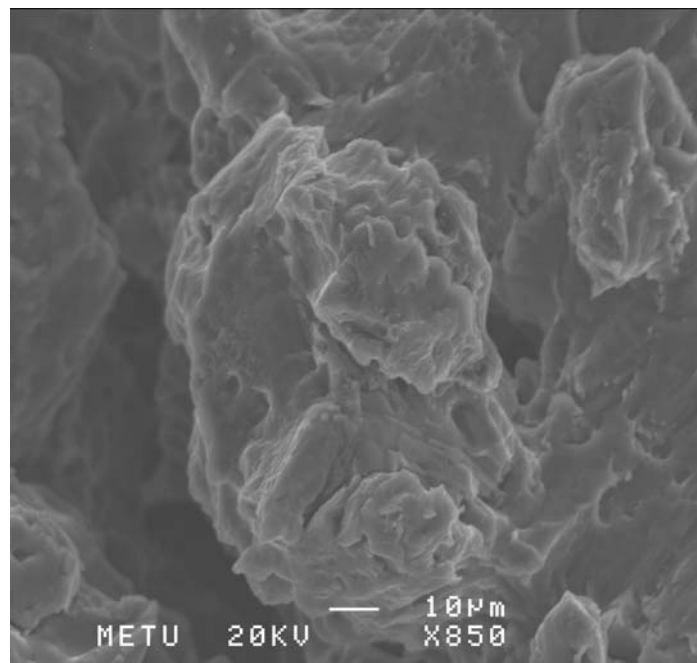


**Figure 63** Fractography of a liquation crack of 7039-5183 aluminum alloy. The crack formation is intergranular

Not only liquation cracks presented for the 7039-5183 or 7039-5356 alloys but also solidification cracks also presented on the weld seam of the alloys. Figure 64 shows the solidification cracks located at the weld metal of 7039-5183 aluminum alloy and Figure 65 shows solidification crack at the weld metal of 7039-5356 aluminum alloy. The smooth and blur regions at the fracture surface reveals the history of the solidification crack formation. During solidification, liquid films form along the grain boundaries. As a result of strain acting on the system these low strength films break apart and then solidify. Consequently first liquidified and then solidified regions or in other terms solidification cracks are seen in the form of smooth regions in the SEM photos.

Figure 66 shows the solidification crack along the fusion line of the 7039 aluminum alloy.

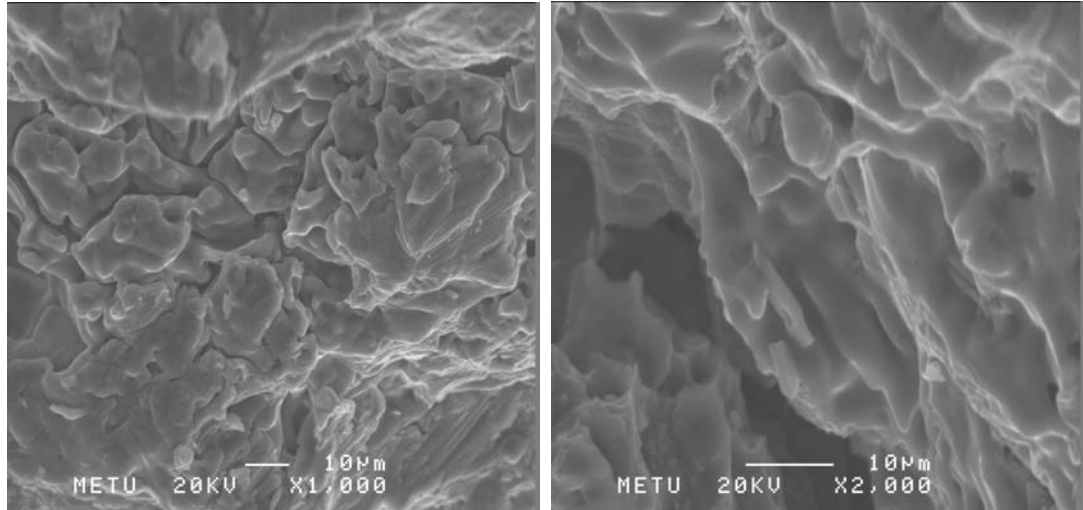


**Figure 64** Fractography of the solidification cracks located at the weld metal of 7039-5183 aluminum alloy.

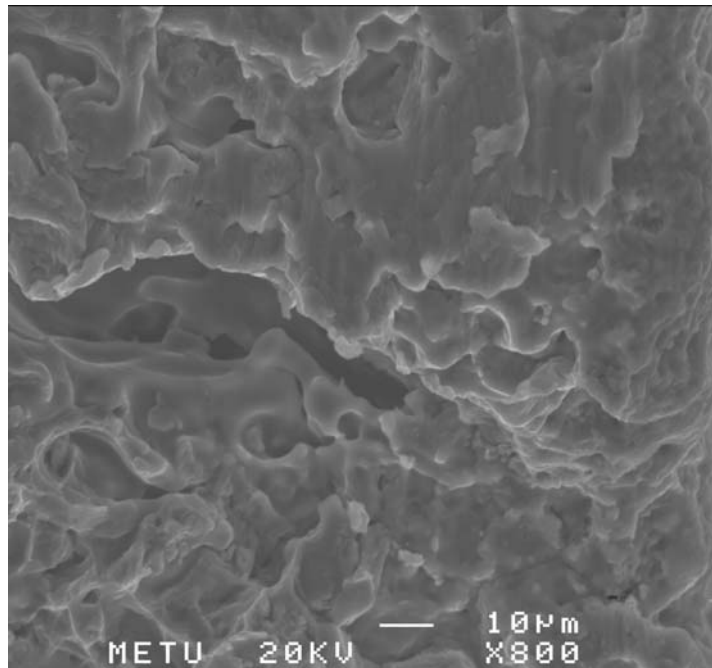


**Figure 65** Fractography of a solidification crack located at the weld metal of 7039-5356 aluminum alloy.

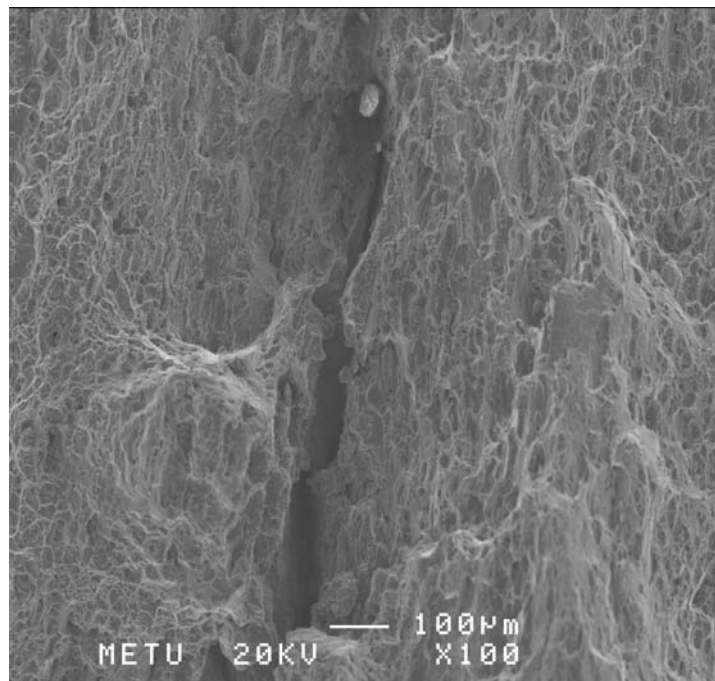


**Figure 66** Fractography of a solidification crack located along the fusion line of 7039 aluminum alloy.

Another finding of the SEM observations was shown at the Figure 67. It points out the dendritic protuberances and the dendritic morphology of the solidification crack. To remind, solidification cracks form at the weld metal in a dendritic manner.

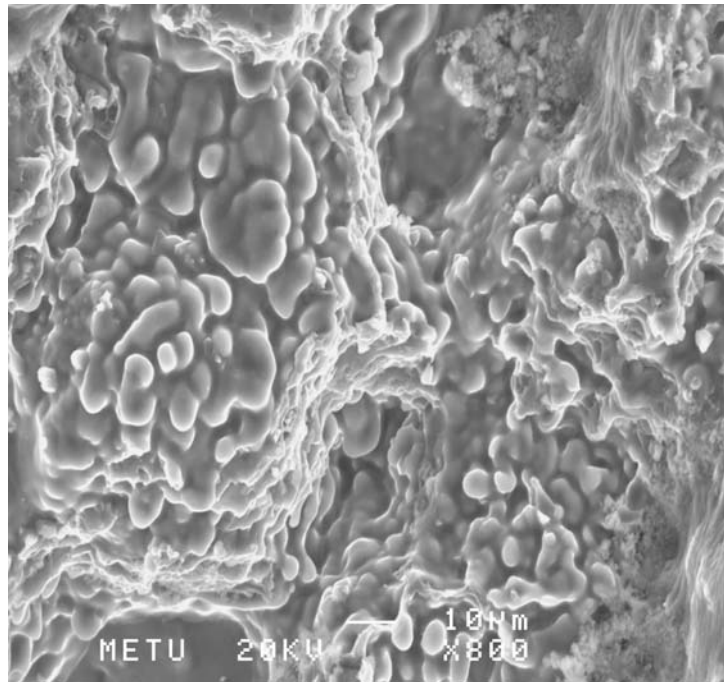


**Figure 67** Dendritic morphology observed at the weld metal of 7039-5356 aluminum alloy

### **5.9.2 SEM Examinations of Fatigue Tested Samples**

The fatigue tested samples were taken to the SEM examination to observe the fatigue behavior of the hot cracks.

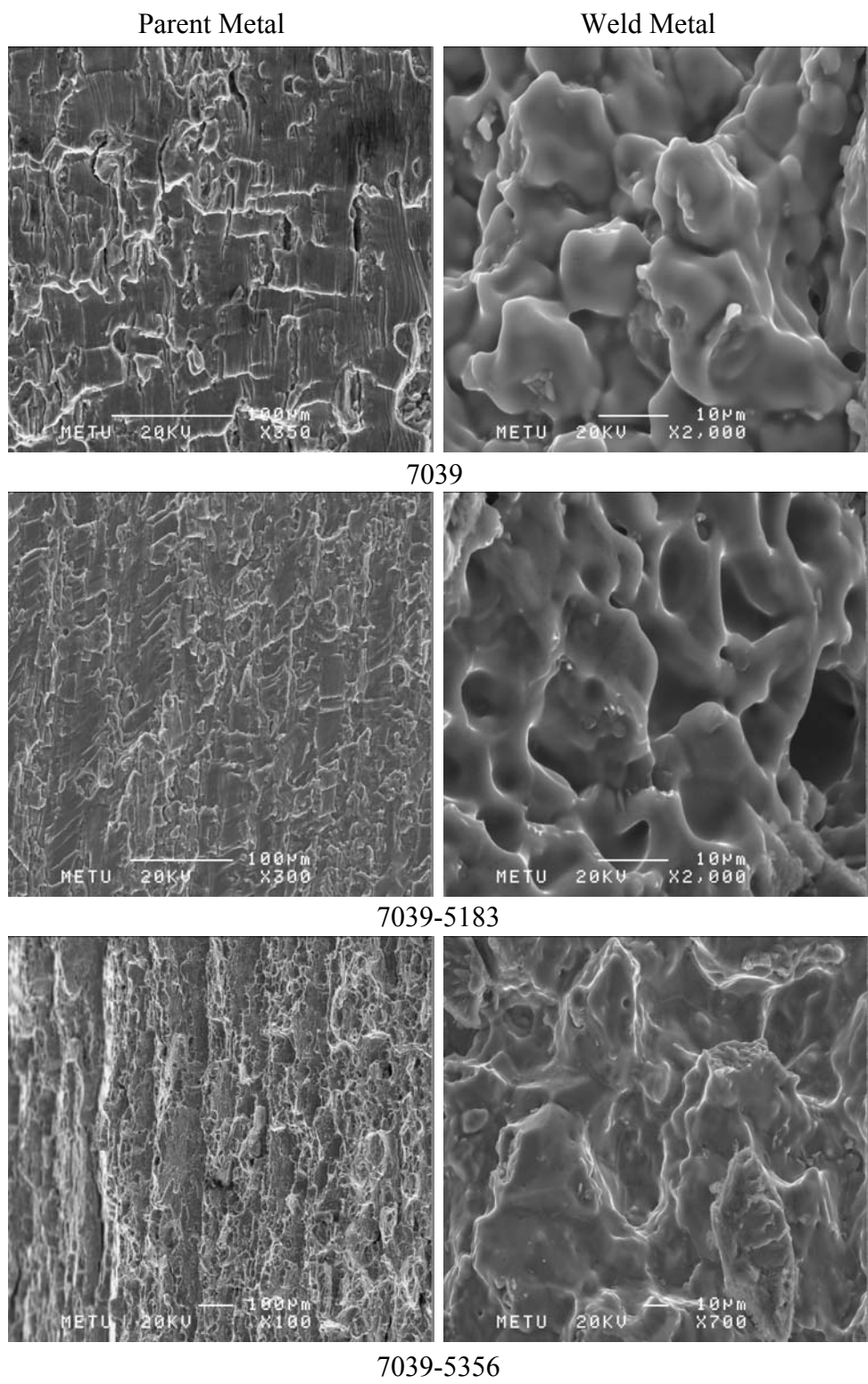


**Figure 68** SEM photographs of the parent metal and weld metal of the fatigue tested samples

SEM observations of the three sets of samples showed that the fracture morphology of the weld metal and parent metal are different. Although the samples are fatigue tested, the weld metal revealed smooth regions that are evidence of pre-liquid parts. Parent metal which is not subjected to melting or solidification revealed typical fatigue fracture morphology. The layered and ductile fractured regions of the parent metal can be seen at Figures 68-69.

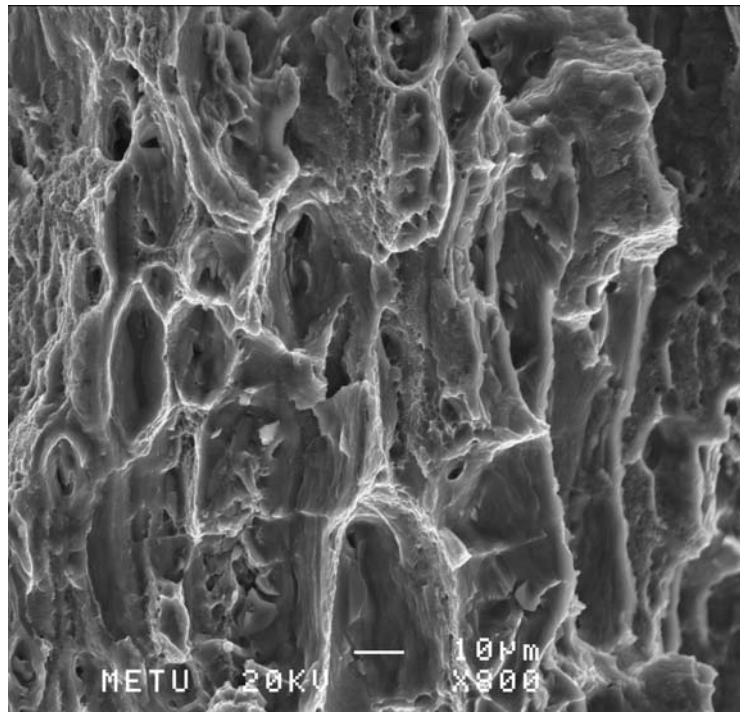


**Figure 69** SEM photograph showing the ductile fracture of the 7039 aluminum alloy taken after fatigue test

In addition to the information gathered related with the fracture morphology of the samples, some remarkable observations are also made with the help of SEM. Figure 70 shows SEM photograph of internal cracks that lie just under the surface at the

weld metal. Such type of cracks did not appear at surface inspections of the samples that were not fatigue tested.

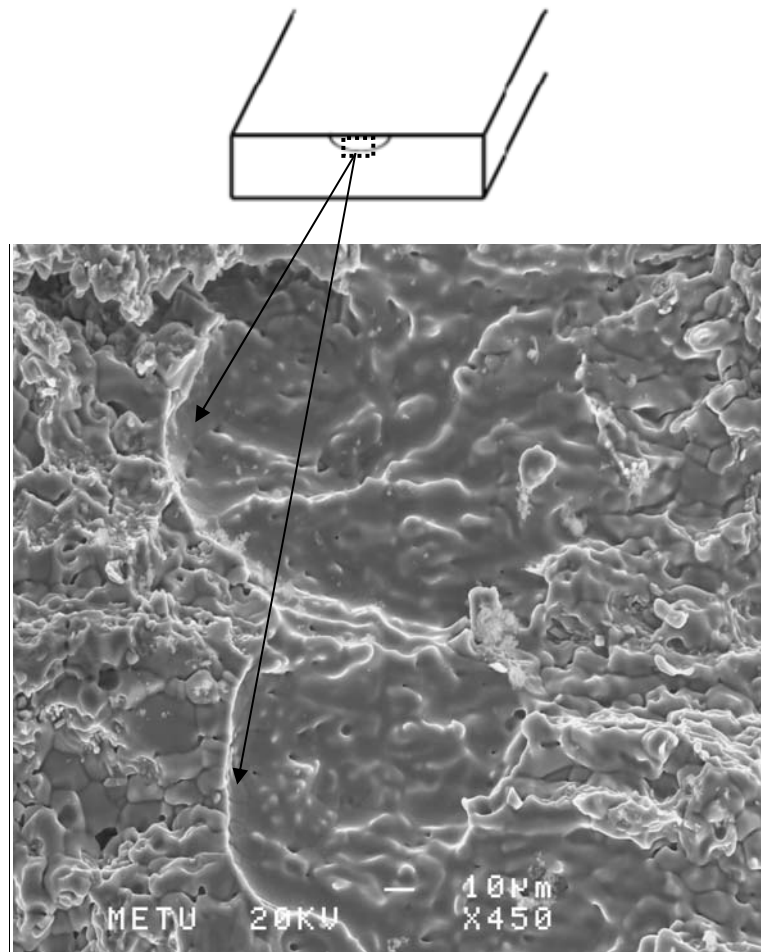


**Figure 70** Cracks that were formed just under the surface of the 7039 aluminum alloy



## CHAPTER 6

### DISCUSSION

This chapter will cover discussion about the effect of welding on the hot cracking susceptibility of the 7039 aluminum alloy.

#### **6.1 Hot cracking behavior of 7039 aluminum alloy**

Hot cracking susceptibility of the 7039 aluminum alloy is evaluated in terms of total crack length, maximum crack length, total crack number and average crack length by using MVT method. MVT results showed that 7039 aluminum alloy is susceptible to hot cracking. Hot cracks are observed as solidification cracks and liquation cracks for the 7039 aluminum alloy. Weld seams produced without using filler aluminum alloys showed susceptibility mostly to solidification cracking; on the other hand liquation and solidification cracks were observed on the weld seams produced with the addition of filler materials.

7039 aluminum alloy also showed centerline cracks on their weld seams. This can be explained by the segregates accumulated at the center part of the alloy. Segregates located at the center cause cracking under sufficient stress and strain.

#### **6.2 Effect of welding parameters on the hot cracking susceptibility**

The main parameters that affect the welding are welding speed and drop current. Both have direct effect on the heat concentrated on the weld seam of the samples. During MVT method welding speed was chosen as the varying parameter and drop current was kept constant. As the welding speed decreased the heat concentrated on the weld seam increased and vice versa. Effect of welding speed can be shown from the macro-photos of the samples (Figure 39). As the welding speed decreased weld penetration depth increased as a result of increased amount of heat. Deep penetration

zones mean that larger zones are affected from the heat. As a result cracking becomes more expectable throughout the weld. As can be seen from the Figures 34-36, hot cracking susceptibility of the samples decreases to a certain point and then increases as the welding speed increases. Reaching an optimum point shows that 7039 aluminum alloy should be welded with an optimum speed to minimize the risk of hot cracking.

### **6.2.1 Effect of welding parameters on the liquation cracking susceptibility**

When the liquation cracking susceptibility of the alloys are compared, it can be seen that as the welding speed increased or as the heat accumulated on the system decreased, the liquation crack susceptibility decreased. Main reason of this is that larger areas were affected when the heat input to the sample was increased. When the heat input increases melting or liquation occurs over a wider range that may increase the probability of liquation crack formation across the sample. Formation of liquation crack becomes more probable across the extended heat affected zone.

Alloying elements have also effect in the liquation crack susceptibilities. The difference between the liquation cracking susceptibility of 7039-5183 and 7039-5356 aluminum alloy sets can be explained with the magnesium and manganese content of the weld seams. According to literature, magnesium has a direct effect in increasing the solidification ranges of alloys. As the solidification range increases mushy zone exists more and under applied stress and strain the zone becomes more prone to liquation cracking. As a result, as the solidification range increases liquation cracking susceptibility of the alloys increase. Effect of magnesium on the solidification ranges can be explained with the Figures 55-56 and Table 8. Having a relatively higher magnesium content, 7039-5356 aluminum alloy has a relatively wider solidification range with respect to 7039-5183 aluminum alloy. On the other part, manganese has also an effect on the mushy zone size that exists during welding and solidification. With the increasing manganese content the mushy zone size decreases. As a result of narrower mushy zone liquation cracking susceptibility also decreases. Table 8 shows the difference in the manganese amount of the weld seam of 7039-5183 aluminum alloy and weld seam of 7039-5356 aluminum alloy.

To conclude, higher manganese and lesser magnesium content than the weld seam of 7039-5183 aluminum alloy contain improved its liquation cracking susceptibility.

### **6.3 Effect of filler materials on the hot cracking susceptibility**

Hot cracking depends on the chemical composition of the alloys. Therefore addition of filler materials has a direct effect on the hot cracking of the alloys. As can be seen from the Figures 30-33, hot cracking susceptibility of the three sets of alloys are different in terms of total crack length, maximum crack length, total crack number and average crack length measurements. Among the three sets of alloys 7039 aluminum alloy weld seam produced with the addition of 5356 aluminum alloy filler material showed the least hot crack susceptibility whereas the set that was welded without using any filler material showed the largest hot cracking susceptibility. The reason of this may be the addition of constituents with low melting. During solidification at the stage after the formation of the cracks, constituents with low melting may heal them and therefore decrease the hot cracking susceptibility.

### **6.4 Effect of filler materials on hardness**

Measurements showed that addition of filler materials has a positive effect in the hardness of the material. Hardness of the weld metal increased as a result of the addition of the filler materials during welding. This can be explained with the strengthening effect of filler materials.

### **6.5 Behavior of hot cracks under fatigue test**

The most critical result obtained related with the fatigue tested samples was the observations made about growth properties of the hot cracks. The fractured surfaces of 7039 aluminum alloy revealed the hot cracks that lie along the fusion line and weld metal. Under cyclic load the cracks grew from those regions towards to the parent metal.

On the other hand the filler material added samples revealed cracks that are initiated from the PMZ and HAZ regions towards parent metal. Although filler material

additions improved the fatigue life of the samples, the presence of liquation cracks could still lead to failure under cyclic load.

When the use of 7039 aluminum alloy in the industry is considered, more importance is becoming attached to this fatigue test. In the industry they are mostly assembled by welding and afterwards they are subjected to cyclic load. Therefore any hot crack that may form during welding has a risk to grow and cause fracture in service.

## CHAPTER 7

### CONCLUSION

This study can be concluded as follows:

1. Modified Varestraint Test Method can be used to determine the hot cracking susceptibility of the 7039 aluminum alloy.
2. Chemical composition of the weld metal is changed with the addition of filler materials during welding. With the addition of filler materials (5183 and 5356 aluminum alloys), 7039 aluminum alloy showed less susceptibility to hot cracking.
3. Hot cracks revealed itself in two types; solidification and liquation cracks. 7039 aluminum alloy welded without using filler materials showed negligible amount of liquation cracking. Solidification cracks were dominant on the weld seam of the 7039 aluminum alloy. For the weld seams produced with the addition of filler alloys, difference is occurred in terms of liquation cracking. 7039 aluminum alloy welded with 5356 aluminum alloy filler material showed higher liquation cracking susceptibility with respect to 5183 aluminum alloy filler material for all welding speeds.
4. Filler material additions during welding changed the chemical composition of the weld seams. The difference in magnesium and manganese content of the weld seams of 7039 aluminum alloy welded with the addition of 5183 aluminum alloy filler material and 5356 aluminum alloy filler material is determinant for their liquation cracking susceptibilities.

5. Increasing welding speed changed the hot cracking susceptibility of the alloys. Hot cracking susceptibility of the alloys decreased to a certain point with increasing welding speed. When the welding speed was further increased hot cracking susceptibility showed an increase. In this respect an optimum welding speed was obtained for all aluminum alloy sets.
6. Liquation cracking susceptibility of the 7039 aluminum alloy welded with 5183 and 5356 aluminum alloy filler materials increased with decreasing welding speed.
7. Decreasing welding speed resulted in higher heat input and therefore increased the welding penetration depth.
8. Micrographs of the samples showed that hot cracking forms intergranularly. Precipitates along the grain boundaries may be the result of intergranular crack initiation.
9. Addition of 5183 and 5356 aluminum alloy filler materials increased the hardness of the weld metal region of 7039 aluminum alloy.

## REFERENCES

1. West E.G., *The Welding of Non-ferrous Metals*. 1951, New York: John Wiley & Sons. Inc. .
2. Mathers G., *The Welding of Aluminium and Its Alloys*. 2002, Cambridge: Woodhead Publishing.
3. Praveen P. and Yarlagadda P. K. D. V., *Meeting challenges in welding of aluminum alloys through pulse gas metal arc welding*. Journal of Materials Processing Technology, 2005. 164-165: p. 1106-1112.
4. *ASM Metals Handbook*. Welding, Brazing and Soldering. Vol. 6. 1993: ASM International.
5. Griffin I. H., B.C.W., Edward M. R., *Welding Processes*. 1984: Cengage Delmar Learning. 400.
6. Kou S., *Welding Metallurgy*. 2003.
7. Granjon H., *Fundamentals of Welding Metallurgy* 1991, Cambridge: Abington Publishing.
8. Savage W.F., L.C.D., Aronson A.H., *Weld Metal Solidification Mechanics*. Welding Journal, 1965. 45: p. 175s-181s.
9. Kelkar G.P., *Weld Cracks – An Engineer’s Worst Nightmare*, WJM Technologies.
10. Cheng C. M., et al., *Hot cracking of welds on heat treatable aluminium alloys*. Science & Technology of Welding & Joining, 2005. 10(3): p. 344-352.
11. Cross C.E., *On the Origin of Weld Solidification Cracking*, in *Hot Cracking Phenomena in Welds*, H.H. Böllinghaus T., Editor. 2005, Springer: Berlin.
12. Apblett W.R., P.W.S., *Factors Which Influence Weld Hot Cracking*. Welding Journal, 1954. 33(2): p. 83s-90s.
13. Davis J. R., *ASM Specialty Handbook Aluminum and Aluminum Alloys*. ASM Specialty Handbook Series. 1993: ASM International.
14. Kou, S., *Solidification and liquation cracking issues in welding*. JOM Journal of the Minerals, Metals and Materials Society, 2003. 55(6): p. 37-42.
15. Chihoski R.A., *The Character Of Stress Fields Around A Weld Arc Moving On An Aluminum Sheet*. Welding Research Supplement, 1972: p. 9s-18s.

16. Pellini W.S., *Strain Theory Of Hot Tearing*. The Foundry, 1952. 80(11): p. 125 - 199.
17. Pumphrey W.I., J.P.H., *A consideration of the nature of brittleness and temperature above the solidus in castings and welds in aluminum alloys*. Journal of Institute Metals, 1948. 75: p. 235–256.
18. Lancaster J. F., *Metallurgy Of Welding*. 6 ed. 1999, Cambridge: Abington Publishing.
19. Borland J. C., *Generalized theory of super-solidus cracking in welds (and castings)*. Welding Journal, 1960 7: p. 508–512.
20. Matsuda F., N.K., Shimokusu Y., Tsukamoto K., Arai K., , *Effect of additional element on weld solidification crack susceptibility of Al-Zn-Mg alloy (Report I)* Transactions of JWRI, 1983. 12.(1): p. 81-87.
21. Huang C., K.S., *Liquation Cracking in Partial-Penetration Aluminum Welds: Effect of Penetration Oscillation and Backfilling*. Welding Journal, 2003. 82: p. 184-194.
22. Kou S., *Solidification and liquation cracking issues in welding*. JOM Journal of the Minerals, Metals and Materials Society, 2003. 55(6): p. 37-42.
23. Mandal N.R., *Aluminum Welding*. Second ed. 2005: Narosa Publishing House.
24. Tirkeş S., *Hot Cracking Susceptibility of Twin Roll Cast Al - Mg Alloys*, PhD Thesis in *Metallurgical and Materials Engineering*. 2009, Middle East Technical University: Ankara. p. 108.
25. Cross C.E. and Coniglio N., *Weld Solidification Cracking: Critical Conditions for Crack Initiation and Growth*. 2008. p. 47-66.
26. Lingenfelter A.C., *Varestraint Testing of Nickel Alloys*. Welding Journal, 1972. 51(9): p. 430s-436s.
27. Savage W.F., L.C.D., *Application of the Varestraint Technique to the Study of Weldability*,. Welding Journal, 1966. 45: p. 497s–503s.
28. Batıgün C., *Welding process related hot cracking tendency in aluminum alloys*, in *9. International Metallurgy and Materials Congress*. 1997: Istanbul.
29. Heuser H., *Value of Different Hot Cracking Tests for the Manufacturer of Filler Metals*. 2005. p. 305-327.
30. Tao M., *Weldability of Al-Zn-Mg Alloys*, in *Faculty of Chemical Technology and Materials Science*. 1997, Delft University of Technology: Delft. p. 180.



31. Cross C. E., *Welding Hot Crack Testing: MVT Test*, in *Catalogue of reference procedures provided by BAM, Chapter 5 - Testing of mechanical-technological properties*, T.B.F.I.f.M.R.a. Testing, Editor. 2005: Berlin.
32. Hemsworth B., B.T., Eaton N.F., *Classification and definition of high temperature welding cracks in alloys*. Metal Construction and British Welding Journal 1969. 1(5-16).
33. Robinson I.B., B.F.R., *Welding Aluminum Alloy 7039*. Welding Journal, 1966. 45(10): p. 433s-444s.
34. Gibbs F.E., *Development of a Weld Filler Alloy for Al-Zn-Mg Alloy 7039*. Welding Journal, 1966. 45: p. 445s-453s.
35. Kim H. T., N.S.W., Hwang S. H., *Study on the Solidification Cracking Behavior of High-Strength Aluminum-Alloy Welds - Effects of Alloying Elements and Solidification Behaviors*. Journal of Materials Science, 1996. 31(11): p. 2859-2864.
36. Cicala E., et al., *Hot cracking in Al-Mg-Si alloy laser welding - operating parameters and their effects*. Materials Science and Engineering A, 2005. 395(1-2): p. 1-9.
37. Matsuda F., et al., *The VDR Cracking Test for Solidification Crack Susceptibility on Weld Metals and Its Application to Aluminum Alloys (Materials, Metallurgy, Weldability)*. Transactions of JWRI, 1979. 8(1): p. 85-95.
38. Caymaz F., *Hot Cracking In Welding Of Aluminum and Some Of Its Alloys*, MSc Thesis in *Metallurgical and Materials Engineering*. 1997, Middle East Technical University: Ankara. p. 128.
39. Brungraber R.J., N.F.G., *Effect of Welding Variables on Aluminum Alloy Weldments*. Welding Journal, 1973. 52(3): p. 97s-103s.
40. Liptak J.A., *Gas Tungsten-Arc Welding Heavy Aluminum Plate*. Welding Journal, 1965. 44(6): p. 276s-281s.
41. Liptak J.A., *Techniques for Welding 7039 Aluminum with Various Inert Gas Processes*. Welding Journal, 1966. 45.
42. Coniglio N., C.C.E., *Weld Parameter and Minor Element Effects on Solidification Crack Initiation in Aluminium*. 2008. p. 277-310.
43. Shibahara M., Serizawa H., and Murakawa H., *Finite Element Method for Hot Cracking Using Temperature Dependent Interface Element (Report II) : Mechanical Study of Houldcroft Test (Mechanics, Strength & Structure Design)*. Transactions of JWRI, 2000. 29(1): p. 59-64.
44. Johnson L., *Formation of Plastic Strains During Welding of Aluminum Alloys*. Welding Journal, 1973. 52(7): p. 298s-305s.

45. Chihoski R.A., *Understanding Weld Cracking in Aluminum Sheet*. Welding Journal, 1972. 51(1): p. 24-30.
46. Batıgün C., T.S., *Effect of line energy on the weld geometry and Mg content of the weld metal in MIG welding of Al-Mg alloys*, in *Welding Technology VI. National Congress*. 2007: Ankara.
47. Mondolfo L. F., *Aluminum Alloys : Structure and Properties*. 1976, London ; Boston :: Butterworths.
48. Mousavi M. G., C.C.E., Grong O., *The Effect of High-Temperature Eutectic-Forming Impurities on Aluminum 7108 Weldability*. 2009. 88(5).
49. Batıgün C., *Determination of Welding Parameter Dependent Hot Cracking Susceptibility of 5086-H32 Aluminium Alloy With The Use of MVT Method*, PhD Thesis in *Metallurgical and Materials Engineering*. 2005, Middle East Technical University: Ankara. p. 238
50. Raghavan V., *Al-Mg-Zn (Aluminum-Magnesium-Zinc)*. Journal of Phase Equilibria and Diffusion, 2007. 28(2): p. 203-208.

## APPENDIX A

### PHASE DIAGRAM OF Al-Mg-Zn

The liquidus projection of Al-Mg-Zn computed by Liang P. et.al., is shown in the Figure A1 [50].

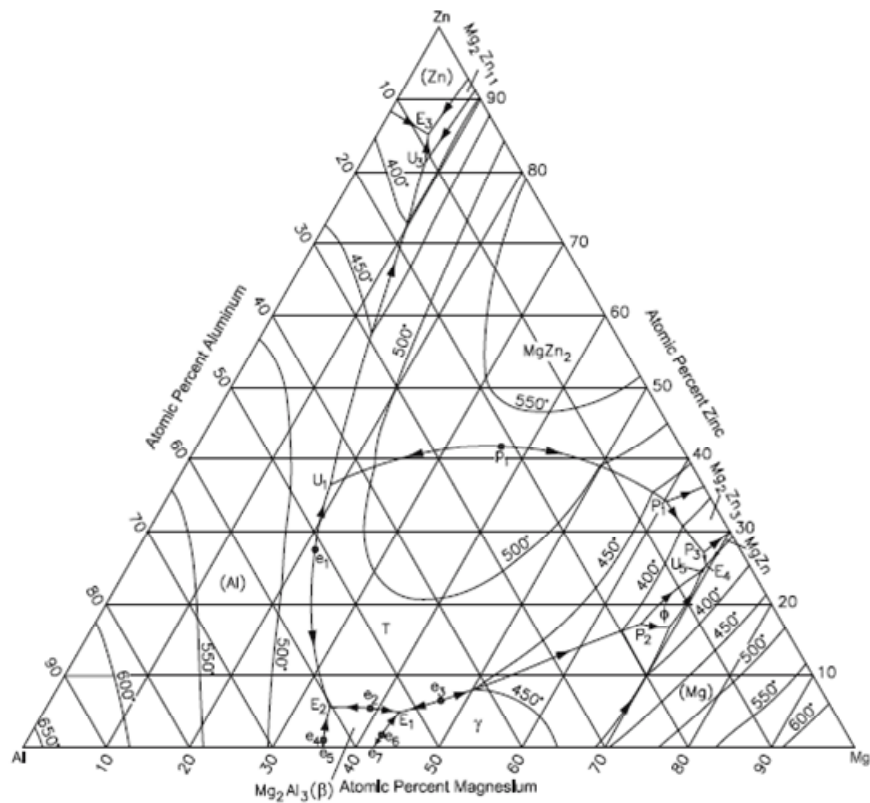


Figure A1 Liquidus projection of Al-Mg-Zn

## APPENDIX B

### CRACK LENGTH AND NUMBER MEASUREMENT RESULTS

Crack length and crack number measurements carried out after MVT method is given in Tables B1 to B3. Tables B4-B5 shows the length and location of liquation cracks. The lengths are given in millimeters.

**Table B1** Crack length measurement results for 7039 aluminum alloy set

<b>7039 Aluminum Alloy</b>					
	<b>50 mm/min</b>	<b>55 mm/min</b>	<b>60 mm/min</b>	<b>65 mm/min</b>	<b>70 mm/min</b>
# 1	5	3,5	1	2	2
# 2	0,5	1,5	2,5	2,75	1,5
# 3	0,5	4	1,25	1,25	1,25
# 4	0,75	1,5	1	3,75	1,5
# 5	0,75	1	3,5	1,5	3,25
# 6	2,5	2	2	1	1,5
# 7	1	1	1,25	0,25	1
# 8	0,5	1	1,5	1,5	
# 9	4,5	0,5	1	1,25	
# 10	2	0,5		1	
# 11	1,5			0,25	
# 12				0,25	
<b>Total Crack Length (mm)</b>	<b>19,5</b>	<b>16,5</b>	<b>15</b>	<b>16,75</b>	<b>12</b>
<b>Total Crack Number</b>	<b>11</b>	<b>10</b>	<b>9</b>	<b>12</b>	<b>7</b>
<b>Average Crack Length (mm)</b>	<b>1,627</b>				

**Table B2** Crack length measurement results for 7039-5183 aluminum alloy set

<b>7039-5183 Aluminum Alloy</b>					
	<b>50 mm/min</b>	<b>55 mm/min</b>	<b>60 mm/min</b>	<b>65 mm/min</b>	<b>70 mm/min</b>
# 1	3,5	3,15	1,12	2,31	2,24
# 2	1,05	2,8	2,05	1,75	2,66
# 3	0,7	2,24	1,4	2,05	1,4
# 4	0,35	2,8	1,1	1,05	2,8
# 5	1,4	2,1	1,8	1,75	1,7
# 6	2,1	1,2	1,1	1,4	1,4
# 7	2,1	0,9	1,96	1,1	2,17
# 8	1,26	0,77		0,35	0,28
# 9	2,45	1,05			0,4
# 10	0,7				
# 11	1,47				
# 12	0,63				
<b>Total Crack Length (mm)</b>	<b>17,71</b>	<b>17,01</b>	<b>10,53</b>	<b>11,76</b>	<b>15,05</b>
<b>Total Crack Number</b>	<b>12</b>	<b>9</b>	<b>7</b>	<b>8</b>	<b>9</b>
<b>Average Crack Length (mm)</b>	<b>1,601</b>				

**Table B3** Crack length measurement results for 7039-5356 aluminum alloy set

<b>7039-5356 Aluminum Alloy</b>					
	<b>50 mm/min</b>	<b>55 mm/min</b>	<b>60 mm/min</b>	<b>65 mm/min</b>	<b>70 mm/min</b>
# 1	0,84	1,47	1,68	1,89	2,8
# 2	3,08	0,49	1,54	1,52	1,1
# 3	1,68	2,31	2,66	1,37	0,56
# 4	0,77	1,54	2,59	1,22	1,05
# 5	1,68	1,71	1,05	1,96	1,4
# 6	1,47	1,33	1,68	1,12	0,77
# 7	0,28	2,94		1,26	0,84
# 8	1,26	0,42			1,61
# 9	1,62				1,05
# 10	0,35				
<b>Total Crack Length (mm)</b>	<b>13,03</b>	<b>12,21</b>	<b>11,2</b>	<b>10,34</b>	<b>11,18</b>
<b>Total Crack Number</b>	<b>10</b>	<b>8</b>	<b>6</b>	<b>7</b>	<b>9</b>
<b>Average Crack Length (mm)</b>	<b>1,449</b>				

**Table B4** The length and location of liquation cracks of 7039-5183 aluminum alloy

Welding ←		7039-5183				
		50 mm/min 120 A	55 mm/min 120 A	60 mm/min 120 A	65 mm/min 120 A	70 mm/min 120 A
1	Crack Length	1,1 mm	1,7 mm	0,98 mm	1 mm	0,4 mm
	Direction					
2	Crack Length	0,35 mm	1,5 mm	0,5 mm	0,6 mm	0,6 mm
	Direction					
3	Crack Length	0,7 mm	0,62 mm	0,7 mm	0,96 mm	0,5 mm
	Direction					
4	Crack Length	0,35 mm	1,6 mm	1 mm	0,4 mm	0,6 mm
	Direction					
5	Crack Length	1,05 mm	1,75 mm	0,8 mm	1,4 mm	
	Direction					
6	Crack Length	1,96 mm		1,6 mm	0,4 mm	
	Direction					
7	Crack Length	0,7 mm			0,4 mm	
	Direction					
8	Crack Length	0,28 mm				
	Direction					
9	Crack Length	0,7 mm				
	Direction					
10	Crack Length	0,4 mm				
	Direction					

**Table B5** The length and location of liquation cracks of 7039-5356 aluminum alloy

Welding ←		7039-5356				
		50 mm/min 120 A	55 mm/min 120 A	60 mm/min 120 A	65 mm/min 120 A	70 mm/min 120 A
1	Crack Length	0,4 mm	0,49 mm	0,84 mm	0,56 mm	0,7 mm
	Direction					
2	Crack Length	2,6 mm	0,14 mm	0,81 mm	0,96 mm	0,42 mm
	Direction					
3	Crack Length	0,89 mm	2,01 mm	1,7 mm	0,7 mm	0,77 mm
	Direction					
4	Crack Length	0,56 mm	0,96 mm	1,1 mm	1,52 mm	0,98 mm
	Direction					
5	Crack Length	0,6 mm	1,1 mm	0,77 mm	0,96 mm	0,14 mm
	Direction					
6	Crack Length	1,1 mm	0,42 mm	0,7 mm	0,7 mm	0,84 mm
	Direction					
7	Crack Length	0,28 mm	2,1 mm			0,63 mm
	Direction					
8	Crack Length	0,7 mm	0,42 mm			
	Direction					
9	Crack Length	1,1 mm				
	Direction					
10	Crack Length	0,35 mm				
	Direction					